Hadronic Effects and Observables in Semileptonic B-Meson Decays

Dissertation

zur Erlangung des akademischen Grades eines Doktors
der Naturwissenschaften

vorgelegt von

M.Sc. Aleksey Rusov

eingereicht bei der Naturwissenschaftlich-Technischen Fakultät
der Universität Siegen

Siegen
Februar 2018

Gutachter der Dissertation:	Prof. Dr. Alexander Khodjamirian Prof. Dr. Thomas Mannel
Datum der Disputation:	16.03.2018
Prüfungskommission:	Prof. Dr. Alexander Khodjamirian Prof. Dr. Thomas Mannel Prof. Dr. Vladimir Braun Prof. Dr. Christian Gutt

Abstract

An accurate phenomenological analysis of rare B-meson decays is important both for precise tests of the Standard Model and in the search for possible New Physics in the flavour sector. In the framework of this thesis, several semileptonic B-meson decays induced by flavour-changing quark currents are studied. The main focus is put on the analysis of the underlying hadronic input including the relevant form factors and nonlocal hadronic amplitudes. With accurate determination of the hadronic input from the QCD-based methods, various observables in inclusive and exclusive semileptonic decays of B mesons are predicted.

This dissertation is written in the form of a cumulative work based on our four articles published in international peer reviewed journals. The first chapter contains a short introduction to the Standard Model and a brief discussion of theoretical methods.

The chapter 2 of the thesis is dedicated to the analysis of the flavour-changing neutral current (FCNC) $b \to d$ observed in the form of the semileptonic $B \to \pi\ell^+\ell^-$ decays. In the latter decays, the underlying hadronic nonlocal contributions are systematically taken into account using the operator-product expansion, QCD factorization and light-cone sum rules. Together with the $B \to \pi$ form factors derived from light-cone sum rules, these nonlocal hadronic amplitudes are used to predict various observables such as the differential rate, direct CP-asymmetry and isospin asymmetry in $B \to \pi\ell^+\ell^-$ decays. In addition, the total width of $B \to \pi\nu\bar{\nu}$ decay is estimated.

The third chapter of the thesis is devoted to the analysis of the higher-twist effects in the QCD light-cone sum rule for the heavy-to-light transition form factors. To this end, the light-cone expansion of the massive quark propagator in the external gluonic field is extended to include new terms containing the derivatives of gluon-field strength. The resulting analytical expressions for the twist-5 and twist-6 contributions to the correlation function are obtained in a factorized approximation, expressed via the product of the lower-twist pion distribution amplitudes and the quark-condensate density. The numerical analysis reveals a smallness of the higher twist effects justifying the conventional truncation of the operator product expansion in the light-cone sum rules up to twist 4.

The chapter 4 of the thesis extends the analysis of hadronic input to other semileptonic decays including $B \to K\ell^+\ell^-$ and $B_s \to K\ell^+\ell^-$. To this end, the light-cone sum rule results for the relevant form factors are updated taking into account the estimate of the higher twist effects. In addition, the corresponding nonlocal hadronic matrix elements are extracted in a systematic way. Moreover, a new way to determine the Wolfenstein parameters of the Cabibbo-Kobayashi-Maskawa matrix is suggested based on the observables in semileptonic FCNC $B \to \pi\ell^+\ell^-$ and $B \to K\ell^+\ell^-$ decays. The prediction for the $B_s \to K\ell\nu_\ell$ partial decay width provides an additional source for the determination of the CKM parameter $|V_{ub}|$.

The last chapter 5 of the thesis deals with the inclusive semileptonic $B \to X_c\tau\nu_\tau$ decays. Using the standard techniques of heavy quark expansion, the decay width and moments of τ-lepton energy distribution are calculated including power corrections up to order Λ^3_{QCD}/m_b^3. The result is compared with the sum of the predictions for the branching fractions of the exclusive semileptonic $B \to (D, D^*, D^{**})\tau\nu_\tau$ decays as well as with the relevant experimental data. In addition, the impact from physics beyond the Standard Model to the inclusive $B \to X_c\tau\nu_\tau$ rate is discussed.

Zusammenfassung

Eine genaue phänomenologische Analyse von seltenen Zerfällen von B-Mesonen ist sowohl für präzise Tests des Standardmodells als auch für die Suche nach möglicher neuer Physik im Flavoursektor wichtig. Im Rahmen dieser Arbeit werden verschiedene semileptonische Zerfälle von B-Mesonen, die durch flavouränderndе Quarkströme induziert werden, untersucht. Der Schwerpunkt liegt dabei auf der Analyse des zugrundeliegenden hadronischen Inputs, einschließlich der relevanten Formfaktoren und nichtlokalen hadronischen Amplituden. Mithilfe einer genauen Bestimmung des hadronischen Inputs, der mittels QCD-basierten Methoden gewonnen wurde, werden verschiedene Observablen von inklusiven und exklusiven semileptonischen Zerfällen von B-Mesonen, vorhergesagt.

Diese Dissertation ist in Form von einer kumulativen Arbeit geschrieben und basiert auf vier Artikeln, die in internationalen, von Experten begutachteten Fachzeitschriften veröffentlicht wurden. Das erste Kapitel enthält eine kurze Einführung in das Standardmodell und eine kurze Diskussion von theoretischen Methoden.

Das Kapitel 2 der Dissertation ist der Analyse des flavouränderndеn neutralen Stroms (FCNC) $b \to d$ gewidmet, der in der Form von semileptonischen $B \to \pi\ell^+\ell^-$ Zerfällen beobachtet werden kann. In den zuletzt genannten Zerfällen, werden die zugrundeliegenden hadronischen nichtlokalen Beiträge unter Verwendung der Operatorproduktentwicklung, der QCD-Faktorisierung und den Lichtskegelsummenregeln, systematisch berücksichtigt. Diese nichtlokalen hadronischen Amplituden werden zusammen mit den aus den Lichtkegelsummenregeln abgeleiteten $B \to \pi$ Formfaktoren, zur Vorhersage verschiedener Observablen wie der differentiellen Rate, der direkten CP-Asymmetrie und der Isospin-Asymmetrie von $B \to \pi\ell^+\ell^-$, verwendet. Zusätzlich wird die totale Breite des Zerfalls $B \to \pi\nu\bar{\nu}$ abgeschätzt.

Das dritte Kapitel der Dissertation ist der Analyse von Effekten höheren Twists, die in der QCD Lichtkegelsummenregel für den Übergang eines schweren Mesons in ein leichtes Meson auftauchen, gewidmet. Zu diesem Zweck wird die Lichtkegelentwicklung des massiven Quarkpropagators in einem externen gluonischen Feld ausgedehnt, um neue Terme, die Ableitungen der Gluonfeldstärke enthalten, zu berücksichtigen. Die daraus resultierenden analytischen Ausdrücke für die Beiträge vom Twist-5 und Twist-6 zu den Korrelationsfunktion, werden in einer faktorisierten Approximation, die durch ein Produkt von Pion-Verteilungsamplituden von niedrigerem Twist und der Quarkkondensatdichte ausgedrückt ist, gewonnen. Die numerische Analyse zeigt, dass die Effekte von höherem Twist klein sind, was das herkömmliche Abbrechen der Operatorproduktentwicklung in den Lichtkegelsummenregeln bei Twist-4, rechtfertigt.

Das Kapitel 4 der Dissertation weitet die Analyse des hadronischen Inputs auf andere semileptonische Zerfälle, einschließlich $B \to K\ell^+\ell^-$ und $B_s \to K\ell^+\ell^-$ aus. Zu diesem Zweck werden die Lichtkegelsummenregel-Ergebnisse für die relevanten Formfaktoren, unter Berücksichtigung der Abschätzung der Effekte von höherem Twist, auf den aktuellen Stand gebracht. Außerdem wird ein neuer Weg vorgeschlagen, die Wolfenstein-Parameter der Cabibbo-Kobayashi-Maskawa-Matrix zu bestimmen, welcher auf den Observablen der semileptonischen FCNC Zerfälle $B \to \pi\ell^+\ell^-$ und $B \to K\ell^+\ell^-$ basiert. Die Vorhersage für die partielle Zerfallsbreite von $B_s \to K\ell\nu_\ell$ bietet eine zusätzliche Möglichkeit den CKM-Parameter $|V_{ub}|$ zu bestimmen.

Das letzte Kapitel 5 der Dissertation beschäftigt sich mit den inklusiven semileptonischen $B \to X_c \tau \nu_\tau$ Zerfällen. Unter Verwendung der Standardtechnik der Heavy-Quark-Expansion, werden die Zerfallsbreite und die Momente der Energieverteilung des τ-Leptons einschließlich der Power-Korrekturen bis zur Ordnung $\Lambda^3_{\rm QCD}/m_b^3$ berechnet. Das Ergebnis wird sowohl mit der Summe der Vorhersagen für die Verzweigungsverhältnisse der exklusiven semileptonischen $B \to (D, D^*, D^{**})\tau\nu_\tau$ Zerfälle als auch mit den relevanten experimentellen Daten verglichen. Zusätzlich wird der Effekt von Physik jenseits des Standardmodells auf die inklusive $B \to X_c \tau \nu_\tau$ Zerfallsrate diskutiert.

Contents

Chapter 1

Introduction

The idea of elementary particles has a long history starting from the time of ancient Greece. The field of particle physics has achieved tremendous development during the previous century due to studies of the cosmic rays and construction of the particle accelerators. Efforts of many theorists and experimentalists led to the foundation of the Standard Model of particle physics – the most successful theory in this field. Being quite a compact theory with a few basic parameters, Standard Model (SM) is able to describe a plenty of various particle processes, some of them with a very impressive accuracy. Up to now, no significant deviation from the SM predictions was found. Nevertheless, as many physicists suppose, there is certainly physics beyond the SM. First of all, it is clear that SM is not a complete theory since it describes only three of the four known fundamental forces (strong, weak and electromagnetic) and does not tell anything about gravity. The second argument is based on a presence of too many input parameters in this theory. The SM also does not incorporate certain phenomena in the cosmology such as dark matter and dark energy. Furthermore, there exist several tensions between SM and physics of heavy hadrons hinting at some New Physics at large energy scales. Nevertheless, it is obvious that SM will survive at least as an effective theory of particle physics, applicable at certain energy scales. This is in a full analogy, for instance, with the classical (Newton) mechanics which is still a very useful and applicable theory for the description of plenty of phenomena in the macroscopic world where one deals with the velocities much smaller the speed of light, whereas a more general, special relativity theory is applicable for any velocities.

There are still open questions about a possible form of the New Physics. What is the particle content of it? At which scale does it appear? How can we detect it? To clarify these issues, from the theory side one still needs to refine phenomenological analysis of a plenty of particle processes to predict various observables with a very high accuracy. Despite SM is a well-established theory, hadronic uncertainties in the decays of mesons and baryons still represent a considerable challenge in their phenomenological analysis. Also from the experimental side, one needs to fulfil as much as possible measurements of the various processes with a high precision by gaining more statistics in particle collisions and by improving the experimental techniques. The joined efforts of experimentalists and theorists is very important for a precision test of the Standard Model as well as for the identification of possible New physics in case if one finds a significant deviation of the SM predictions from the measurements.

In the light of such situation in particle physics, an analysis of hadronic effects in

several semileptonic decays of heavy hadrons was performed in this thesis. The thesis is written as a cumulative work presenting the results of our research in a form of four articles published in the leading international peer reviewed journals. In the rest of this chapter, a short overview of the SM and a brief description of theoretical methods used in the research are given. The four subsequent chapters contain the corresponding articles on the topics of the research. The first one (Chapter 2) is devoted to the analysis of the hadronic input and observables in exclusive semileptonic $B \to \pi\ell^+\ell^-$ decays. In Chapter 3, a new estimate of higher twist effects in light-cone sum rule for the heavy-to-light transition vector form factor is given. Chapter 4 contains the results of the analysis of semileptonic exclusive $B_s \to K\ell\bar{\nu}_\ell$ and $B_{(s)} \to \pi(K)\ell^+\ell^-$ decays at large hadronic recoil, including the updated results for the relevant form factors from QCD light-cone sum rules and a new way to extract the Cabibbo-Kobayashi-Maskawa matrix elements. In Chapter 5, the analysis of the semitauonic inclusive $B \to X_c\tau\nu_\tau$ decay up to order $\Lambda^3_{\rm QCD}/m_b^3$ is presented. The thesis is concluded by a summary and discussion of the obtained results.

1.1 The Standard Model

A detailed overview of the SM certainly goes beyond the scope of this thesis. There is a plenty of remarkable reviews and excellent books available in the literature, e.g. [1, 2, 3, 4, 5, 6]. Here we aim at a brief outline of the foundations of the Standard Model and its application in the context of the thesis.

1.1.1 Particle content

The Standard Model (SM) is a basis of the modern elementary particle physics describing the electromagnetic, weak and strong interactions as well as classifying all elementary particles. According to the Standard Model, all matter around us consists of the building blocks – elementary particles. There are two basic types of such particles called quarks and leptons. These particles are fermions since they have spin 1/2. There are six different types of both quarks and leptons organised in pairs forming in total three generations. The hierarchy of the particles together with some of their properties is presented in Table 1.1. The lightest and most stable particles belong to the first generation, while the heavier and less stable particle form the second and third generations. Each particle has an antiparticle having the opposite values of the electric charge and of other additive quantum numbers.

There is another type of fundamental particles, gauge bosons, which are defined as physical force carriers. They mediate the electromagnetic, weak and strong interactions. All gauge bosons in the Standard Model have an integer spin $S = 1$. The massless photon mediates the electromagnetic force between electrically charged particles. The photons as well as their interactions with charged fermions are well described by quantum electrodynamics (QED). The weak interactions between particles are mediated by W^+, W^- and Z gauge bosons. These bosons are massive and therefore the weak interaction takes place only at very small, sub-nuclear distances. W^+ and W^- bosons carry an electric charge

Class	Type	Generation	Charge	Mass
Quarks	u, up	I	+2/3	$\sim 2.5\,\mathrm{MeV}$
(Spin 1/2)	d, down	I	-1/3	$\sim 5\,\mathrm{MeV}$
	s, strange	II	+2/3	$\sim 100\,\mathrm{MeV}$
	c, charm	II	-1/3	$\sim 1.3\,\mathrm{GeV}$
	b, bottom	III	+2/3	$\sim 4.7\,\mathrm{GeV}$
	t, top	III	-1/3	$\sim 175\,\mathrm{GeV}$
Leptons	e, electron	I	-1	$0.511\,\mathrm{MeV}$
(Spin 1/2)	ν_e, electron neutrino	I	0	$< 0.23\,\mathrm{eV}$
	μ, muon	II	-1	$105.7\,\mathrm{MeV}$
	ν_μ, muon neutrino	II	0	$< 0.23\,\mathrm{eV}$
	τ, tau	III	-1	$1.777\,\mathrm{GeV}$
	ν_τ, tau neutrino	III	0	$< 0.23\,\mathrm{eV}$
Gauge bosons	γ, photon		0	0
(Spin 1)	Z-boson		0	$91.2\,\mathrm{GeV}$
	$W^{\pm}$-bosons		± 1	$80.4\,\mathrm{GeV}$
	g, gluon		0	0
Scalar bosons (Spin 0)	H, Higgs boson		0	$125\,\mathrm{GeV}$

Table 1.1: Elementary particles in the Standard Model [1]. The bounds on neutrino masses follow from $\sum_j m_{\nu_j} < 0.23$ eV given in [7]

of +1 and -1 and by this reason they participate in the electromagnetic interactions. Furthermore, they have a specific property to interact exclusively with the left-handed particles. The Z-boson is a electrically neutral particle and interacts both with left- and right-handed particles although in asymmetric way. The gluons are the mediators of the strong interactions. There are eight types (colors) of gluons interacting with the color charged quarks. Since gluons have color charge, they can also interact with themselves. The quark-gluon interactions are described by quantum chromodynamics (QCD).

Furthermore, there is another particle playing an important role in the Standard Model and discovered recently at Large Hadron Collider (LHC) [8, 9]. This is the Higgs boson. Being a scalar neutral particle, Higgs boson generates the masses of all fermions and $W^{\pm}$ and Z bosons by means of the spontaneous symmetry breaking mechanism.

1.1.2 Electroweak sector

The electroweak sector of the Standard model unifies the electromagnetic and weak interactions. It is based on the gauge symmetry group $SU(2)_L \times U(1)$. Theory of the electroweak interactions was originally developed by Glashow [10], Weinberg [11]

and Salam [12]. According to the electroweak theory, the fermions, leptons and quarks forming left-handed doublets and right-handed singlets, transform under the fundamental representations of the symmetry group $SU(2)_L \times U(1)$:

$$\Psi_L = \begin{pmatrix} \psi_L^u \\ \psi_L^d \end{pmatrix} = \begin{pmatrix} (\nu_e)_L \\ e_L \end{pmatrix}, \begin{pmatrix} (\nu_\mu)_L \\ \mu_L \end{pmatrix}, \begin{pmatrix} (\nu_\tau)_L \\ \tau_L \end{pmatrix}, \begin{pmatrix} u_L \\ d_L \end{pmatrix}, \begin{pmatrix} c_L \\ s_L \end{pmatrix}, \begin{pmatrix} t_L \\ b_L \end{pmatrix}, \quad (1.1)$$

$$\psi_R = e_R,\, \mu_R,\, \tau_R,\, u_R,\, d_R,\, s_R,\, c_R,\, b_R,\, t_R. \quad (1.2)$$

In the above, the left-handed and right-handed components of the fermion field ψ are defined as:

$$\psi_L = \frac{1-\gamma_5}{2}\psi, \qquad \psi_R = \frac{1+\gamma_5}{2}\psi. \quad (1.3)$$

The representations (1.2), (1.1) can be ordered by the quantum numbers of the weak isospin I, its third projection I_3 and the weak hypercharge Y. The doublets of the left-handed fields have isospin $I = 1/2$ and the right-handed singlets have $I = 0$. These basic quantum numbers are related with the electric charge Q via the Gell-Mann-Nishijima relation:

$$Q = I_3 + \frac{Y}{2}. \quad (1.4)$$

Weak hypercharge Y characterises the whole multiplet. From Eq. (1.4) it follows that $Y = 2\,\bar{Q}$ with $\bar{Q}$ being the average charge of the multiplet.

The electroweak Lagrangian is generically presented as a sum of the several parts, including the gauge boson, fermion, Higgs and Yukawas ones:

$$\mathcal{L}_{EW} = \mathcal{L}_G + \mathcal{L}_F + \mathcal{L}_H + \mathcal{L}_Y. \quad (1.5)$$

The gauge boson part is given by

$$\mathcal{L}_G = -\frac{1}{4} W^a_{\mu\nu} W^{a\,\mu\nu} - \frac{1}{4} B_{\mu\nu} B^{\mu\nu}, \quad (1.6)$$

where the strength tensors of the $SU(2)$-gauge fields $W^a_\mu\,(a = 1, 2, 3)$ and $U(1)$ gauge field B_μ are:

$$W^a_{\mu\nu} = \partial_\mu W^a_\nu - \partial_\nu W^a_\mu + g\,\varepsilon^{abc}\, W^b_\mu\, W^c_\nu, \quad (1.7)$$

$$B_{\mu\nu} = \partial_\mu B_\nu - \partial_\nu B_\mu, \quad (1.8)$$

with g and ε^{abc} being the gauge coupling and the structure constants of the $SU(2)_L$ group, respectively. Under the exact $SU(2)_L \times U(1)$ symmetry the gauge bosons are massless. They acquires their masses after spontaneous symmetry breaking $SU(2)_L \times U(1) \to U(1)$ by means of the Higgs mechanism as explained below.

The fermion part of the electroweak Lagrangian is given by

$$\mathcal{L}_F = \sum_\Psi \bar{\Psi}_L\, i\not{D}_L \Psi_L + \sum_\psi \bar{\psi}_R\, i\not{D}_R \psi_R, \quad (1.9)$$

where doublets Ψ_L and singlets ψ_R are presented in (1.1) and (1.2), respectively, and the summations over Ψ, ψ include all flavours of fermions (quarks and leptons). The covariant derivatives are given by expressions

$$(D_L)_\mu = \partial_\mu - ig\frac{\sigma^a W^a_\mu}{2} + ig'\frac{Y_L}{2}B_\mu, \tag{1.10}$$

$$(D_R)_\mu = \partial_\mu + ig'\frac{Y_R}{2}B_\mu, \tag{1.11}$$

where g' is a gauge coupling of the $U(1)$ gauge group, and $\sigma^a\,(a=1,2,3)$ are the Pauli matrices related with the generators T^a of the $SU(2)$ group as $T^a = \sigma^a/2$. The values of the hypercharge Y_L, Y_R for doublets and singlets follow from (1.4):

$$Y(\nu_L) = Y(e_L) = -1, \qquad Y(u_L) = Y(d_L) = +\frac{1}{3}, \tag{1.12}$$

$$Y(e_R) = -2, \qquad Y(d_R) = -\frac{2}{3}, \qquad Y(u_R) = +\frac{4}{3}, \tag{1.13}$$

and identically for the particles of the second and third generations. The W^a_μ, B_μ are the four gauge fields, which are related with the physical fields of $W^\pm$ and Z bosons and photon field A_μ:

$$W^{(*)}_\mu = \frac{W^1_\mu \pm i\, W^2_\mu}{\sqrt{2}}, \tag{1.14}$$

$$Z_\mu = \cos\theta_W\, W^3_\mu + \sin\theta_W\, B_\mu, \tag{1.15}$$

$$A_\mu = -\sin\theta_W\, W^3_\mu + \cos\theta_W\, B_\mu, \tag{1.16}$$

where the mixing Weinberg angle θ_W is determined as

$$\cos\theta_W = \frac{g}{\sqrt{q^2+g'^2}}. \tag{1.17}$$

Using the expressions for the covariant derivatives (1.10), (1.11) and the definitions (1.14), (1.15), (1.16), one obtains from (1.9) the explicit expressions for the Lagrangians of boson-fermion interaction:

$$\mathcal{L}_{\psi A} = -e\sum_\psi Q_\psi(\bar\psi\gamma_\mu\psi)A^\mu, \tag{1.18}$$

$$\mathcal{L}_{\psi W} = \frac{g}{\sqrt{2}}\sum_\Psi\left[(\bar\psi^d_L\gamma_\mu\psi^u_L)W^\mu + \text{h.c.}\right], \tag{1.19}$$

$$\mathcal{L}_{\psi Z} = \frac{g}{4\cos\theta_W}\sum_\Psi\left[(\bar\psi^u\gamma_\mu(a_u-\gamma_5)\psi^u) - (\bar\psi^d\gamma_\mu(a_d-\gamma_5)\psi^d)\right]Z^\mu, \tag{1.20}$$

where

$$a_u = 1 - 4Q_u\sin^2\theta_W, \qquad a_d = 1 + 4Q_d\sin^2\theta_W, \tag{1.21}$$

and the elementary electric charge e is related with g and g':

$$e = \frac{gg'}{\sqrt{g^2+g'^2}} = g\sin\theta_W = g'\cos\theta_W. \tag{1.22}$$

The Lagrangian (1.18) contains only a sum over electrically charged particles and reproduces quantum electrodynamics. Note, that the Lagrangian (1.19) does not incorporate the effect of mixing which takes place in case of quarks. This issue will be discussed in sect. 1.1.4.

The Yukawa part of the SM Lagrangian can be splitted into two pieces:

$$\mathcal{L}_Y = \mathcal{L}_Y^{\text{leptons}} + \mathcal{L}_Y^{\text{quarks}}. \tag{1.23}$$

The first term in (1.23) describes the Yukawa interaction of the leptons with the Higgs boson:

$$\mathcal{L}_Y^{\text{leptons}} = -Y_{ij}^{(\ell)} \, (\bar{L}_L^i \phi) \ell_R^j + \text{h.c.} \tag{1.24}$$

where $L_L^i = (\nu_\ell^i, \, \ell^i)^T (\ell^i = e, \mu, \tau)$ is a doublet of the left-handed leptons, ℓ_R^i is the right-handed lepton singlet, the Higgs doublet ϕ is defined by (1.26) (see next section) and $Y_{ij}^{(\ell)}$ is the 3×3 matrix of lepton Yukawa couplings. Note, that neutrinos are assumed to be massless in the SM, and by this reason the term with right-handed neutrinos is not present in (1.24). In the SM, the lepton number is conserved and lepton mixing is absent. Therefore, the lepton Yukawa matrix should be diagonal $Y_{ij}^{(\ell)} = \delta_{ij} Y_{ii}^{(\ell)}$. The Lagrangian $\mathcal{L}_Y^{\text{quarks}}$ will be discussed in sect. 1.1.4.

In the Standard Model, the electroweak symmetry is broken down to the electromagnetic gauge symmetry $U(1)_{\text{em}}$ by the Higgs mechanism. In its minimal formulation it requires a single Higgs field which is a doublet under $SU(2)$. The fermion masses arise from gauge-invariant Yukawa interactions of the fermion and Higgs fields by means of the spontaneous symmetry breaking mechanism as explained below.

1.1.3 Higgs sector

The Standard Model predicts an existence of the field with non-zero vacuum expectation value (VEV). Such feature of this field leads to the electroweak symmetry breaking [13, 14, 15, 16]. The Higgs sector of the Standard Model is described by the Lagrangian:

$$\mathcal{L}_H = (D_\mu \phi)^\dagger (D^\mu \phi) - V(\phi), \tag{1.25}$$

where the $SU(2)_L$ doublet of the complex Higgs fields ϕ with $Y = 1$ is introduced:

$$\phi(x) = \begin{pmatrix} \phi^+(x) \\ \phi^0(x) \end{pmatrix}, \tag{1.26}$$

and covariant derivative D_μ is defined as:

$$D_\mu = \partial_\mu - ig \frac{\sigma^a W_\mu^a}{2} + \, i \frac{g'}{2} B_\mu. \tag{1.27}$$

The Higgs potential $V(\phi)$ is given by the expression:

$$V(\phi) = -\mu^2 \phi^\dagger \phi + \frac{\lambda}{4} (\phi^\dagger \phi)^2, \qquad \mu^2 > 0, \, \lambda > 0. \tag{1.28}$$

Minimisation of the potential (1.28) leads to the minimum $\phi_0^\dagger \phi_0 = 2\mu^2/\lambda$. The minimal value of the Higgs field doublet can be chosen in the form

$$\phi_0 \equiv \langle \phi \rangle = \frac{1}{\sqrt{2}} \begin{pmatrix} 0 \\ v \end{pmatrix}, \tag{1.29}$$

with $v = 2\mu/\sqrt{\lambda}$ being the vacuum expectation value (VEV). In general case, the doublet of complex Higgs fields ϕ has four independent components. Three of them can be eliminated by a suitable gauge transformation allowing to present the Higgs doublet in the following form (the unitary gauge):

$$\phi(x) = \frac{1}{\sqrt{2}} \begin{pmatrix} 0 \\ v + h(x) \end{pmatrix}, \tag{1.30}$$

where real field $h(x)$ describes the physical Higgs boson. For completiness, we also quote a definition of the charge conjugate Higgs field $\tilde{\phi}$ in the unitary gauge:

$$\tilde{\phi}(x) \equiv i\sigma_2 \phi(x) = \frac{1}{\sqrt{2}} \begin{pmatrix} v + h(x) \\ 0 \end{pmatrix}. \tag{1.31}$$

Implementation of the Higgs doublet in the form (1.30) to the Lagrangian (1.25) yields the mass terms of the $W^\pm$ and Z bosons and the mass of the Higgs boson $m_h = \sqrt{2}\mu$. Note, that the photon appears to be massless as it must be. Additionally, one obtains the trilinear and quadrilinear vertices of the interactions of the Higgs with the W and Z bosons and the self-interactions of the Higgs field including the triple and quartic vertices.

1.1.4 The Cabibbo-Kobayashi-Maskawa quark-mixing matrix

The quark mixing is induced by the Yukawa interaction of the quark and Higgs fields. This interaction is described by the Lagrangian

$$\mathcal{L}_Y^{\text{quarks}} = -Y_{ij}^{(d)} (\bar{Q}_L^i \phi)\, d_R^j - Y_{ij}^{(u)} (\bar{Q}_L^i \tilde{\phi})\, u_R^j + \text{h.c.}, \tag{1.32}$$

where $Q_L^i = (u_L^i,\, d_L^i)^T$, $i = 1, 2, 3$ is the $SU(2)$-left-handed doublet of the quark fields ($u^i = u, c, t$ and $d^i = d, s, b$), u_R^j and d_R^j are the up- and down-type quark singlets, and the Higgs fields doublet ϕ and $\tilde{\phi}$ are defined in eqs. (1.26) and (1.31). $Y^{(u,d)}$ are the complex 3×3 matrices of the Yukawa couplings. The mass terms are obtained from replacing $\phi(x)$ by its VEV, $\phi \to \langle \phi \rangle$ according to (1.29) that yields:

$$\mathcal{L}_Y^{\text{quarks}} \to \mathcal{L}_Y^{\text{quarks}} = -\frac{v}{\sqrt{2}} Y_{ij}^{(d)} \bar{d}_L^i\, d_R^j - \frac{v}{\sqrt{2}} Y_{ij}^{(u)} \bar{u}_L^i\, u_R^j + \text{h.c.}. \tag{1.33}$$

(the same is valid for leptons, see (1.24)). The bilinear quark fields terms in (1.33) can be diagonalized with the help of four unitary 3×3 matrices $V_{L,R}^{u,d}$ yielding the mass eigenstates

$$[\tilde{u}_{L,R}]^i = [V_{L,R}^u]^{ij}\, [u_{L,R}]^j, \qquad [\tilde{d}_{L,R}]^i = [V_{L,R}^d]^{ij}\, [d_{L,R}]^j, \tag{1.34}$$

and the diagonal mass matrices

$$M_q = \frac{v}{\sqrt{2}} V_L^q \, Y^{(q)} \, V_R^{q\dagger}, \qquad q = u, d. \tag{1.35}$$

Introducing the quark mass eigenstates (1.34) does not change the diagonal terms in the Lagrangian, i.e. the kinetic terms and the interactions terms with the neutral bosons (1.18), (1.20) due to the unitarity of the transformations. The only modification appears in the interaction of the charged W-boson with the quark fields (1.19) yielding a product of the unitary matrices

$$V_L^u V_L^{d\dagger} \equiv V_{\rm CKM} = \begin{pmatrix} V_{ud} & V_{us} & V_{ub} \\ V_{cd} & V_{cs} & V_{cb} \\ V_{td} & V_{ts} & V_{tb} \end{pmatrix}, \tag{1.36}$$

which is called the Cabibbo-Kobayashi-Maskawa (CKM) quark-mixing matrix. Finally, the Lagrangian of the interaction of the quark mass eigenstates with W-boson can be presented as follows (the tildes over quark fields are omitted):

$$\mathcal{L}_{Wq} = \frac{g}{\sqrt{2}} (\bar{u}_L, \bar{c}_L, \bar{t}_L) \gamma^\mu V_{\rm CKM} \begin{pmatrix} d_L \\ s_L \\ b_L \end{pmatrix} W_\mu^\dagger + \text{h.c.}. \tag{1.37}$$

As one can see, the Lagrangian (1.37) allows for flavour-changing transition not only between quarks of the same generation but also for transition between different generations, e.g. $b \to u$. This is a very important feature of the weak interactions allowing b-quark to decay to lower mass quarks u, d, s, c and leading to a plenty of possible decays of B mesons containing one b quark. The CKM matrix (1.36) is a complex 3×3 unitary matrix and was originally introduced in [17, 18]. It can be parametrised in terms of three mixing-angles $\theta_{12}, \theta_{13}, \theta_{23}$ and one CP-violating phase δ [20]:

$$V_{\rm CKM} = \begin{pmatrix} c_{12}\, c_{13} & s_{12}\, c_{13} & s_{13}\, e^{-i\delta} \\ -s_{12}\, c_{23} - c_{12}\, s_{23}\, s_{13}\, e^{i\delta} & c_{12}\, c_{23} - s_{12}\, s_{23}\, s_{13}\, e^{\imath\delta} & s_{23}\, c_{13} \\ s_{12}\, s_{23} - c_{12}\, c_{23}\, s_{13}\, e^{i\delta} & -c_{12}\, s_{23} - s_{12}\, c_{23}\, s_{13}\, e^{i\delta} & c_{23}\, c_{13} \end{pmatrix}, \tag{1.38}$$

where $s_{ij} = \sin\theta_{ij}$, $c_{ij} = \cos\theta_{ij}$. The angels can be chosen to lie in the first quadrant.

From experiment it was found that $s_{13} \ll s_{23} \ll s_{12} \ll 1$. To exhibit this hierarchy it was found convenient to represent the CKM matrix in the terms of the 4 parameters A, λ, ρ, η defined as [19]:

$$s_{12} = \lambda = \frac{|V_{us}|}{\sqrt{|V_{ud}|^2 + |V_{us}|^2}}, \tag{1.39}$$

$$s_{23} = A\lambda^2 = \lambda \frac{|V_{cb}|}{|V_{us}|}, \tag{1.40}$$

$$s_{13} e^{i\delta} = V_{ub}^* = A\lambda^3(\rho + i\eta). \tag{1.41}$$

λ is a small parameters, and to order λ^4 the CKM matrix takes the form:

$$V_{\rm CKM} = \begin{pmatrix} 1-\lambda^2/2 & \lambda & A\lambda^3(\rho - i\eta) \\ -\lambda & 1-\lambda^2/2 & A\lambda^2 \\ A\lambda^3(1-\rho-i\eta) & -A\lambda^2 & 1 \end{pmatrix} + \mathcal{O}(\lambda^4). \tag{1.42}$$

Additionally, one defines $\bar{\rho} + i\bar{\eta} = -(V_{ud}V_{ub}^*)/(V_{cd}V_{cb}^*)$, where parameters $\bar{\rho}$ and $\bar{\eta}$ are related with ρ and η as:

$$\bar{\rho} = \rho\left(1 - \frac{\lambda^2}{2} + \mathcal{O}(\lambda^4)\right), \tag{1.43}$$

$$\bar{\eta} = \eta\left(1 - \frac{\lambda^2}{2} + \mathcal{O}(\lambda^4)\right). \tag{1.44}$$

The unitarity of the CKM matrix implies ($V\,V^\dagger = V^\dagger\,V = I$):

$$\sum_k V_{ik}\,V_{jk}^* = \delta_{ij} \quad \text{and} \quad \sum_k V_{kj}\,V_{ki}^* = \delta_{ij}, \tag{1.45}$$

yielding in particular the commonly used constraint (applied in the thesis, see chapter 2):

$$V_{ud}V_{ub}^* + V_{cd}V_{cb}^* + V_{td}V_{td}^* = 0. \tag{1.46}$$

The values of the CKM matrix elements V_{ij} can be extracted from the experimental data on the relevant decays. The review of the ways of the CKM matrix elements determination as well as global fit of CKM parameters is given in, e.g. [1]. In the context of the thesis, we suggested a new way of the CKM parameters determination based on observables in $B \to K\ell^+\ell^-$ and $B \to \pi\ell^+\ell^-$ decays (see Chapter 4).

1.1.5 Quantum chromodynamics

Quantum chromodynamics (QCD) is the gauge theory of strong interaction based on the symmetry group $SU(3)_C$. The basic fermions are quarks in three different color states forming the fundamental representations of $SU(3)_C$ group. They are described by triplets of quark fields $q = q_i\,(i = 1, 2, 3)$ for each quark flavour $q = u, d, s, c, b, t$. The Lagrangian of QCD can be presented in a compact form:

$$\mathcal{L}_{QCD} = -\frac{1}{4}G_{\mu\nu}^a G^{a\,\mu\nu} + \sum_{q=u,d,s\ldots} \bar{q}(i\not{D} - m_q)q, \tag{1.47}$$

where $G_{\mu\nu}^a\,(a = 1, \ldots 8)$ is the gluon field strength tensor:

$$G_{\mu\nu}^a = \partial_\mu A_\nu^a - \partial_\nu A_\mu^a + g_s f_{abc} A_\mu^b A_\nu^c, \tag{1.48}$$

$A_\mu^a\,(a = 1, \ldots 8)$ denotes the gluon field, f_{abc} are the $SU(3)$ structure constants, and g_s is the $SU(3)_C$ gauge (strong) coupling. The covariant derivative D_μ in (1.47) is defined as:

$$D_\mu = \partial_\mu - ig_s G_\mu^a \frac{\lambda^a}{2}, \tag{1.49}$$

where λ^a denotes the Gell-Mann matrices related with the $SU(3)$ generators $T^a = \lambda^a/2$.

Non-abelian nature of the symmetry group $SU(3)$ causes non-trivial quark-gluon dynamics including (in addition to the analogous in QED quark-gluon vertex) also the triple and quartic gluon self interactions as one can see from (1.47) and (1.48). Moreover, the non-abelian feature of the $SU(3)$ group leads to another nontrivial property related with the dependence of the strong coupling constant $\alpha_s = g_s^2/(4\pi)$ on energy scale, which completely differs from the analogous one in QED. As it was found first in [23, 24], at small distances, the self-coupling of gluons leads to anti-screening effects, resulting in a weakening of the coupling constant α_s. This is referred to as **asymptotic freedom**. Therefore, at small distances quarks are quasi-free and can be teated in nonperturbative way. On the other hand, the coupling constant α_s increases for large distances. This leads to the so-called **confinement** of quarks in hadrons. Due to this effect, the energy needed to separate two quarks at large distances becomes so large, that it exceeds the threshold for the creation of new quark-antiquark pairs, which then again form colourless states with the original quarks. This process is also referred to as **hadronisation**.

The properties of the strong interactions described above make theoretical analysis of the hadrons very complicated. In the practical calculation of processes with hadrons one deals with the matrix elements of the quark currents sandwiched between hadronic states. These hadronic matrix elements formally account for all possible quarks-gluon interaction dynamics inside the hadrons and therefore they could not be treated in the perturbative way. To this end, one has to develop methods allowing to evaluate interaction amplitudes beyond the ordinary QCD perturbation theory. In recent decades, several nonperturbative methods were developed providing a way to extract the hadronic input. This issue is a subject of discussion in subsequent chapters.

1.2 B mesons and their decays

The main object of research in this thesis are the flavour changing processes $b \to q$ observed as decays of B mesons. B mesons are the bound states of light u, d or s quark and heavy b quark. The latter decays to the lighter c, s, d, u-quarks. Analysis of the B-meson decays provides the most powerful test of the SM in the flavour sector. In particular, one uses these decays for an accurate determination of the elements of CKM matrix. Additionally, it is crucial for search of possible New Physics. A list pseudoscalar and vector B-mesons with some of their properties is given in Table 1.2.

Since B mesons contain unstable b-quark, they are not present in the matter surrounding us, and therefore they have to be produced at large energies at particle colliders. In order to measure various decay observables as precisely as possible one needs to produce a huge number of B-mesons. There are two main ways to achieve this goal. First, B mesons are produced at hadron colliders like the Tevatron at Fermilab in proton-antiproton ($p\bar{p}$) collision and the Large Hadron Collider (LHC) at CERN in proton-proton (pp) collisions. These colliders were not specially designed for a creation of B-mesons, but in inelastic proton-proton collisions, high-energy gluons can collide and produce a pair of b-quarks which then hadronise in B-hadrons (mesons or baryons) accompanied by a large number of other charged and neutral particles. The total $b\bar{b}$ cross-section measured by the

B-meson	quark content	J^P	mass (MeV)	mean life (10^{-12} s)
B^-, B^+	$\bar{u}b$, $u\bar{b}$	0^-	5279.31 ± 0.15	1.638 ± 0.004
$\bar{B}^0$, B^0	$\bar{d}b$, $d\bar{b}$	0^-	5279.62 ± 0.15	1.520 ± 0.004
$\bar{B}^*$, B^*	$\bar{d}b$, $d\bar{b}$	1^-	5324.65 ± 0.25	
$\bar{B}^0_s$, B^0_s	$\bar{s}b$, $s\bar{b}$	0^-	5366.82 ± 0.22	1.510 ± 0.005
B^-_c, B^+_c	$\bar{c}b$, $c\bar{b}$	0^-	6275.1 ± 1.0	0.507 ± 0.009

Table 1.2: A list of the most well studied B-mesons with their quantum numbers, masses and mean lifes [1]

LHCb collaboration on a specially designed detector optimised for the measurements of B-hadrons [27]

$$\sigma(pp \to b\bar{b}X) = (284 \pm 20 \pm 49)\,\mu\text{b}, \qquad \sqrt{s} = 7\,\text{TeV}$$

yields at the accumulated integrated luminosity $\int \mathcal{L}\,dt = 3\,\text{fb}^{-1}$ about 10^{11} $\bar{b}b$ pairs.

Another way to create B-mesons is a collision of electron and positron beams at the fixed center-mass energy of 10.579 GeV corresponding to the production of $\Upsilon(4S)$-states decaying at $> 96\%$ cases [1] to $B\bar{B}$-pairs. Such a mechanism of B-meson production is realised at so-called B-factories (for instance, electron-positron PEP accelerator with the BaBar detector at SLAC collaboration and electron-positron KEK accelerator at Belle). The $\bar{b}b$ production at such B-factories is lower than at proton-proton colliders but does not suffer much from background effects.

The heaviness of the b-quark belonging to the third generation allows for a plenty of various possible B-meson decay channels. The full list of the measured B-meson decay modes together with the values of the branching fractions and CP-asymmetries is provided by Particle Data Group [1]. The possible B-meson decay modes can be classified according to their final states. There are three large classes:

- **Leptonic decays.**

  These decays have only leptons in the final state. The examples are $B \to \tau\nu_\tau$, $B_s \to \mu^+\mu^-$. Such decays are easier for the theoretical analysis since they have a simplest hadronic structure involving only one nonperturbative parameter — B-meson decay constant f_B, which parametrises the matrix element of the axial-vector quark current sandwiched between vacuum and B-meson state,

  $$\langle 0|\bar{q}(0)\gamma_\mu\gamma_5 b(0)|B_q(p)\rangle = i\,f_{B_q}\,p_\mu, \tag{1.50}$$

  where $q = u, d, s$ or c. Let us consider as an example leptonic $B^+ \to \tau^+\nu_\tau$ decay. This processes is described by single Feynman diagram shown at Fig. 1.1. The branching fraction of $B^+ \to \tau^+\nu_\tau$ decay has quite a simple form

  $$\text{Br}(B^+ \to \tau^+\nu_\tau) = \frac{G_F^2 f_B^2 |V_{ub}|^2}{8\pi} m_B m_\tau^2 \left(1 - \frac{m_\tau^2}{m_B^2}\right)^2 \tau_B, \tag{1.51}$$

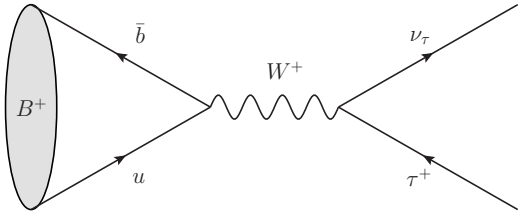

Figure 1.1: Feynman diagram of the leptonic $B^+ \to \tau^+\nu_\tau$ decay

and is proportional to the squared product of CKM matrix element V_{ub} and decay constant f_B. The latter one is a nonperturbative quantity to be extracted using some nonperturbative method (QCD sum rules, Lattice QCD, etc) or from experimental data if one fixes V_{ub}, say, from the global CKM fit.

- **Semileptonic decays.**

  These decays have both leptons and hadrons in the final state. The hadronic structure of the semileptonic decays is more complicated since one needs to deal with the hadrons both in the initial and final states. The nonperturbative physics for exclusive channels (e.g. $B^- \to \pi^0\mu^-\bar{\nu}_\mu$) is described in terms of form factors parametrising the matrix element of the quark current between initial and final hadronic states. In the inclusive semileptonic decays, e.g. $B^- \to X_c\tau^-\bar{\nu}_\tau$, [1] one deals with the nonperturbative parameters arising in the heavy-quark expansion of the forward matrix element of the quark currents. Since the analysis of the B-meson semileptonic decays is an object of study in this thesis, these issues will be discussed in more details in a subsequent chapters.

- **Non-leptonic decays.**

  These decays have only hadrons in the final states. Some examples are $B \to D\pi$, $B \to \pi\pi\pi$ decays. Nonleptonic decays are the most complicated ones due to purely hadronic amplitudes. They as a rule can be treated only by making additional assumptions that allow then for a factorization of the underlying matrix element. A detailed overview of these decays and relevant calculation methods goes beyond the scope of this thesis.

Semileptonic B-meson decays can be arranged in two large classes depending on the type of flavour changing transition:

- **Flavour changing charged current $b \to u, c$.**

  These processes proceed at tree level via W-boson exchange. The $b \to p\ell\nu$ $(p = u, c)$ transition is described by the following effective Hamiltonian:

$$\mathcal{H}_{\text{eff}}^{b\to p\ell\nu} = -\frac{4G_F V_{pb}}{\sqrt{2}}(\bar{p}_L\gamma_\mu b_L)(\bar{\ell}_L\gamma^\mu\nu_L) + \text{h.c.}, \qquad p = u,\, c \tag{1.52}$$

[1] there a summation over all hadronic states X_c is assumed with X_c being any single- or multi-hadron state containing a c-quark

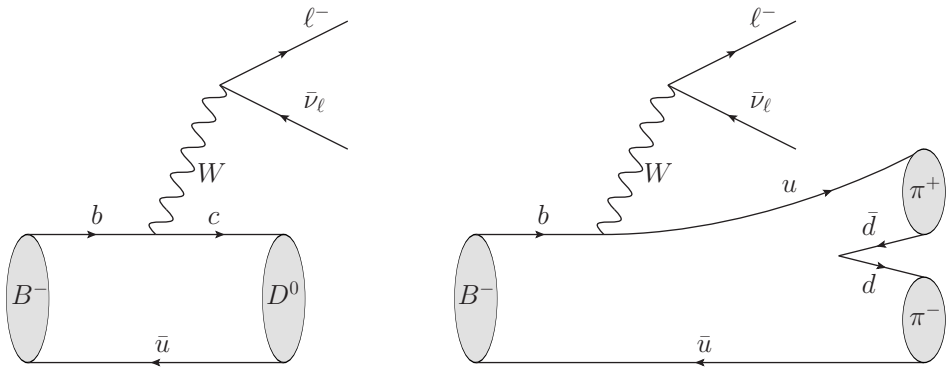

Figure 1.2: Diagrams of the semileptonic $B^- \to D^0 \ell^- \bar{\nu}_\ell$ and $B^- \to \pi^- \pi^+ \ell^- \bar{\nu}_\ell$ decays as examples of the processes induced by flavour-changing charged quark currents $b \to u, c$

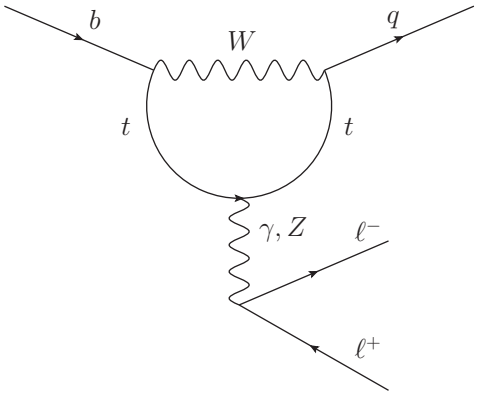

Figure 1.3: Penguin diagram describing FCNC $b \to q\ell^+\ell^-$ transition with $q = d, s$ in the SM

which is easily derived from the Standard Model Lagrangian (see eqs. (1.19) and (1.37)) by integrating out the heavy W-boson provided that the typical momentum transfer of the decay is of order $\sim m_b \ll m_W$. In (1.52) G_F denotes the effective four-fermion interaction coupling – Fermi constant, which is related with weak gauge coupling g as:

$$\frac{G_F}{\sqrt{2}} = \frac{g^2}{8m_W^2}. \tag{1.53}$$

The underlying $b \to p\ell\nu$ process is observed in the form of the exclusive or inclusive $B \to X_p \ell \bar{\nu}$ decays. Some examples of the corresponding diagrams are shown in Fig. 1.2.

- **Flavour changing neutral current (FCNC) $b \to d, s$.**

  As one can see from (1.37), the FCNC transitions are forbidden at tree level in the SM. Nevertheless, they can be induced via loops. One example of the diagram describing $b \to q\ell^+\ell^-$ $(q = d, s)$ transition is given in Fig. 1.3 (so-called penguin

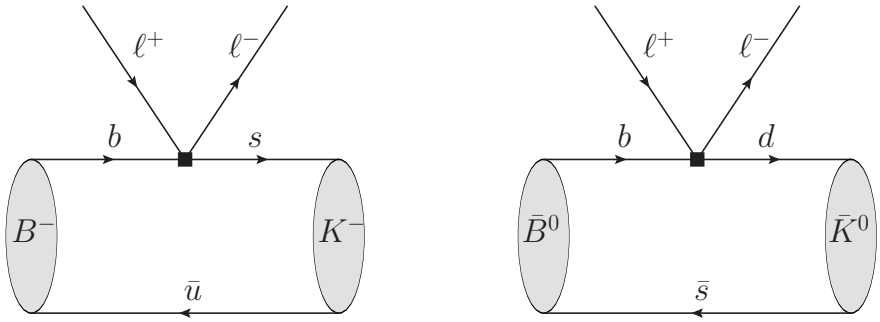

Figure 1.4: Diagrams of the semileptonic $B^- \to K^-\ell^+\ell^-$ and $\bar{B}_s^0 \to \bar{K}^0\ell^+\ell^-$ decays as examples of the processes induced by FCNC $b \to s, d$. The black squares denote the effective $b \to d, s$ vertices.

diagram). The full set of the diagrams describing the FCNC $b \to d$ transition in the SM can be found in [21]. At these diagrams, the heavy particles like W and Z bosons and t quark with masses larger then the factorization scale $\mu \sim m_b$ are integrated out. Their contributions are absorbed in the short-distance Wilson coefficients $C_i(\mu)$. Integrating out the heavy degrees of freedom yields also the local dimension-six effective operators $\mathcal{O}_i$. This leads to the following effective Hamiltonian describing FCNC transition $b \to q\ell^+\ell^-$ $(q = d, s)$ [21]

$$\mathcal{H}_{\text{eff}}^{b\to q\ell^+\ell^-} = \frac{4G_F}{\sqrt{2}} \left(\lambda_u^{(q)} \sum_{i=1}^{2} C_i\, \mathcal{O}_i^u + \lambda_c^{(q)} \sum_{i=1}^{2} C_i\, \mathcal{O}_i^c - \lambda_t^{(q)} \sum_{i=3}^{10} C_i\, \mathcal{O}_i \right) + \text{h.c.} \quad (1.54)$$

where $\lambda_p^{(q)} = V_{pb}V_{pq}^*$, $(p = u, c, t)$ are the products of CKM matrix elements, satisfying the unitary relation (1.46). The list of the effective operators $\mathcal{O}_i$ and the values of Wilson coefficients C_i at different scales are given in the Appendix A of the Chapter 2, see also sect. 4.3.

The underlying $b \to q\ell^+\ell^-$ process is observed in the form of the exclusive or inclusive $B \to X_q\ell^+\ell^-$ decays. Some examples of the corresponding diagrams are shown in Fig. 1.4.

1.3 Hadronic input in semileptonic B-meson decays

In order to predict the decay rates and other observables in the semileptonic B-meson decays one needs to specify the relevant hadronic input which appears in the amplitudes of the considered processes. The hadronic input relevant for the semileptonic B-meson decays considered in the thesis includes the following:

- **Heavy-to-light transition form factors.**

In the calculation of the differential decay rate of the exclusive semileptonic $B \to P\ell^+\ell^-$ processes, where B denotes pseudoscalar $B^\pm, B_d^0$ or B_s^0 meson and $P = \pi, K$ is pseudoscalar light meson, one encounters the matrix elements of the flavour-changing

current sandwiched between the final P-meson and initial B-meson states. This matrix element is a purely nonperturbative object accounting for long-distance dynamics of quark-gluon interaction in the meson-to-meson transition. In this case, one applies a general Lorenz decomposition of the matrix element and parametrises it in terms of the scalar functions of momentum transfer squared q^2. For the matrix element of the vector $b \to q\,(q = u, d, s)$ quark current in case of pseudoscalar-to-pseudoscalar meson transition the following standard convention is used [2]:

$$\begin{aligned}\langle P(p)|\bar{q}\gamma^\mu b|B(p+q)\rangle &= f_{BP}^{+}(q^2)\left[2p^\mu + \left(1 - \frac{m_B^2 - m_P^2}{q^2}\right)q^\mu\right] \\ &+ f_{BP}^{0}(q^2)\,\frac{m_B^2 - m_P^2}{q^2}\,q^\mu, \end{aligned} \tag{1.55}$$

where $f_{BP}^{+}(q^2)$ and $f_{BP}^{0}(q^2)$ are the $B \to P$ transition **vector** and **scalar form factors**. This is the only hadronic input needed for the calculation of the semileptonic exclusive $B \to P\ell\nu_\ell$ decay. In the analysis of the FCNC exclusive semileptonic processes one encounters an additional matrix elements of the tensor quark current. This matrix element for pseudoscalar-to-pseudoscalar meson transition is parametrised as

$$\langle P(p)|\bar{q}\sigma^{\mu\nu}q_\nu b|B(p+q)\rangle = \frac{i f_{BP}^{T}(q^2)}{m_B + m_P}\left[2q^2 p^\mu + \left(q^2 - \left(m_B^2 - m_P^2\right)\right)q^\mu\right], \tag{1.56}$$

introducing a new $B \to P$ transition **tensor form factor** $f_{BP}^{T}(q^2)$. Note that all matrix elements specified above are *local*: the $q \equiv q(0)$ and $b \equiv b(0)$ quark field operators are defined at the same point in the coordinate space (for convenience at $x = 0$). The $B \to P$ form factors are nonperturbative quantities which can be calculated using some nonperturbative method. In the context of this thesis we exploit the light-cone sum rule (LCSR) to predict these form factors at large recoil of P meson or, equivalently, in the region of small values of q^2.

- **The nonlocal hadronic amplitudes.**

The amplitude of the FCNC exclusive $B \to P\ell^-\ell^+$ decay contains an additional hadronic input apart from the standard form factors. This input includes the hadronic effects generated by the dimension-6 effective operators combined with the electromagnetic emission of the lepton pair. They can be represented as a correlation function of the time-ordered product of effective operators with the quark electromagnetic current, $j_\mu^{\rm em}(x) = \sum_{q=u,d,s,c,b} Q_q \bar{q}(x)\gamma_\mu q(x)$, sandwiched between B- and P-meson states:

$$\begin{aligned}\mathcal{H}_{(BP)\mu}^{(p)} &= i\int d^4x\, e^{iqx}\langle P(p)|\mathrm{T}\big\{j_\mu^{\rm em}(x), \big[C_1\mathcal{O}_1^p(0) + C_2\mathcal{O}_2^p(0) \\ &+ \sum_{k=3-6,8g} C_k\mathcal{O}_k(0)\big]\big\}|B(p+q)\rangle = \big[(p\cdot q)q_\mu - q^2 p_\mu\big]\,\mathcal{H}_{BP}^{(p)}(q^2), \qquad (p = u, c). \end{aligned} \tag{1.57}$$

which are described in terms of additional Lorentz invariant amplitudes denoted as $\mathcal{H}_{BP}^{(c)}(q^2)$ and $\mathcal{H}_{BP}^{(u)}(q^2)$ and called **nonlocal hadronic amplitudes**. Contracting the

[2] Note that parametrisation of the matrix element depends on the quantum numbers J^P of the initial and final states. We consider mostly pseudoscalar ($J^P = 0^-$) to pseudoscalar ($J^P = 0^-$) transitions

quark fields in (1.57) under the time-ordered product yields different contribution described by diagrams demonstrated in Chapter 2. These nonlocal amplitudes are calculated using LCSR and QCD factorization (QCDF) methods as well as general quark-hadron duality approach.

- **Nonperturbative parameters in heavy-quark expansion**

The decay width of the inclusive semileptonic $B \to X_c \tau \nu_\tau$ decay can be expressed by means of the optical theorem through the discontinuity of the time-product of the correlation function of quark currents. Applying the heavy-quark expansion for this correlator yields a set of the basic nonperturbative parameters (up to order $\Lambda^3_{\rm QCD}/m_b^3$):

$$
\begin{aligned}
2m_B\,\mu_\pi^2 &= -\langle B(p)|\bar b_v (iD)^2 b_v|B(p)\rangle, && (1.58)\\
2m_B\,\mu_G^2 &= \langle B(p)|\bar b_v (iD_\mu)(iD_\nu)(-i\sigma^{\mu\nu}) b_v|B(p)\rangle, && (1.59)\\
2m_B\,\rho_D^3 &= \langle B(p)|\bar b_v (iD_\mu)(iv\cdot D)(iD^\mu) b_v|B(p)\rangle, && (1.60)\\
2m_B\,\rho_{LS}^3 &= \langle B(p)|\bar b_v (iD_\mu)(iv\cdot D)(iD_\nu)(-i\sigma^{\mu\nu}) b_v|B(p)\rangle, && (1.61)
\end{aligned}
$$

where v denotes the four-velocity of the decaying B meson, D_μ is the covariant derivative, $\sigma^{\mu\nu} = (i/2)[\gamma^\mu, \gamma^\nu]$, b_v denotes a phase redefined b-quark field (see (1.65)), μ_π^2 and μ_G^2 are the **kinetic** and **chromomagnetic terms**, and ρ_D^3 and ρ_{LS}^3 are the **Darwin** and **spin-orbit terms**. As a rule, the values of these parameters are extracted from the experimental data on the observables in inclusive $B \to X_c \ell \bar\nu_\ell$ decays with light leptons $\ell = e$ or μ, see Chapter 5.

1.4 Methods

Here we briefly outline the three main calculational methods used in the thesis to obtain the hadronic input. All these methods are based on QCD.

1.4.1 Light-cone sum rules

The method of QCD sum rules was developed originally by Shifman, Vainshtein and Zakharov (SVZ) in [29, 30]. The detailed overview of the QCD sum rule method including in particular the light-cone sum rules (LCSR) is given e.g., in [31]. The LCSR method was developed based on a combination of the SVZ-technique and the theory of hard exclusive processes [32, 33], see also [34, 35]. The starting point of LCSR is a construction of a "proper" correlation function which is connected with the object of calculation, e.g. form factor, via hadronic dispersion relation and quark-hadron duality. This correlation function contains a time-ordered product of two or more currents including the interpolating current(s) of the particle(s) and transition operator. Then one needs to determine a kinematic domain where the integrand in the correlation function becomes dominant near the light-cone $x^2 = 0$. In this kinematic domain one applies the light-cone operator product expansion (LC OPE) presenting the correlation function in the form of the convolution of the hard-scattering kernels with the relevant light-cone distribution amplitudes (DAs). The OPE result for the correlation function represents an expansion in different parameters: in strong coupling α_s, in twists and multiplicities

(e.g. quark-antiquark, quark-antiquark-gluon, etc.) of the DAs. After OPE one needs to write down a dispersion relation in external momentum in order to connect the OPE result with the hadronic matrix element. In the dispersion relation one isolates the ground state contribution from the contribution of the excited and multi-hadron states with the same quantum numbers. The OPE for correlation function is presented as a rule in the form of the dispersion integral of a spectral density. The hadronic spectral density of the excited states is approximated by imaginary part of the OPE result in the same variable with help of the quark-hadron duality. Such approximation leads to introducing an additional parameter – so-called continuum threshold. Its value is chosen to equalize the integral over the spectral density and the dispersion OPE integral. Finally, one applies the Borel transformation in the external momentum introducing new Borel parameter. This transformation eliminates all polynomial divergences and also leads to an exponential suppression of the contribution of the excited states. The value of the continuum threshold is fixed by calculation of the mass of lowest hadron from differentiated sum rule. A description of the LCSR method applied to the $B \to P$ form factors is given in Appendix A of Chapter 4.

1.4.2 QCD factorization

A detailed discussion of the QCD factorization (QCDF) approach can be found in [36, 37, 38]. This approach is most popular in the theoretical analysis of the nonleptonic heavy hadron decays. The QCDF formalism allows one to compute systematically the matrix elements of the effective operators in the heavy-quark limit $m_b \gg \Lambda_{\rm QCD}$, when the mass of the b-quark is much larger that the typical hadronic scale $\Lambda_{\rm QCD}$. This limit leads to some important simplifications. Let us consider as an example the non-leptonic exclusive decay $B \to M_1 M_2$ with two light mesons M_1 and M_2 in the final state. The corresponding matrix element can be presented in the form [36]

$$\langle M_1 M_2|Q|B\rangle = \langle M_1|j_1|B\rangle\langle M_2|j_2|0\rangle \times \Big[1 + \sum r_n \alpha_s^n + \mathcal{O}(\Lambda_{\rm QCD}/m_b)\Big] \qquad (1.62)$$

where $Q = j_1 \times j_2$ is one of the effective dimension-six local operators in the effective Hamiltonian. In the heavy-quark limit neglecting any perturbative corrections $\mathcal{O}(\alpha_s)$ one gets a naive factorization of the matrix element as a product of the form factor and decay constant. This approximation is improved within the hard-scattering approach based on assumption of hard-gluon exchange dominance [37]. Within this assumption in the heavy-quark limit the matrix element of the dimension-6 effective operator Q_i for the $B \to M_1 M_2$ decay can be presented in the form [37, 39]

$$\begin{aligned} \langle M_1 M_2|Q_i|B\rangle &= \sum_j F_j^{B\to M_1}(m_2^2) \int_0^1 du\, T_{ij}^I(u) f_{M_2} \Phi_{M_2} + (M_1 \leftrightarrow M_2) \qquad (1.63) \\ &+ \int_0^1 ds\, du\, dv\, T_i^{II}(s,u,v) f_B \Phi_B(s) f_{M_1} \Phi_{M_1}(u) f_{M_2} \Phi_{M_2}(v) \end{aligned}$$

where $F^{B\to M_1}$ is a corresponding $B \to M_1$ form factor, f_B, f_{M_1}, f_{M_2} are the decay constants of the heavy B and light M_1 and M_2 mesons, and $\Phi_B, \Phi_{M_1}, \Phi_{M_2}$ are the relevant

light-cone distributions amplitudes. Hard-scattering kernels T_{ij}^I and T_i^{II} are calculable quantities which can be presented in the form of the perturbative series in α_s, and the integration in (1.64) is performed over the light-cone momentum fractions of the constituent quarks inside the mesons. Note that in the heavy-quark limit the meson LCDA's are needed only at leading twist approximation [39].

The main advantage of the QCDF method as one can see from (1.64) is a reduction of the complicated hadronic matrix element of four-quark operators to more simple non-perturbative objects (form factors and LCDA's). This approximation works well for the B-meson decays where $m_b \gg \Lambda_{\rm QCD}$ is well justified.

As it was shown in [40], the QCDF approach allows also to compute non-factorizable corrections to exclusive $B \to V\ell^+\ell^-$ and $B \to V\gamma$ decays in the heavy quark mass limit. The same method has been used for the calculation of the rare radiative decays $B \to K^*\gamma$, $B \to \rho\gamma$ and $B \to \omega\gamma$, and the electroweak penguin decays $B \to K^*\ell^+\ell^-$ and $B \to \rho\ell^+\ell^-$ [41]. In the context of the thesis, QCDF is used for the calculation of some diagrams contributing to the nonlocal hadronic amplitudes at space-like region of q^2, see sect. III in Chapter 2.

1.4.3 Heavy quark expansion

The heavy quark expansion (HQE) is a useful tool for the calculation of inclusive heavy hadron decays. The first discussion of inclusive semileptonic decays in this framework has been given by [42], and was then developed in subsequent works [43, 44, 45].

To calculate the inclusive heavy-hadron decay within the HQE method one deals with the correlation function of the time-ordered product of the flavour-changing $Q \to q$ quark currents:

$$T_{\mu\nu} = \int d^4x\, e^{ix(q-m_Q v)} \langle H(P)|T\{\bar{Q}_v(x)\gamma_\mu(1-\gamma_5)q(x), \bar{q}(0)\gamma_\nu(1-\gamma_5)Q_v(0)|H(P)\rangle, \quad (1.64)$$

where H denotes a heavy meson with the four-momentum P and four-velocity v, and Q is a heavy quark. In (1.64), a phase redefinition of the heavy quark filed Q is performed as follows:

$$Q_v(x) = e^{im_Q\, v\cdot x} Q(x). \quad (1.65)$$

This allows one to reduce strong oscillations due to large fraction $m_Q v$ of the Q-quark momentum. Afterwards, one contracts the q-quark fields in (1.64) yielding the propagator of the q-quark moving in the background field of the soft gluon in the heavy H meson. After rescaling the Q-quark momentum $p_Q = m_Q\, v + k$, one expands the correlator (1.64) in powers of $k/m_Q \sim \Lambda_{\rm QCD}/m_Q$ obtaining the matrix elements

$$\langle H(P)|\bar{Q}_v(iD_{\mu_1})\dots(iD_{\mu_n})Q_v|H(P)\rangle. \quad (1.66)$$

These matrix elements are then reduced to the basic parameters up to certain order $1/m_Q^n$ with help of the procedure described in [46].

The resulting inclusive decay rate is related with the correlator (1.64):

$$d\Gamma \sim {\rm Im} T_{\mu\nu} L^{\mu\nu} d\Phi, \quad (1.67)$$

where $L^{\mu\nu}$ is a leptonic tensor and $d\Phi$ denotes the phase space element. Therefore, the decay rate and other observables acquire a form of the expansion in powers $\Lambda_{\rm QCD}/m_Q$ expressed in terms of short-distance coefficients and nonperturbative parameters (e.g. (1.58) – (1.61)). More details on this issue are presented in Chapter 5.

1.5 Observables in semileptonic B-meson decays

There is a set of the observables in the semileptonic B-meson decays which are of considerable interest from experimental point of view. The SM predictions for these quantities together with their measurements by experimental collaborations (for instance at LHCb or at B-factories) allow for a precision test of the SM and are also very helpful in search for possible New Physics, in case a sizeable deviation from the SM predictions is found. In the framework of this thesis, we consider the following set of observables relevant in exclusive $B \to P\ell\nu_\ell$, $B \to P\ell^+\ell^-$ and inclusive $B \to X_c\ell\nu_\ell$ decays:

- **Branching fraction**

  The branching fraction of the generic $B \to f$ decay channel is defined as:

  $$\mathcal{B}(B \to f) = \frac{\Gamma(B \to f)}{\Gamma_{\rm tot}(B)}, \tag{1.68}$$

  where $\Gamma_{\rm tot}(B) = 1/\tau_B$ is a total B-meson decay width, and τ_B is its mean life.

- **Binned in q^2 branching fraction**

  The q^2 binned branching fraction of the semileptonic B-meson decay is defined as the partially integrated branching fraction normalised to the bin width:

  $$\mathcal{B}(\bar{B} \to P\ell^+\ell^-[q_1^2, q_2^2]) \equiv \frac{1}{q_2^2 - q_1^2} \int\limits_{q_1^2}^{q_2^2} dq^2 \frac{dB(\bar{B} \to P\ell^+\ell^-)}{dq^2}. \tag{1.69}$$

  In this thesis, most of the decay rates were predicted at large hadronic recoil region due to the limitation of the LCSR method applicability: $q_1^2, q_2^2 \in [0 - 12]\,\text{GeV}^2$.

- ***CP*-averaged q^2-binned branching fraction**

  In the Particle Data Group review [1] most of the experimental values of the branching fractions are CP-averaged:

  $$\mathcal{B}_{BP}[q_1^2, q_2^2] \equiv \frac{1}{2}\Big(\mathcal{B}(\bar{B} \to P\ell^+\ell^-[q_1^2, q_2^2]) + \mathcal{B}(B \to \bar{P}\ell^+\ell^-[q_1^2, q_2^2])\Big). \tag{1.70}$$

- **Binned direct *CP*-asymmetry**

  One of the specific feature of the FCNC $b \to d$ processes is a non-vanishing CP-asymmetry (as it is explained in Chapter 2). To this end, one defines:

  $$\mathcal{A}_{CP}^{BP}[q_1^2, q_2^2] = \frac{\mathcal{B}(\bar{B} \to P\ell^+\ell^-[q_1^2, q_2^2]) - \mathcal{B}(B \to \bar{P}\ell^+\ell^-[q_1^2, q_2^2])}{\mathcal{B}(\bar{B} \to P\ell^+\ell^-[q_1^2, q_2^2]) + \mathcal{B}(B \to \bar{P}\ell^+\ell^-[q_1^2, q_2^2])}. \tag{1.71}$$

- **Binned isospin asymmetry**

  A difference in the patterns of diagrams contributing to the isospin related modes of FCNC $\bar{B}^0 \to P^0\ell^+\ell^-$ and $B^- \to \bar{P}^-\ell^+\ell^-$ produces non-trivial isospin asymmetry defined as follows:

$$\mathcal{A}_{\rm I}^{BP}[q_1^2, q_2^2] = \frac{\Gamma(\bar{B}^0 \to P^0\ell^+\ell^-[q_1^2, q_2^2]) - C_I\Gamma(B^- \to \bar{P}^-\ell^+\ell^-[q_1^2, q_2^2])}{\Gamma(\bar{B}^0 \to P^0\ell^+\ell^-[q_1^2, q_2^2]) + C_I\Gamma(B^- \to \bar{P}^-\ell^+\ell^-[q_1^2, q_2^2])}, \tag{1.72}$$

  where C_I is an isospin factor originating from the difference in the quark content of the charged and neutral final state mesons; for instance, in $B \to \pi\ell^+\ell^-$ decays $C_I = 1/2$ since $\pi^0 \sim 1/\sqrt{2}\,(d\bar{d} - u\bar{u})$.

- **Moments of lepton-energy distribution**

  In the inclusive semileptonic decays it is reasonable to consider the moments of the lepton-energy distribution defined as:

$$M_\ell^n \equiv \langle E_\ell^n \rangle_{E_\ell > E_{\rm cut}} = \frac{\int_{E_{\rm cut}}^{E_{\rm max}} dE_\ell\, E_\ell^n \dfrac{d\Gamma}{dE_\ell}}{\int_{E_{\rm cut}}^{E_{\rm max}} dE_\ell \dfrac{d\Gamma}{dE_\ell}} \tag{1.73}$$

  and also the relevant central ones:

$$\overline{M}_\ell^n \equiv \langle (E_\ell - \langle E_\ell \rangle)^n \rangle_{E_\ell > E_{\rm cut}}, \tag{1.74}$$

  with $E_{\rm cut}$ being a energy cut applied in the experiment to the final state lepton.

There is also another interesting observable – the forward-backward asymmetry – defined as

$$\mathcal{A}_{\mathcal{FB}}(q^2) = \frac{\displaystyle\int_1^0 d\cos\theta \frac{d\Gamma}{dq^2 d\cos\theta} - \int_0^{-1} d\cos\theta \frac{d\Gamma}{dq^2 d\cos\theta}}{\displaystyle\int_1^0 d\cos\theta \frac{d\Gamma}{dq^2 d\cos\theta} + \int_0^{-1} d\cos\theta \frac{d\Gamma}{dq^2 d\cos\theta}}. \tag{1.75}$$

In the SM, it was found that for pseudoscalar-to-pseudoscalar semileptonic exclusive B-meson decays with the massless leptons in the final state the forward-backward asymmetry vanishes due to absence of the linear terms in $\cos\theta$ in the double differential distributions.

1.6 References

[1] C. Patrignani *et al.* [Particle Data Group], *Review of Particle Physics*, Chin. Phys. C **40** (2016) no.10, 100001.

[2] M.E. Peskin and D.V. Schroeder, *An Introduction to quantum field theory*, Addison-Wesley, 1995.

[3] M.D. Schwartz, *Quantum Field Theory and the Standard Model*, Cambridge University Press, 2014.

[4] J.F. Donoghue, E. Golowich, B.R. Holstein, *Dynamics of the Standard Model*, Cambridge University Press, 1994.

[5] T. Muta, *Foundation of Quantum Chromodynamics: an Introduction to Perturbative Methods in Gauge Theories*, World Scientific Publishing Company, 1998.

[6] W. Hollik, *Quantum field theory and the Standard Model*, arXiv:1012.3883 [hep-ph].

[7] P.A.R. Ade *et al.* [Planck Collaboration], *Planck 2015 results. XIII. Cosmological parameters*, Astron. Astrophys. **594** (2016) A13, arXiv:1502.01589 [astro-ph.CO].

[8] G. Aad *et al.* [ATLAS Collaboration], *Observation of a new particle in the search for the Standard Model Higgs boson with the ATLAS detector at the LHC*, Phys. Lett. B **716** (2012) 1, arXiv:1207.7214 [hep-ex].

[9] S. Chatrchyan *et al.* [CMS Collaboration], *Observation of a new boson at a mass of 125 GeV with the CMS experiment at the LHC*, Phys. Lett. B **716** (2012) 30, arXiv:1207.7235 [hep-ex].

[10] S. L. Glashow, *Partial Symmetries of Weak Interactions*, Nucl. Phys. **22** (1961) 579.

[11] S. Weinberg, *A Model of Leptons*, Phys. Rev. Lett. **19** (1967) 1264.

[12] A. Salam, *Weak and Electromagnetic Interactions*, Conf. Proc. C **680519** (1968) 367.

[13] P. W. Higgs, *Spontaneous Symmetry Breakdown without Massless Bosons*, Phys. Rev. **145** (1966) 1156.

[14] P. W. Higgs, *Broken Symmetries and the Masses of Gauge Bosons*, Phys. Rev. Lett. **13** (1964) 508.

[15] P. W. Higgs, *Broken symmetries, massless particles and gauge fields*, Phys. Lett. **12** (1964) 132.

[16] F. Englert and R. Brout, *Broken Symmetry and the Mass of Gauge Vector Mesons*, Phys. Rev. Lett. **13** (1964) 321.

[17] N. Cabibbo, *Unitary Symmetry and Leptonic Decays*, Phys. Rev. Lett. **10** (1963) 531.

[18] M. Kobayashi and T. Maskawa, *CP Violation in the Renormalizable Theory of Weak Interaction*, Prog. Theor. Phys. **49** (1973) 652.

[19] L. Wolfenstein, *Parametrization of the Kobayashi-Maskawa Matrix*, Phys. Rev. Lett. **51** (1983) 1945.

[20] L. L. Chau and W. Y. Keung, *Comments on the Parametrization of the Kobayashi-Maskawa Matrix*, Phys. Rev. Lett. **53** (1984) 1802.

[21] G. Buchalla, A. J. Buras and M. E. Lautenbacher, *Weak decays beyond leading logarithms*, Rev. Mod. Phys. **68** (1996) 1125, hep-ph/9512380.

[22] D. J. Gross and F. Wilczek, *Ultraviolet Behavior of Nonabelian Gauge Theories*, Phys. Rev. Lett. **30** (1973) 1343.

[23] D. J. Gross and F. Wilczek, *Asymptotically Free Gauge Theories. 1*, Phys. Rev. D **8** (1973) 3633.

[24] H. D. Politzer, *Reliable Perturbative Results for Strong Interactions?*, Phys. Rev. Lett. **30** (1973) 1346.

[25] H. Fritzsch, M. Gell-Mann and H. Leutwyler, *Advantages of the Color Octet Gluon Picture*, Phys. Lett. **47B** (1973) 365.

[26] S. L. Glashow, J. Iliopoulos and L. Maiani, *Weak Interactions with Lepton-Hadron Symmetry*, Phys. Rev. D **2** (1970) 1285.

[27] R. Aaij *et al.* [LHCb Collaboration], *Measurement of* $\sigma(pp \to b\bar{b}X)$ *at* $\sqrt{s} = 7$ TeV *in the forward region*, Phys. Lett. B **694** (2010) 209, arXiv:1009.2731 [hep-ex].

[28] R. Aaij *et al.* [LHCb Collaboration], *Measurement of the b-quark production cross-section in 7 and 13 TeV pp collisions*, Phys. Rev. Lett. **118** (2017) no.5, 052002 Erratum: [Phys. Rev. Lett. **119** (2017) no.16, 169901], arXiv:1612.05140 [hep-ex].

[29] M. A. Shifman, A. I. Vainshtein and V. I. Zakharov, *QCD and Resonance Physics: Applications*, Nucl. Phys. B **147** (1979) 448.

[30] M. A. Shifman, A. I. Vainshtein and V. I. Zakharov, *QCD and Resonance Physics. Theoretical Foundations*, Nucl. Phys. B **147** (1979) 385.

[31] P. Colangelo and A. Khodjamirian, *QCD sum rules, a modern perspective*, In *Shifman, M. (ed.): At the frontier of particle physics, vol. 3* 1495-1576, hep-ph/0010175.

[32] I.I. Balitsky, V.M. Braun and A.V. Kolesnichenko, $\Sigma^+ \to P\gamma$ *Decay in QCD. (In Russian)*, Sov. J. Nucl. Phys. **44** (1986) 1028 [Yad. Fiz. **44** (1986) 1582].

[33] V.L. Chernyak and I.R. Zhitnitsky, *B meson exclusive decays into baryons*, Nucl. Phys. B **345** (1990) 137.

[34] V.M. Belyaev, A. Khodjamirian and R. Ruckl, *QCD calculation of the* $B \to \pi, K$ *form-factors*, Z. Phys. C **60** (1993) 349, hep-ph/9305348.

[35] V.M. Belyaev, V.M. Braun, A. Khodjamirian and R. Ruckl, *$D^*D\pi$ and $B^*B\pi$ couplings in QCD*, Phys. Rev. D **51** (1995) 6177, hep-ph/9410280.

[36] M. Beneke, G. Buchalla, M. Neubert and C. T. Sachrajda, *QCD factorization for $B \to \pi\pi$ decays: Strong phases and CP violation in the heavy quark limit*, Phys. Rev. Lett. **83** (1999) 1914, hep-ph/9905312.

[37] M. Beneke, G. Buchalla, M. Neubert and C. T. Sachrajda, *QCD factorization for exclusive, nonleptonic B meson decays: General arguments and the case of heavy light final states*, Nucl. Phys. B **591** (2000) 313, hep-ph/0006124.

[38] M. Beneke, G. Buchalla, M. Neubert and C. T. Sachrajda, *QCD factorization in $B \to \pi K$, $\pi\pi$ decays and extraction of Wolfenstein parameters*, Nucl. Phys. B **606** (2001) 245, hep-ph/0104110.

[39] M. Beneke and M. Neubert, *QCD factorization for $B \to PP$ and $B \to PV$ decays*, Nucl. Phys. B **675** (2003) 333, hep-ph/0308039.

[40] M. Beneke, T. Feldmann and D. Seidel, *Systematic approach to exclusive $B \to Vl^+l^-$, $V\gamma$ decays*, Nucl. Phys. B **612** (2001) 25, hep-ph/0106067.

[41] M. Beneke, T. Feldmann and D. Seidel, *Exclusive radiative and electroweak $b \to d$ and $b \to s$ penguin decays at NLO*, Eur. Phys. J. C **41** (2005) 173, hep-ph/0412400.

[42] J. Chay, H. Georgi and B. Grinstein, *Lepton energy distributions in heavy meson decays from QCD*, Phys. Lett. B **247** (1990) 399.

[43] I. I. Y. Bigi, M. A. Shifman, N. G. Uraltsev and A. I. Vainshtein, *QCD predictions for lepton spectra in inclusive heavy flavor decays*, Phys. Rev. Lett. **71** (1993) 496, hep-ph/9304225.

[44] A.V. Manohar and M. B. Wise, *Inclusive semileptonic B and polarized Lambda(b) decays from QCD*, Phys. Rev. D **49** (1994) 1310, hep-ph/9308246.

[45] T. Mannel, *Operator product expansion for inclusive semileptonic decays in heavy quark effective field theory*," Nucl. Phys. B **413** (1994) 396, hep-ph/9308262.

[46] B. M. Dassinger, T. Mannel and S. Turczyk, *Inclusive semi-leptonic B decays to order $1/m_b^4$*, JHEP **0703** (2007) 087, hep-ph/0611168.

Chapter 2

Hadronic effects and observables in $B \to \pi \ell^+ \ell^-$ decay at large recoil

Published as an article in:
Ch. Hambrock, A. Khodjamirian, A.V. Rusov, Phys.Rev. **D92** (2015) no.7, 074020

Contributions of the authors to the article.
A.V. Rusov performed analytical derivation of all expressions obtained in the paper and carried out numerical analysis. Additionally, A.V. Rusov prepared the draft of the manuscript. Dr. Ch. Hambrock performed an independent numerical simulation providing a cross check of the results. Prof. Dr. A. Khodjamirian suggested the outline of this project, supervised the calculations, discussed them and worked on the final version of the manuscript.

PHYSICAL REVIEW D **92,** 074020 (2015)

Hadronic effects and observables in $B \to \pi \ell^+ \ell^-$ decay at large recoil

Christian Hambrock, Alexander Khodjamirian, and Aleksey Rusov[*]

Theoretische Physik 1, Naturwissenschaftlich-Technische Fakultät, Universität Siegen, D-57068 Siegen, Germany

(Received 30 June 2015; published 14 October 2015)

We calculate the amplitude of the rare flavor-changing neutral-current decay $B \to \pi \ell^+ \ell^-$ at large recoil of the pion. The nonlocal contributions in which the weak effective operators are combined with the electromagnetic lepton-pair emission are systematically taken into account. These amplitudes are calculated at off-shell values of the lepton-pair mass squared, $q^2 < 0$, employing the operator-product expansion, QCD factorization and light-cone sum rules. The results are fitted to hadronic dispersion relations in q^2, including the intermediate vector meson contributions. The dispersion relations are then used in the physical region $q^2 > 0$. Our main result is the process-dependent addition $\Delta C_9^{(B\pi)}(q^2)$ to the Wilson coefficient C_9 obtained at $4m_\ell^2 < q^2 \lesssim m_{J/\psi}^2$. Together with the $B \to \pi$ form factors from light-cone sum rules, this quantity is used to predict the differential rate, direct CP asymmetry and isospin asymmetry in $B \to \pi \ell^+ \ell^-$. We also estimate the total rate of the rare decay $B \to \pi \nu \bar{\nu}$.

DOI: 10.1103/PhysRevD.92.074020 PACS numbers: 12.38.Lg, 13.20.He, 11.30.Er

I. INTRODUCTION

The first measurement of the $B^+ \to \pi^+ \mu^+ \mu^-$ decay by the LHCb Collaboration [1] paved the way for more detailed measurements of $b \to d \ell^+ \ell^-$ decays. These results will complement the available data on $b \to s \ell^+ \ell^-$ decays, providing new important insight in the dynamics of flavor-changing neutral-current (FCNC) transitions in the Standard Model (SM) and beyond.

One important feature of exclusive $b \to d \ell^+ \ell^-$ decays is a nonvanishing direct CP asymmetry. In the SM this effect is caused by the interference between the dominant short-distance contributions of semileptonic and magnetic dipole operators and the contributions of other effective operators accompanied by the electromagnetic lepton-pair emission. The amplitudes of the latter contributions are process dependent, and are defined as hadronic matrix elements of *nonlocal* operator products. Importantly, the parts of the exclusive $b \to d \ell^+ \ell^-$ decay amplitudes proportional to $\lambda_u \equiv V_{ub} V_{ud}^*$ and $\lambda_c \equiv V_{cb} V_{cd}^*$ are of the same order of Cabibbo suppression and, in addition to a relative CKM phase, have different strong phases originating from the nonlocal amplitudes. The main goal of this work is to calculate the hadronic matrix elements of nonlocal contributions to $B \to \pi \ell^+ \ell^-$ at large recoil of the pion, that is, at small and intermediate lepton-pair mass, $q^2 \ll m_B^2$.

An advanced theoretical description of the exclusive semileptonic FCNC decays was developed on the basis of the QCD factorization (QCDF) approach [2], applied first to the decays $B \to K^{(*)} \ell^+ \ell^-$ in Ref. [3] and to $B \to \rho \ell^+ \ell^-$ in Ref. [4]; see also further applications to $B \to K \ell^+ \ell^-$ [5,6], and to $B \to \pi \ell^+ \ell^-$ [7]. An approach combining QCD light-cone sum rules with QCDF at $q^2 > 0$ for $B \to K^{(*)} \ell^+ \ell^-$ was used in [8].

In QCDF, the nonlocal effects in these decays are described in terms of hard-scattering quark-gluon amplitudes with virtual photon emission, convoluted with light-cone distribution amplitudes (DAs) of the initial B meson and final light meson. Soft gluons, responsible for the onset of long-distance effects in the channel of the electromagnetic current, including vector resonance formation and nonfactorizable interactions with initial and final meson remain beyond the reach of QCDF. Hence, these contributions have to be kept small, protected by their power suppression. In particular, one avoids the intervals of lepton-pair mass squared q^2 in the vicinity of vector meson masses, $q^2 \sim m_V^2$ $(V = \rho, \omega, \ldots, J/\psi, \ldots)$, where nonlocal effects are largely influenced by long-distance quark-gluon dynamics. This constraint defines the region of applicability of QCDF, that is, roughly from $q^2_{\rm min} = 2\ {\rm GeV}^2$ up to $q^2_{\rm max} = 6\ {\rm GeV}^2$. In this region, quark-hadron duality approximation is tacitly assumed for the contributions of radially excited and continuum hadronic states with the quantum numbers of light vector mesons.

Note that in the $B \to \pi \ell^+ \ell^-$ decay, as compared to $B \to K \ell^+ \ell^-$, the role of nonlocal effects related to ρ and ω resonances in the q^2 channel grows due to the current-current operators with large Wilson coefficients in the $\sim \lambda_u$ part. For the same reason, the weak annihilation combined with virtual photon emission, being suppressed in $B \to K \ell^+ \ell^-$ decays, becomes one of the dominant nonlocal effects in $B \to \pi \ell^+ \ell^-$. In the QCDF approach one describes the weak annihilation contribution [3] in terms of a virtual photon emission off the spectator antiquark in the B meson, followed by the subsequent annihilation to a

[*]On leave from the Department of Theoretical Physics, Yaroslavl State University, Russia.

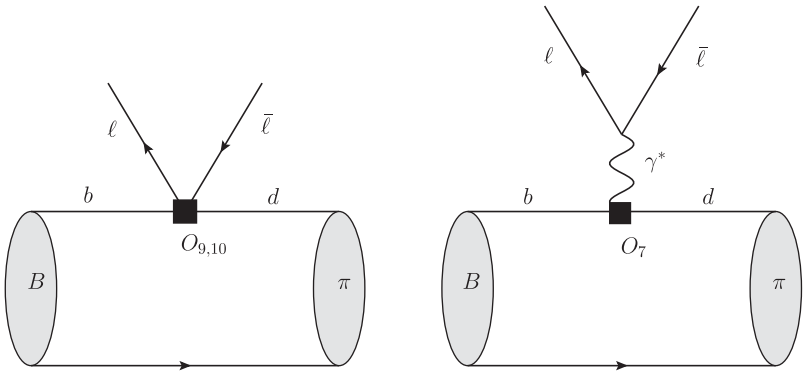

FIG. 1. FCNC contributions to $B \to \pi\ell^+\ell^-$ due to the effective operators $O_{9,10}$ (left) and $O_{7\gamma}$ (right) denoted as black squares.

final pion state. The accuracy of this leading-power diagram approximation, presumably quite sufficient for $B \to K\ell^+\ell^-$ decay, becomes crucial for $B \to \pi\ell^+\ell^-$.

In this paper we calculate the nonlocal effects in $B \to \pi\ell^+\ell^-$, using the method formulated in Ref. [9] and applied in Ref. [10] to $B \to K\ell^+\ell^-$. One avoids applying QCDF directly in the physical region $q^2 > 0$ and calculates the amplitudes of nonlocal contributions at deep spacelike $q^2 < 0$, $|q^2| \gg \Lambda^2_{\rm QCD}$, where the operator-product expansion (OPE) and QCDF can safely be used. The OPE contributions include the leading-order (LO) loops and weak annihilation, the NLO perturbative corrections to the loops and hard-spectator scattering. Furthermore, we include important nonfactorizable soft-gluon effects via dedicated LCSR calculations of hadronic matrix elements. The amplitudes of nonlocal effects are then represented in a form of hadronic dispersion relations in the variable q^2 where vector mesons are included explicitly. The residues of vector-meson poles related to nonleptonic $B \to V\pi$ decays are fixed, using experimental data and/or QCDF estimates. The nonresonant part of the hadronic dispersion integral is parametrized combining quark-hadron duality with a polynomial ansatz. Finally, the unknown parameters in the dispersion relation—most importantly, the strong phases of resonance and nonresonant contributions—are fitted to the QCD calculation at $q^2 < 0$. The advantage of describing nonlocal contributions to the FCNC decay amplitude in terms of hadronic dispersion relation is that the latter is valid in the whole large-recoil region specified as $4m_\ell^2 < q^2 < m^2_{J/\psi}$.

In $B \to \pi\ell^+\ell^-$ decays the combinations of CKM factors λ_u and λ_c are comparable in size. Correspondingly, we have to calculate separately two hadronic matrix elements of nonlocal effects multiplying λ_u and λ_c. A similar CKM separation has to be done in the amplitudes of nonleptonic $B \to V\pi$ decays, used to fix the residues of vector-meson poles in the hadronic dispersion relations. To obtain the separate parts of nonleptonic $B \to V\pi$ amplitudes for $V = \rho, \omega$ we employ the QCDF results [11] and control the resulting amplitudes with the data on branching ratios and CP-asymmetries of these nonleptonic decays.

The plan of this paper is as follows. In Sec. II we present the structure of the $B \to \pi\ell^+\ell^-$ decay amplitude and define the hadronic matrix element of nonlocal contributions. Section III contains a detailed calculation of these amplitudes at $q^2 < 0$. In Sec. IV we perform the relevant numerical analysis. In Sec. V the necessary inputs for the nonleptonic $B \to V\pi$ decay amplitudes are presented. Section VI is devoted to the analysis of the hadronic dispersion relations. Matching the latter to the result of QCD calculation, we then obtain $\Delta C_9^{(B\pi)}(q^2 > 0)$. In Sec. VII our predictions for the observables in the $B \to \pi\ell^+\ell^-$ decay are presented, including the decay rate, direct CP asymmetry and isospin asymmetry. In Sec. VIII we estimate the rate for $B \to \pi\nu\bar{\nu}$ decay. Section IX contains the concluding discussion. The two appendixes contain (A the operators and Wilson coefficients of the effective Hamiltonian of $b \to d\ell^+\ell^-$ transitions and (B) the QCDF expressions used for the amplitudes of $B \to \rho(\omega)\pi$ nonleptonic decays.

II. THE $B \to \pi\ell^+\ell^-$ DECAY AMPLITUDE

The effective weak Hamiltonian of the $b \to d\ell^+\ell^-$ transitions $(\ell = e, \mu, \tau)$ has the following form [12,13] in the SM:

$$H_{\rm eff}^{b\to d} = \frac{4G_F}{\sqrt{2}}\left(\lambda_u \sum_{i=1}^{2} C_i \mathcal{O}_i^u + \lambda_c \sum_{i=1}^{2} C_i \mathcal{O}_i^c - \lambda_t \sum_{i=3}^{10} C_i \mathcal{O}_i\right) + \text{H.c.}, \quad (1)$$

where $\lambda_p = V_{pb}V_{pd}^*$, $(p = u, c, t)$ are the products of CKM matrix elements. In contrast to the $b \to s\ell^+\ell^-$ transitions, all three terms in the unitary relation have the same order of Cabibbo suppression, $\lambda_u \sim \lambda_c \sim \lambda_t \sim \lambda^3$, λ being the Wolfenstein parameter. Hereafter, we assume CKM unitarity and replace $\lambda_t = -(\lambda_u + \lambda_c)$. The local dimension-6 operators $\mathcal{O}_i$ in (1) together with the numerical values of their Wilson coefficients C_i at relevant scales are presented in the Appendix A.

The amplitude of the $B \to \pi\ell^+\ell^-$ decay reads

$$A(B\to\pi\ell^+\ell^-) = -\langle\pi(p)\ell^+\ell^-|H_{\rm eff}^{b\to d}|B(p+q)\rangle$$
$$= \frac{G_F}{\sqrt{2}}\frac{\alpha_{\rm em}}{\pi}\lambda_t\left[(\bar\ell\gamma^\mu\ell)p_\mu\left(C_9 f_{B\pi}^+(q^2)+\frac{2m_b}{m_B+m_\pi}C_7^{\rm eff}f_{B\pi}^T(q^2)\right)\right.$$
$$\left.+(\bar\ell\gamma^\mu\gamma_5\ell)p_\mu C_{10}f_{B\pi}^+(q^2)+16\pi^2\frac{\bar\ell\gamma^\mu\ell}{q^2}\left(\frac{\lambda_u}{\lambda_t}\mathcal{H}_\mu^{(u)}+\frac{\lambda_c}{\lambda_t}\mathcal{H}_\mu^{(c)}\right)\right], \quad (2)$$

where p^μ and q^μ are the four-momenta of the π-meson and lepton pair, respectively.

In (2), the dominant contributions of the operators $O_{9,10}$ and $O_{7\gamma}$ are separated (Fig. 1) and their hadronic matrix elements are expressed in terms of the vector and tensor $B\to\pi$ form factors, $f_{B\pi}^+(q^2)$ and $f_{B\pi}^T(q^2)$, respectively, defined in the standard way,

$$\langle\pi(p)|\bar d\gamma^\mu b|B(p+q)\rangle$$
$$= f_{B\pi}^+(q^2)\left[2p^\mu+\left(1-\frac{m_B^2-m_\pi^2}{q^2}\right)q^\mu\right]$$
$$+f_{B\pi}^0(q^2)\frac{m_B^2-m_\pi^2}{q^2}q^\mu, \quad (3)$$

$$\langle\pi(p)|\bar d\sigma^{\mu\nu}q_\nu b|B(p+q)\rangle$$
$$= \frac{if_{B\pi}^T(q^2)}{m_B+m_\pi}[2q^2p^\mu+(q^2-(m_B^2-m_\pi^2))q^\mu]. \quad (4)$$

For definiteness, hereafter we consider the $B^-\to\pi^-\ell^+\ell^-$ mode, unless stated otherwise. We assume isospin symmetry for the $b\to d$ and $b\to u$ transition form factors. The $B^-\to\pi^-$ form factor $f_{B\pi}^+$ in Eq. (3) is equal to the one in the $\bar B^0\to\pi^+\ell^-\nu_\ell$ semileptonic decay and the form factors in the $\bar B^0\to\pi^0\ell^+\ell^-$ decay amplitude have an extra factor $1/\sqrt{2}$. For the CP-conjugated modes $B^+\to\pi^+\ell^+\ell^-$ and $B^0\to\pi^0\ell^+\ell^-$, respectively, one has to use the Hermitian conjugated effective operators with complex conjugated CKM factors λ_p^*.

The current-current, quark-penguin and chromomagnetic operators in the effective Hamiltonian (1) contribute to the decay amplitude (2), with the lepton pair produced via virtual photon. After factorizing out the lepton pair, the expression for these nonlocal effects is arranged in (2) in a form of correlation functions of the time-ordered product of quark operators with the quark electromagnetic current, $j_\mu^{\rm em}=\sum_{q=u,d,s,c,b}Q_q\bar q\gamma_\mu q$, sandwiched between B and π states,

$$\mathcal{H}_\mu^{(p)} = i\int d^4x e^{iqx}\langle\pi(p)|{\rm T}\left\{j_\mu^{\rm em}(x),\left[C_1\mathcal{O}_1^p(0)+C_2\mathcal{O}_2^p(0)\right.\right.$$
$$\left.\left.+\sum_{k=3-6,8g}C_k\mathcal{O}_k(0)\right]\right\}|B(p+q)\rangle = [(p\cdot q)q_\mu-q^2p_\mu]\mathcal{H}^{(p)}(q^2), \quad (p=u,c), \quad (5)$$

where the index $p=u,c$ hereafter distinguishes the hadronic matrix elements in Eq. (2), multiplying, respectively, the CKM factors λ_u,λ_c. Substituting (5) in (2) and taking into account the conservation of the leptonic current, we write down the decay amplitude in a more compact form,

$$A(B\to\pi\ell^+\ell^-) = \frac{G_F}{\sqrt{2}}\lambda_t\frac{\alpha_{\rm em}}{\pi}f_{B\pi}^+(q^2)\left[(\bar\ell\gamma^\mu\ell)p_\mu\left(C_9+\Delta C_9^{(B\pi)}(q^2)+\frac{2m_b}{m_B+m_\pi}C_7^{\rm eff}r_{B\pi}^T(q^2)\right)+(\bar\ell\gamma^\mu\gamma_5\ell)p_\mu C_{10}\right], \quad (6)$$

where the invariant amplitudes introduced in Eq. (5) form a process-dependent and q^2-dependent addition to the Wilson coefficient C_9,

$$\Delta C_9^{(B\pi)}(q^2)\equiv -16\pi^2\frac{(\lambda_u\mathcal{H}^{(u)}(q^2)+\lambda_c\mathcal{H}^{(c)}(q^2))}{\lambda_t f_{B\pi}^+(q^2)}. \quad (7)$$

In Eq. (6) we also introduce the ratio of tensor and vector form factors,

$$r_{B\pi}^T(q^2)\equiv\frac{f_{B\pi}^T(q^2)}{f_{B\pi}^+(q^2)}. \quad (8)$$

In the case of $b\to s\ell^+\ell^-$ transitions, the factor λ_u is usually neglected so that $\lambda_c=-\lambda_t$, and one recovers the corresponding expression for $\Delta C_9^{(BK)}(q^2)$ in $B\to K\ell^+\ell^-$ used in Ref. [10].

III. NONLOCAL EFFECTS AT SPACELIKE q^2

In this section we present separate contributions to the nonlocal amplitudes $\mathcal{H}^{(u)}(q^2)$ and $\mathcal{H}^{(c)}(q^2)$ defined in (5) and calculated at $q^2<0$, in the same approximation that was adopted in Ref. [10] for $B\to K\ell^+\ell^-$.

A. Factorizable loops

At LO in the quark-gluon coupling, the contributions of the four-quark operators to $B \to \pi \ell^+ \ell^-$ have two possible quark topologies. One of them corresponds to the factorizable quark-loop diagrams with different flavors [see Fig. 2(a)]. Their expressions are obtained from, e.g., the ones presented in Ref. [10], separating the $\sim\lambda_u$ and $\sim\lambda_c$ parts,

$$\mathcal{H}^{(u)}_{\mathrm{fact,LO}}(q^2) = \frac{1}{12\pi^2}\left(\frac{C_1}{3} + C_2\right) g_0(q^2) f^+_{B\pi}(q^2) + \mathcal{H}^{(3-6)}_{\mathrm{fact,LO}}(q^2), \tag{9}$$

$$\mathcal{H}^{(c)}_{\mathrm{fact,LO}}(q^2) = \frac{1}{12\pi^2}\left(\frac{C_1}{3} + C_2\right) g(q^2, m_c^2) f^+_{B\pi}(q^2) + \mathcal{H}^{(3-6)}_{\mathrm{fact,LO}}(q^2), \tag{10}$$

where the common term stemming from the quark-penguin operators O_{3-6} is

$$\begin{aligned}\mathcal{H}^{(3-6)}_{\mathrm{fact,LO}}(q^2) = \frac{1}{24\pi^2}\Bigg[&-\left(\frac{4}{3}C_3 + \frac{4}{3}C_4 + C_5 + \frac{C_6}{3}\right)\left(g(q^2, m_b^2) + g(q^2, m_s^2)\right) \\ &+ 2\left(C_3 + \frac{1}{3}C_4 + C_5 + \frac{C_6}{3}\right) g(q^2, m_c^2) \\ &+ \left(C_3 + \frac{C_4}{3} + C_5 + \frac{C_6}{3}\right) g_0(q^2) \\ &+ \left(C_3 + \frac{C_4}{3} + C_5 + \frac{C_6}{3}\right)\Bigg] f^+_{B\pi}(q^2).\end{aligned} \tag{11}$$

For the loop function we use the expression valid at $q^2 < 0$,

$$g(q^2, m_q^2) = \frac{4m_q^2}{q^2} + \frac{2}{3} - \ln\frac{m_q^2}{\mu^2} + \sqrt{1 - \frac{4m_q^2}{q^2}}\left(\frac{2m_q^2}{q^2} + 1\right) \times \ln\left(\frac{\sqrt{4m_q^2 - q^2} - \sqrt{-q^2}}{\sqrt{4m_q^2 - q^2} + \sqrt{-q^2}}\right), \tag{12}$$

where m_q is the quark mass if $q = b, c, s$ and μ is the renormalization scale. For u- and d-quark loops the quark masses are neglected; in this case the loop function takes the form

$$g_0(q^2) = \lim_{m_q^2 \to 0} g(q^2, m_q^2) = \frac{2}{3} - \ln\left(\frac{-q^2}{\mu^2}\right). \tag{13}$$

In Eqs. (9) and (10) the "full" $B \to \pi$ form factor is the same as in the contributions of $O_{9,10}$ operators to the decay amplitude (2). For this form factor we will use LCSR results that are valid also at $q^2 < 0$.

Note that in the LO approximation, when gluon exchanges between the loop and the rest of the diagram in Fig. 2(a) are neglected, the nonlocal amplitudes $H^{(u,c)}_{\mathrm{fact,LO}}(q^2)$ can also be calculated within LCSR approach. One has to define the vacuum-to-pion 3-point correlation function of the B-meson interpolating current, the four-quark operator and the electromagnetic current. After the quark loop is factorized out at large spacelike q^2, the remaining correlation function coincides with the one used to calculate the $B \to \pi$ form factor from LCSR. The resulting sum rule is then reduced to the loop factor multiplied by the LCSR expression for the $B \to \pi$ form factor, reproducing Eqs. (9), (10).

B. Weak annihilation

The second possible topology at LO is the weak annihilation (WA) with the diagrams shown in Fig. 2(b).

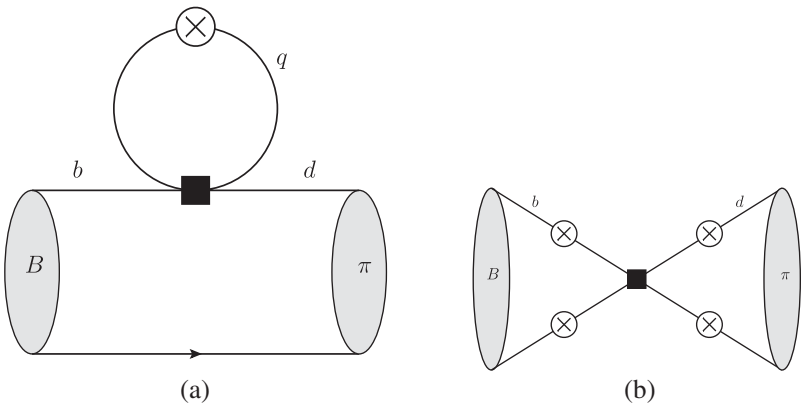

FIG. 2. Leading-order diagrams of nonlocal effects in $B \to \pi \ell^+ \ell^-$ due to the four-quark effective operators $O^{u,c}_{1,2}$ and O_{3-6}: the quark-loop (a) and weak annihilation (b). The black square denotes the operator and crossed circles indicate possible points of the virtual photon emission.

In QCDF, neglecting the inverse heavy b-quark mass corrections, the leading diagram is the one where the virtual photon is emitted off the spectator quark $q = u, d$ in the B meson, with the resulting expression [3,5]:

$$\mathcal{H}^{(p)}_{\rm WA}(q^2) = \frac{1}{8N_c}\frac{f_B f_\pi m_b}{m_B^2}\int_0^\infty \frac{d\omega}{\omega}\phi_B^-(\omega) \times \int_0^1 du\varphi_\pi(u)T_-^{(0),p}(u,\omega), \quad (p=u,c), \tag{14}$$

where f_π and f_B are the π- and B-meson decay constants, respectively, and the hard-scattering amplitude

$$T_-^{(0),p}(u,\omega) = Q_q\tilde{C}^p_{\rm WA}\frac{4m_B}{m_b}\frac{m_B\omega}{m_B\omega - q^2}, \quad (p=u,c) \tag{15}$$

is convoluted with the B-meson DA $\phi_B^-(\omega)$ defined as in Refs. [14,15] and $\varphi_\pi(u)$ is the twist-2 pion DA. The factor

$$\tilde{C}^p_{\rm WA} = \delta_{pu}(\delta_{qu}(C_2+3C_1)+\delta_{qd}(C_1+3C_2)) + C_3 + 3C_4 \tag{16}$$

is the combination of Wilson coefficients depending on the flavor content of the B meson. To obtain the amplitudes $\mathcal{H}^{(p)}_{\rm WA}(q^2)$, one takes into account that the LO kernel (15) is independent of the variable u, hence the integral over $\varphi_\pi(u)$ is reduced to its unit normalization. Adopting the exponential ansatz [14] for the B-meson DAs,

$$\phi_B^+(\omega) = \frac{\omega}{\lambda_B^2}e^{-\omega/\lambda_B}, \qquad \phi_B^-(\omega) = \frac{1}{\lambda_B}e^{-\omega/\lambda_B}, \tag{17}$$

where λ_B is the inverse moment, we obtain the following expression for the amplitude valid at $q^2 < 0$:

$$\mathcal{H}^{(p)}_{\rm WA}(q^2) = -\frac{Q_q f_B f_\pi}{2N_c m_B\lambda_B}e^{-q^2/m_B\lambda_B}{\rm Ei}\left(\frac{q^2}{m_B\lambda_B}\right)\tilde{C}^p_{\rm WA}, \tag{18}$$

where ${\rm Ei}(x) = -\int_{-x}^{\infty} dt e^{-t}/t$.

In contrast to $B\to K\ell^+\ell^-$ transitions, the WA mechanism due to the enhanced current-current operators $O^u_{1,2}$ provides one of the dominant contributions to the $\mathcal{H}^{(u)}_{\rm WA}(q^2)$ amplitude in $B\to\pi\ell^+\ell^-$. Moreover, the resulting difference between the WA amplitudes in $B^-\to\pi^-\ell^+\ell^-$ and $\bar{B}^0\to\pi^0\ell^+\ell^-$ contributes to the isospin asymmetry in $B\to\pi\ell^+\ell^-$.

Since the role of WA effects becomes important, it is desirable to improve the accuracy beyond the leading diagram contribution considered here. We checked that adding all subleading diagrams in Fig. 2(b) to the virtual photon emission from the spectator quark does not produce a visible effect for the $O_{1,2}$ contributions. There still remain power suppressed corrections generated by the higher twists in the pion DAs, and the contributions of the operators $O_{5,6}$ yet unaccounted in QCDF. In the future the perturbative nonfactorizable corrections to the diagrams in Fig. 2(b) also have to be calculated.

In principle, it is also possible to calculate the WA contribution employing the LCSR approach with the B-meson DAs. The correlation function will be described by the diagram similar to Fig. 2(b), but with the on-shell pion replaced by the interpolating quark current with the virtuality p^2. After employing the hadronic dispersion relation and quark-hadron duality in the pion channel, in the factorizable approximation, the two-point part of this correlation function will yield the QCD sum rule for the pion decay constant squared. The result for $\mathcal{H}^{(p)}_{\rm WA}(q^2)$ will then yield the expression (18).

C. Factorizable NLO contributions

The NLO corrections to the quark loops generated by the current-current operators $O^{u,c}_{1,2}$ are given by the two-loop diagrams shown in Figs. 3(a)–3(c). The contributions of quark-penguin operators are neglected, being suppressed by small Wilson coefficients and α_s simultaneously. At the same order of the perturbative expansion, the chromomagnetic operator O_{8g} is described with the diagrams shown in Figs. 3(d) and 3(e). These factorizable NLO contributions were taken into account in QCDF [3,4], employing the quark-level two-loop diagrams calculated in Ref. [16] (see also Refs. [17,18]). The NLO contribution of $O^c_{1,2}$ to $\mathcal{H}^{(c)}$ can be literally taken from Ref. [10], replacing $f^+_{BK}(q^2)$ by $f^+_{B\pi}(q^2)$. The corresponding contribution to $\mathcal{H}^{(u)}$ has the same structure, so that we can present both contribution by one compact expression,

$$\mathcal{H}^{(p)}_{\rm fact,NLO} = -\frac{\alpha_s}{32\pi^3}\frac{m_b}{m_B}\Big\{C_1F^{(7)}_{2,p}(q^2) + C_8^{\rm eff}F_8^{(7)}(q^2) + \frac{m_B}{2m_b}\Big[C_1F_2^{(9)} + 2C_2\Big(F^{(9)}_{1,p}(q^2) + \frac{1}{6}F^{(9)}_{2,p}(q^2)\Big) + C_8^{\rm eff}F_8^{(9)}(q^2)\Big]\Big\}f^+_{B\pi}(q^2), \tag{19}$$

where $p = u, c$. The definitions and nomenclature of the indices of the functions $F^{(7,9)}_{1,p}$, $F^{(7,9)}_{2,p}$ and $F_8^{(7,9)}$ are the same as in Refs. [16,17]. The only difference is that $F^{(7,9)}_{1,c}$ and $F^{(7,9)}_{2,c}$ are expressed as a double expansion in $\hat{s} = q^2/m_b^2$ and $\hat{m}_c^2 = m_c^2/m_b^2$, whereas $F^{(7,9)}_{1,u}$ and $F^{(7,9)}_{2,u}$ are expanded only in powers $\hat{s} = q^2/m_b^2$ since we work in the limit $m_u = 0$. It has been shown in Refs. [16,17] that keeping the terms up to the third power of $\hat{s}$ and $\hat{m}_c^2$ provides a sufficient numerical accuracy in the region $0.05 \le \hat{s} \le 0.25$. Here we use this expansion for $q^2 < 0$, restricting ourselves to $1.0 \le |q^2| \le 4.0$ GeV^2, i.e. staying within the same region. For $F_8^{(7,9)}$ we use the expression derived in Ref. [3].

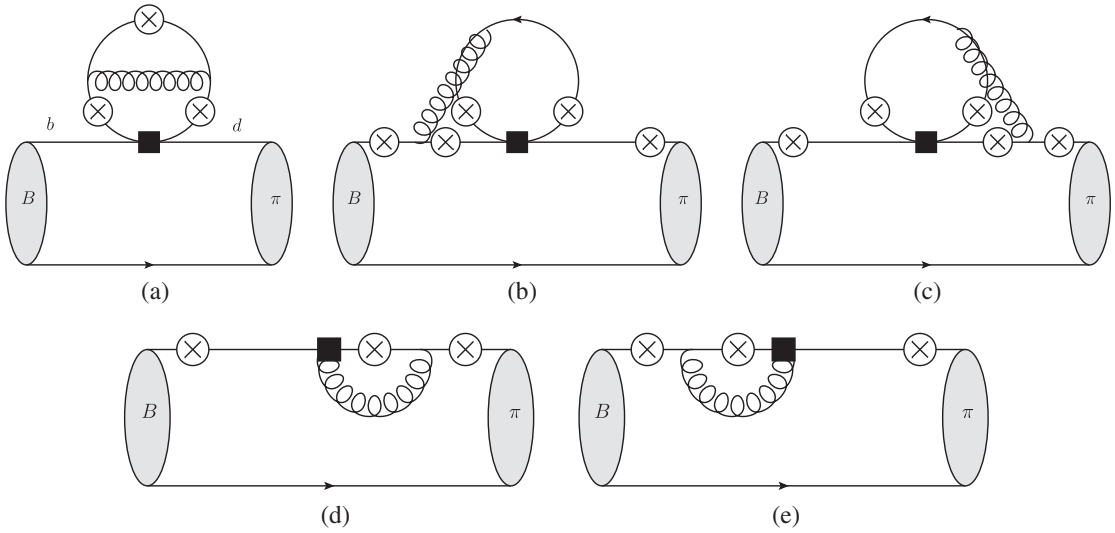

FIG. 3. Factorizable NLO quark-loop contributions to $B \to \pi \ell^+ \ell^-$, due to the four-quark effective operators $O_{1,2}^{u,c}$ (a,b,c) and the chromomagnetic operator O_{8g} (d,e). The notation is the same as in Fig. 2.

We remind that at NLO, the nonlocal contributions acquire the imaginary part also at $q^2 < 0$, that is, not related to the singularities in the variable q^2. The origin of this imaginary part and its relation to the final-state strong interaction is the same as for $B \to K \ell^+ \ell^-$ and is explained in detail in Ref. [10].

Note that analytic expressions for the two-loop virtual corrections to the matrix elements of the O_1^u and O_2^u operators are available from Ref. [18]. These expressions are valid at $q^2 > 0$ and agree with the expansion in q^2/m_b^2 obtained in Ref. [17]. However, we cannot use the results of Ref. [18] straightforwardly in our calculation at $q^2 < 0$, without separating the imaginary contributions inherent to the negative q^2 region from the contributions appearing due to the cuts of quark-gluon diagrams at $q^2 > 0$. Hence, we prefer to use the expanded form of these corrections [17] in which the phases stemming from the positivity of q^2, e.g. the terms proportional to $i\pi$ and originating from the $\log q^2$ terms, can be easily recognized and separated. As we work at sufficiently small values of $|q^2|$, the accuracy of the expansion in Ref. [17] is sufficient.

Contrary to the LO contributions considered in the previous subsections, the factorizable NLO ones are not simply accessible within the LCSR approach. Indeed, in order to reach the same $O(\alpha_s)$ accuracy, the calculation of the underlying correlation function has to include two-loop diagrams with several scales, a task exceeding the currently reached level of complexity in the multiloop calculations.

D. Nonfactorizable soft-gluon contributions

We also take into account the nonfactorizable contributions to the amplitudes $\mathcal{H}^{(p)}(q^2)$ emerging due to a soft-gluon emission from the quark loops, as shown in Fig. 4.

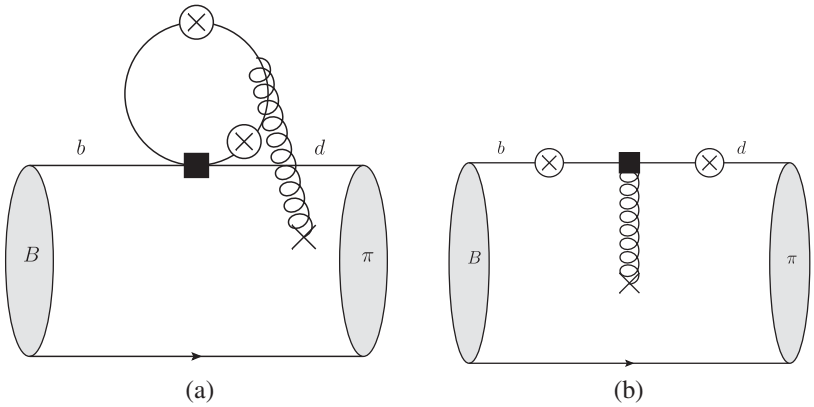

FIG. 4. Nonfactorizable soft-gluon contributions to $B \to \pi \ell^+ \ell^-$ due to (a) the four-quark effective operators $O_{1,2}^{u,c}$ and O_{3-6} and (b) the chromomagnetic O_{8g} operator. The soft gluon is represented by the gluon line with a cross. The rest of notation is the same as in the previous figures.

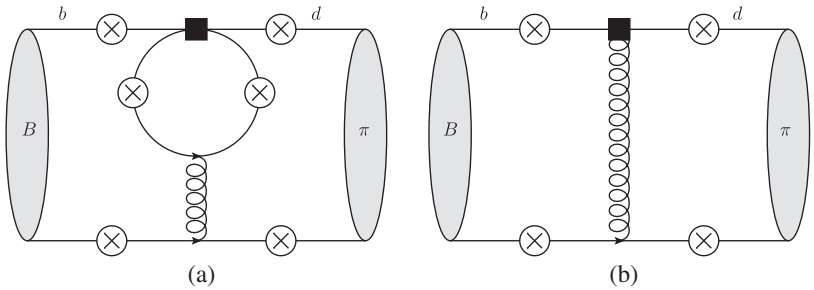

FIG. 5. Nonfactorizable spectator contributions to $B \to \pi \ell^+ \ell^-$ due to (a) the four-quark effective operators $O_{1,2}^{u,c}$, O_{3-6} and (b) the chromomagnetic operator O_{8g}.

These hadronic matrix elements cannot be reduced to a $B \to \pi$ form factor. It is also not possible to attribute the soft gluon to one of the hadrons in the $B \to \pi$ transition. The soft-gluon contributions are nevertheless well defined at $q^2 < 0$ and $|q^2| \gg \Lambda_{\rm QCD}^2$. As shown in Ref. [9], their suppression with respect to the factorizable loops is controlled by the powers of $1/(4m_c^2 - q^2)$ and $1/|q^2|$, stemming, respectively, from the c-quark and massless loops with soft gluon. The corresponding hadronic matrix elements were first calculated for the c-quark loops in Ref. [9] for $B \to K^{(*)} \ell^+ \ell^-$. The calculation was done in two steps: (1) applying the light-cone OPE at deep spacelike q^2 for the quark loop with soft-gluon emission, and (2) calculating the $B \to K^{(*)}$ hadronic matrix element of the emerging quark-antiquark-gluon operator using LCSRs with the B-meson three-particle DAs. Completing this result to include the loops with all possible quark flavors is straightforward and was already done for $B \to K \ell^+ \ell^-$ in Ref. [10]; to obtain the corresponding contribution to $\mathcal{H}^{(c)}(q^2)$ in $B \to \pi \ell^+ \ell^-$, we only need to replace the kaon by the pion. The soft-gluon nonfactorizable contribution of the operator O_1^u contributing to $\mathcal{H}^{(u)}(q^2)$ is also easily obtained. The result for this contribution is cast in a compact form,

$$\begin{aligned}\mathcal{H}_{\rm soft}^{(p)}(q^2) = &\frac{4}{3}(\delta_{pc} C_1 + C_4 - C_6)\tilde{A}(m_c^2, q^2) \\ &+ \frac{2}{3}(2\delta_{pu} C_1 + C_4 - C_6)\tilde{A}(0, q^2) \\ &- \frac{2}{3}(C_3 + C_4 - C_6)(\tilde{A}(m_s^2, q^2) \\ &+ \tilde{A}(m_b^2, q^2)). \end{aligned} \tag{20}$$

A cumbersome expression for the nonfactorizable hadronic matrix element $\tilde{A}(m_q^2, q^2)$ obtained from LCSR can be found in Ref. [9] [see Eq. (4.8) therein], where the dependence on the quark mass squared is explicitly shown and is indicated in the above expression. To adjust this expression to the $B \to \pi \ell^+ \ell^-$ transition, one has to replace the decay constant, meson mass and threshold parameter in the equation $f_K \to f_\pi$, $m_K \to m_\pi$, $s_0^K \to s_0^\pi$, thus taking into account the flavor $SU(3)$ violation. In the sum rule for $\tilde{A}(m_q^2, q^2)$, we use the ansatz for the three-particle B-meson DAs suggested in Ref. [24], where the parameter $\lambda_E^2 = 3/2\lambda_B^2$ is directly related to the inverse moment of the two-particle DA ϕ_B^+ specified in Eq. (17).

The soft-gluon contribution of the chromomagnetic operator O_{8g} is described by the diagram in Fig. 4(b), where instead of the loop factor, one has a pointlike emission of the soft-gluon field. One modifies the correlation function accordingly and arrives at the LCSR that was already derived in Ref. [10] and presented in Eq. (4.7) therein.[1] Making the necessary replacements for $B \to \pi \ell^+ \ell^-$, we obtain

$$\begin{aligned}\mathcal{H}_{{\rm soft},O_{8g}}^{(u)}(q^2) &= \mathcal{H}_{{\rm soft},O_{8g}}^{(c)}(q^2) \\ &= [\mathcal{H}_{{\rm soft},O_{8g}}^{(BK)}(q^2)]_{f_K \to f_\pi, m_K \to m_\pi, s_0^K \to s_0^\pi}. \end{aligned} \tag{21}$$

As in the case of $B \to K \ell^+ \ell^-$ transitions, this contribution turns out to be very small.

E. Nonfactorizable spectator scattering

An important nonlocal contribution to the $B \to \pi \ell^+ \ell^-$ amplitude in NLO emerges due to a hard gluon emitted from the intermediate quark loop or from the O_{8g}-operator vertex, and absorbed by the spectator quark in the $B \to \pi$ transition, as shown in Fig. 5. Following [10], we will use the QCDF result [3] for this contribution. The following expression is valid for both $p = u$ and $p = c$ parts of the nonlocal amplitude:

[1] We notice that in the related equation (4.4) a factor C_{8g} on the rhs is missing.

$$\mathcal{H}^{(p)}_{\text{nonf,spect}}(q^2) = \frac{\alpha_s C_F}{32\pi N_c}\frac{f_B f_\pi m_b}{m_B^2}\left(\int_0^\infty \frac{d\omega}{\omega}\phi_B^+(\omega)\int_0^1 du\varphi_\pi(u)T_+^{(1),p}(u,\omega) + \int_0^\infty \frac{d\omega}{\omega}\phi_B^-(\omega)\int_0^1 du\varphi_\pi(u)T_-^{(1),p}(u,\omega)\right). \tag{22}$$

The hard-scattering kernels entering the above expression have the form

$$T_+^{(1),p}(u,\omega) = -\frac{m_B}{m_b}\left(\frac{2}{3}t_\parallel(u,m_c)(\delta_{pc}C_1 + C_4 - C_6) - \frac{1}{3}t_\parallel(u,m_b)(C_3 + C_4 - C_6) - \frac{1}{3}t_\parallel(u,m_s)(C_3 + C_4 - C_6) + \frac{1}{3}(2\delta_{pu}C_1 + C_4 - C_6)t_\parallel(u,0)\right), \tag{23}$$

$$T_-^{(1),p}(u,\omega) = -Q_q\frac{m_B\omega}{m_B\omega - q^2 - i\epsilon}\left[\frac{8m_B}{3m_b}\left(h(m_c^2,\bar{u}m_B^2 + uq^2)(\delta_{pc}C_1 + C_4 + C_6) + h(m_b^2,\bar{u}m_B^2 + uq^2)(C_3 + C_4 + C_6) + h(0,\bar{u}m_B^2 + uq^2)(\delta_{pu}C_1 + C_3 + 3C_4 + 3C_6) - \frac{2}{3}(C_3 - C_5 - 15C_6)\right) + \frac{8C_8^{\text{eff}}}{\bar{u} + uq^2/m_B^2}\right], \tag{24}$$

where Q_q is the electric charge of the spectator quark in the B meson ($q = u, d$) and the functions $t_\parallel(u, m_q)$ and $h(m_q^2, q^2)$ can be found in Ref. [3].

The two-particle B-meson DAs $\phi_B^\pm(\omega)$ are given in Eq. (17); for the twist-2 pion DA we employ the standard Gegenbauer expansion,

$$\varphi_\pi(u,\mu) = 6u(1-u)(1 + a_2^\pi(\mu)C_2^{(3/2)}(u) + a_4^\pi(\mu)C_4^{(3/2)}(u)). \tag{25}$$

The fact that the amplitudes in (22) depend on the charge of the spectator quark in the B meson triggers another important contribution to the isospin asymmetry in $B \to \pi\ell^+\ell^-$.

Summing up all contributions considered in this section, we obtain the two nonlocal amplitudes in the adopted approximation

$$\mathcal{H}^{(p)}(q^2) = \mathcal{H}^{(p)}_{\text{fact,LO}}(q^2) + \mathcal{H}^{(p)}_{\text{WA}}(q^2) + \mathcal{H}^{(p)}_{\text{fact,NLO}}(q^2) + \mathcal{H}^{(p)}_{\text{soft}}(q^2) + \mathcal{H}^{(p)}_{\text{soft,O}_8}(q^2) + \mathcal{H}^{(p)}_{\text{nonf,spect}}(q^2), \quad (p = u, c). \tag{26}$$

IV. NUMERICAL ANALYSIS

Here we perform the numerical analysis of the nonlocal amplitudes (26) at spacelike $q^2 < 0$, more definitely, in the region $1\ \text{GeV}^2 \le |q^2| \lesssim 4\ \text{GeV}^2$, where the OPE and QCDF approximation can be trusted. The input parameters and references to their source are listed in Table I, the charged and neutral B-meson and pion masses are taken from [19], and the numerical values of the Wilson coefficients are presented in Appendix A. As a default renormalization and factorization scale we assume $\mu = 3$ GeV, the same as in Ref. [10]. It will be varied in the interval $2.5 < \mu < 4.5$ GeV to study the μ dependence.

For the vector $B \to \pi$ form factor the most recent update [20] of LCSR prediction is adopted, in a form fitted to the three-parameter BCL parameterization,

TABLE I. Intervals of the input parameters used in the calculation of $\mathcal{H}^{(u,c)}(q^2 < 0)$.

Input parameter	References
$\alpha_s(m_Z) = 0.1185 \pm 0.0006$	
$\bar{m}_c(\bar{m}_c) = (1.275 \pm 0.025)$ GeV	
$\bar{m}_b(\bar{m}_b) = (4.18 \pm 0.03)$ GeV	[19]
$m_s(2\ \text{GeV}) = (95 \pm 5)$ MeV	
$f_B = 207^{+17}_{-9}$ MeV	[21]
$\lambda_B = (460 \pm 110)$ MeV	[22]
$f_\pi = 130.4$ MeV	[19]
$a_2^\pi(1\ \text{GeV}) = 0.17 \pm 0.08$	
$a_4^\pi(1\ \text{GeV}) = 0.06 \pm 0.10$	[23]
Sum rules in the pion channel	
$M^2 = 1.0 \pm 0.5\ \text{GeV}^2$, $s_0^\pi = 0.7\ \text{GeV}^2$	[24]
$f_{B\pi}^+(0) = 0.307 \pm 0.020$	
$b_1^+ = -1.31 \pm 0.42$	[20]
$b_2^+ = -0.904 \pm 0.444$	

$$f_{B\pi}^{+}(q^2) = \frac{f_{B\pi}^{+}(0)}{1-q^2/m_{B^*}^2}\left\{1 + b_1^{+}[z(q^2,t_0) - z(0,t_0) - \frac{1}{3}(z(q^2,t_0)^3 - z(0,t_0)^3)\right] + b_2^{+}\left[z(q^2,t_0)^2 - z(0,t_0)^2 + \frac{2}{3}(z(q^2,t_0)^3 - z(0,t_0)^3)\right]\right\}, \quad (27)$$

with $t_0 = (m_B + m_\pi)(\sqrt{m_B} - \sqrt{m_\pi})^2$, where the normalization and shape parameters are presented in Table I. The decay constant of B meson is determined from two-point sum rules, where we use the recent analysis [21]; the inverse moment of the B-meson DA is also represented by the interval of QCD sum rule prediction [22]. The intervals of Gegenbauer moments in the pion DAs used in the QCDF expressions are the same as in the LCSR for the $B \to \pi$ form factor [20,23].

Substituting the central input in the expressions presented in the previous section, we calculate the two amplitudes $\mathcal{H}^{(u)}(q^2 < 0)$ and $\mathcal{H}^{(c)}(q^2 < 0)$ for $B^- \to \pi^-\ell^+\ell^-$ and plot their real and imaginary parts in Figs. 6 and 7, respectively, showing also the separate contributions. For comparison, the amplitude $\mathcal{H}^{(u)}(q^2 < 0)$ is plotted in Fig. 8 for $\bar{B}^0 \to \pi^0\ell^+\ell^-$, whereas the amplitude $\mathcal{H}^{(c)}(q^2 < 0)$ for the latter mode is numerically similar to the one for $B^- \to \pi^-\ell^+\ell^-$ and is not shown.

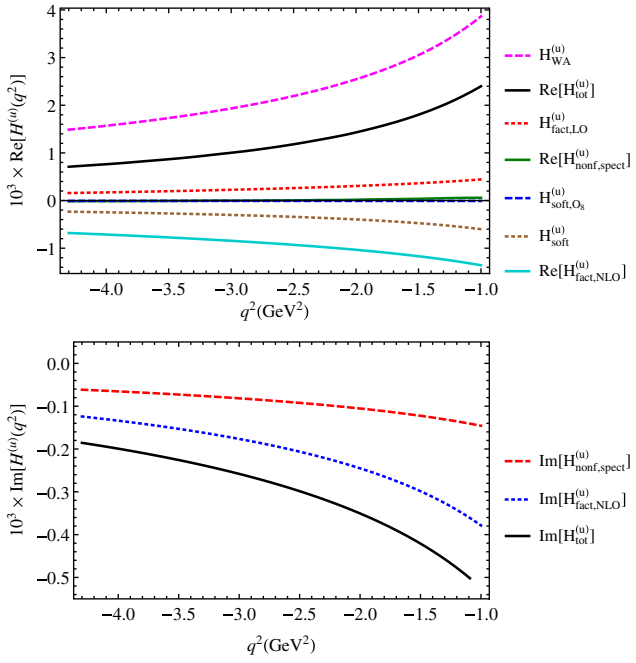

FIG. 6 (color online). Nonlocal amplitude $\mathcal{H}^{(u)}(q^2)$ for $B^- \to \pi^-\ell^+\ell^-$ at $q^2 < 0$ calculated at the central values of the input; the real (imaginary) part is in the upper (lower) panel. $H^{(u)}_{tot}(q^2)$ is the sum of the separate contributions specified in Eq. (26).

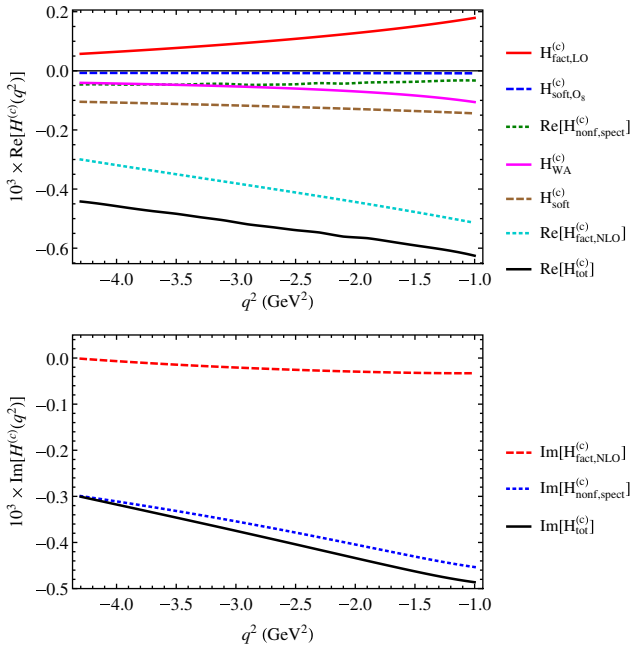

FIG. 7 (color online). The same as in Fig. 6 for the amplitude $\mathcal{H}^{(c)}(q^2)$ for $B^- \to \pi^-\ell^+\ell^-$.

From the numerical analysis we can draw several conclusions:

(a) The contributions to $\mathcal{H}^{(c)}(q^2)$ are approximately the same as the corresponding ones for the $B \to K\ell^+\ell^-$

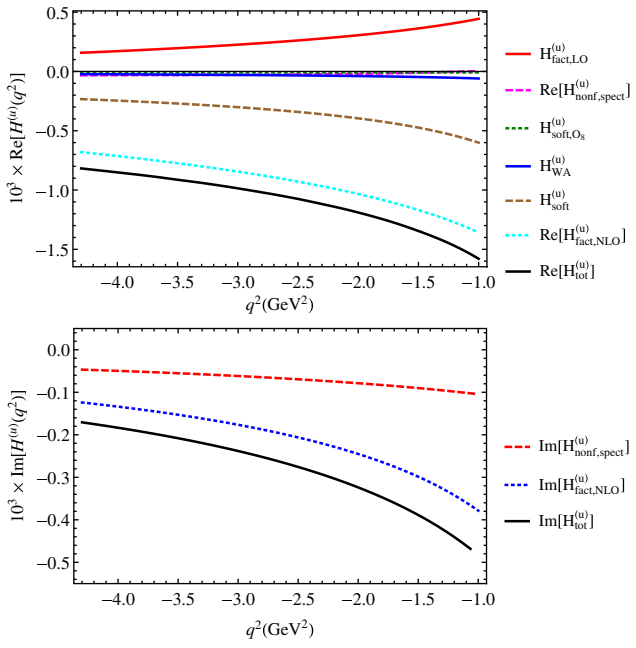

FIG. 8 (color online). The same as in Fig. 6 for the amplitude $\mathcal{H}^{(u)}(q^2)$ in $\bar{B}^0 \to \pi^0\ell^+\ell^-$.

obtained in Ref. [10]; the differences reflect the violation of the flavor $SU(3)$ symmetry.

(b) The contributions to $\mathcal{H}^{(u)}(q^2)$, in $B^- \to \pi^-\ell^+\ell^-$ presented in Fig. 6 are clearly dominated by the weak annihilation term, enhancing the real part of $\mathcal{H}^{(u)}(q^2)$ considerably. This effect is less pronounced for $\bar{B}^0 \to \pi^-\ell^+\ell^-$, as expected.

(c) The nonfactorizable soft-gluon contribution due to the operators $O_{1,2}^{u,c}$ are important and the corresponding contributions of O_{3-6} are not negligible. Meanwhile, the contribution due to the operator O_{8g} with a soft gluon is very small.

The uncertainties of the functions $\mathcal{H}^{(c)}(q^2<0)$ and $\mathcal{H}^{(u)}(q^2<0)$ are estimated varying the inputs within their adopted intervals indicated in Table I. The largest uncertainties originate from the variation of f_B, λ_B and the correlated variation of the parameters of $f_{B\pi}^+$. To stay on the conservative side, we neglect possible correlations between the individual input entries in Table I. We also varied the renormalization/factorization scale around the default "optimal" value $\mu = 3.0$ GeV. The results do not significantly change the estimated total uncertainty and we therefore neglect the scale dependence in the error estimates performed below.

V. NONLEPTONIC $B \to V\pi$ DECAY AMPLITUDES

We now turn to weak nonleptonic $B \to V\pi$ decays with neutral vector mesons $V = \rho^0, \omega, \phi, J/\psi, \psi(2S)$ in the final state. The intervals of the absolute values of their amplitudes have to be estimated and used as an input in the hadronic dispersion relations for $\mathcal{H}^{(u,c)}(q^2)$ to be fitted to the calculated $\mathcal{H}^{(u,c)}(q^2<0)$.

The amplitude of a $B^- \to V\pi^-$ decay is parametrized as

$$A(B^- \to V\pi^-) = \langle V(q)\pi^-(p)|H_{\text{eff(NL)}}^{b\to d}|B^-(p+q)\rangle = \frac{4G_F}{\sqrt{2}} m_V (\varepsilon_V^* \cdot p)(\lambda_u A^u_{B^-V\pi^-} + \lambda_c A^c_{B^-V\pi^-}), \tag{28}$$

where q (ε_V) is the 4-momentum (polarization vector) of the vector meson with $q^2 = m_V^2$. For the charge-conjugated mode $B^+ \to V\pi^+$ one has to replace $\lambda_{u,c} \to \lambda_{u,c}^*$ in the above relation, whereas the hadronic amplitudes remain unchanged, $A^{u,c}_{B^-V\pi^-} = A^{u,c}_{B^+V\pi^+}$. For the neutral $\bar{B}^0 \to V\pi^0$ decay modes we denote the corresponding amplitudes as $A^{u,c}_{\bar{B}^0V\pi^0} = A^{u,c}_{B^0V\pi^0}$. The effective Hamiltonian $H^{b\to d}_{\text{eff(NL)}}$ in Eq. (28) contains the operators $O_{1,2}^{u,c}$, O_{3-6}, O_{8g} given in Appendix A, and we neglect the electroweak quark-penguin operators with $O(\alpha_{\text{em}})$ suppressed Wilson coefficients. From Eq. (28) one obtains the expression for the CP-averaged width,

$$\Gamma(B^\mp \to V\pi^\mp) \equiv \frac{1}{2}[\Gamma(B^- \to V\pi^-) + \Gamma(B^+ \to V\pi^+)] = \frac{G_F^2\lambda^{3/2}(m_B^2, m_\pi^2, m_V^2)}{8\pi m_B^3} \times (|\lambda_u|^2|A^u_{B^-V\pi^-}|^2 + |\lambda_c|^2|A^c_{B^-V\pi^-}|^2 + 2|\lambda_u\lambda_c||A^u_{B^-V\pi^-}||A^c_{B^-V\pi^-}|\cos\delta\cos\Delta), \tag{29}$$

where $\lambda(a,b,c) = a^2 + b^2 + c^2 - 2ab - 2ac - 2bc$. In the above, we explicitly isolate the relative strong phase δ between the amplitudes $A^u_{B^-V\pi^-}$ and $A^c_{B^-V\pi^-}$ and denote $\Delta \equiv \arg(\lambda_u) - \arg(\lambda_c)$. The direct CP asymmetry takes the following form:

$$\mathcal{A}_{CP}(B^\mp \to V\pi^\mp) \equiv \frac{\Gamma(B^- \to V\pi^-) - \Gamma(B^+ \to V\pi^+)}{2\Gamma(B^\mp \to V\pi^\pm)} = -2\sin\delta\sin\Delta\left(\left|\frac{\lambda_u A^u_{B^-V\pi^-}}{\lambda_c A^c_{B^-V\pi^-}}\right| + \left|\frac{\lambda_c A^c_{B^-V\pi^-}}{\lambda_u A^u_{B^-V\pi^-}}\right| + 2\cos\delta\cos\Delta\right)^{-1}. \tag{30}$$

Analogous expressions are obtained for the neutral $B \to V\pi^0$ modes, replacing $B^- \to \bar{B}^0$ and $B^+ \to B^0$.

For the input in the two dispersion relations for the amplitudes $\mathcal{H}^{(u)}(q^2)$ and $\mathcal{H}^{(c)}(q^2)$ we need to separately determine the moduli of the hadronic amplitudes $|A^u_{B^-V\pi^-}|$ and $|A^c_{B^-V\pi^-}|$. In principle, one can use the two observables in Eqs. (28) and (30), but the presence of the third unknown parameter, the relative strong phase, hinders the determination. Therefore, the situation is more complex here than for the nonleptonic $B \to VK$ decays used in the analysis of $B \to K\ell^+\ell^-$ in Ref. [10] where only the contributions proportional to λ_c were retained and the amplitudes $|A^c_{BVK}|$ were directly obtained from the measured $B \to VK$ branching fractions.

On the other hand, there is a possibility to estimate separate contributions to the nonleptonic amplitudes applying the QCDF approach [2]. The latter is known to provide a reasonably good description of the charmless channels $B^- \to \rho^0\pi^-$ and $B^- \to \omega^0\pi^-$. Here we use the results of Ref. [11] where the QCDF description for $B \to VP$ decays was elaborated in detail. The necessary expressions for the amplitude decomposition and the additional input parameters including the $B \to V$ form factors, decay constants and the Gegenbauer moments of the DAs of $V = \rho, \omega$ are collected in Appendix B. The resulting absolute values of the amplitudes are presented in Table II. To check the validity of these estimates, we calculated the observables (28) and (30), and compared the results with the experiment and with the earlier predictions of Ref. [11] (see Table III), observing a reasonable agreement. In the transition from the widths to branching fractions we use the lifetimes of B

TABLE II. Inputs for the absolute values $|A^{u,c}_{BV\pi}|$ of the $B \to V\pi$ amplitudes (in MeV).

Mode	$\lvert A^{u}_{BV\pi}\rvert$	$\lvert A^{c}_{BV\pi}\rvert$
$B^{\mp} \to \rho^0\pi^{\mp}$	$20.8^{+2.7}_{-2.3}$	$1.3^{+1.1}_{-0.4}$
$B^{\mp} \to \omega\pi^{\mp}$	$19.1^{+2.7}_{-2.0}$	$0.3^{+0.4}_{-0.1}$
$B^{\mp} \to J/\psi\pi^{\mp}$	$0.5^{+9.7}_{-0.5}$	$29.2^{+1.4}_{-1.5}$
$B^{\mp} \to \psi(2S)\pi^{\mp}$	$3.5^{+6.7}_{-3.5}$	$32.3^{+2.0}_{-2.1}$
$B^0 \to \rho^0\pi^0$	$9.9^{+1.3}_{-1.4}$	0
$B^0 \to \omega\pi^0$	0	0
$B^0 \to J/\psi\pi^0$	$0.3^{+6.9}_{-0.3}$	$20.6^{+1.0}_{-1.1}$
$B^0 \to \psi(2S)\pi^0$	$2.4^{+4.7}_{-2.4}$	$22.8^{+1.4}_{-1.5}$

mesons from Ref. [19]. Note that in the dispersion relations we will not isolate the intermediate ϕ-meson pole, hence we do not specify the $B \to \phi\pi$ nonleptonic amplitudes here. These decays originate either due to the $q = s$ part of the quark-penguin operators O_{3-6} with suppressed Wilson coefficients, or due to the $O_{1,2}$ operators combined with a transition via intermediate gluons into an $\bar{s}s$ state. The latter is Okubo-Zweig-Iizuka suppressed (cf. the smallness of ϕ decays into pions). The measured upper limit $\mathrm{BR}(B^- \to \phi\pi^-) < 1.5 \times 10^{-7}$ [19], being significantly smaller than the measured branching fractions of $B^- \to \rho(\omega)\pi^-$ decays (see Table III), convinces us that the intermediate ϕ-meson contribution to $B \to \pi\ell^+\ell^-$ is small. Furthermore we do not separate the radial excitations $\rho', \ldots, \omega', \ldots$, approximating their contributions to the hadronic spectral density by the quark-hadron duality ansatz; hence we do not need to consider here the nonleptonic decays of the type $B \to \rho'(1450)\pi$.

For the neutral $B^0 \to V\pi^0$ modes, the QCDF prediction [11] fails to predict the partial width $B^0 \to \rho^0\pi^0$, the experimental value being significantly larger. Without going into more detailed discussion of this problem, guided by the hierarchy of amplitudes in the charged mode, $A^{c}_{B^0\rho^0\pi^0} \ll A^{u}_{B^0\rho^0\pi^0}$, we simply assume $A^{c}_{B^0\rho^0\pi^0} = 0$ and extract $|A^{u}_{B^0\rho^0\pi^0}|$ from the measured partial width employing Eq. (29). For the $B^0 \to \omega\pi^0$ mode only the upper limit on the branching fraction is available [19], indicating that this decay amplitude is suppressed in comparison to the other modes; hence we put $A^{u}_{B^0\omega\pi^0} \approx A^{c}_{B^0\omega\pi^0} \approx 0$ as is specified in Table II.

Turning to the charmonium channels $B \to \psi\pi$, where $\psi = J/\psi, \psi(2S)$, we do not expect the QCDF approach to work there due to a heavy final state and enhanced nonfactorizable, power-suppressed effects (see, e.g., the discussion in Ref. [9]). On the other hand, one anticipates that these nonleptonic decays are dominated by the emission topology due to the operators $O^{c}_{1,2}$ with large Wilson coefficients and a small admixture of O_{3-6} ($q = c$). The contributions of the operators $O^{u}_{1,2}$ and O_{3-6} ($q \neq c$) are expected to be strongly suppressed. Theoretical estimates for the analogous contributions to $B \to \psi K$ transitions (see, e.g., [25] and [26]) yield the amplitudes of gluonic transitions of light-quark loops to charmonium states at the level of 10^{-3} of the dominant contributions of $O^{c}_{1,2}$ operators. With an extra Cabibbo enhancement of the λ_u terms in $B \to \psi\pi$ with respect to $B \to \psi K$, a considerable suppression still remains. Hence we expect that $|A^{u}_{B^-\psi\pi^-}| \ll |A^{c}_{B^-\psi\pi^-}|$. In this situation the relative strong phase does not considerably influence the extraction of the large $\sim\lambda_c$ term, whereas the uncertainty of the small $\sim\lambda_u$ term is tolerable. Therefore, we use the current experimental data on the branching fractions and CP asymmetries of the above decays [19] and perform the fit of these data to Eqs. (29) and (30), extracting the absolute values of the amplitudes $|A^{u}_{B^-\psi\pi^-}|$ and $|A^{u}_{B^-\psi\pi^-}|$ and allowing the relative phase δ to change from 0 to 2π. The resulting intervals are presented in Table II. Finally, for the neutral $\bar{B}^0 \to \psi\pi^0$ modes, we make use of the isospin symmetry relation, $A^{u,c}_{B^0\psi\pi^0} \simeq 1/\sqrt{2}A^{u,c}_{B^-\psi\pi^-}$, since for the dominant ψ emission mechanism of these decays there is only one independent isospin amplitude. This assumption is supported by the measurement [19] yielding $\Gamma(B^0 \to J/\psi\pi^0) \simeq 1/2\Gamma(B^+ \to J/\psi\pi^+)$. The resulting estimates are also presented in Table II.

TABLE III. Comparison of the experimental data [19] and theoretical predictions for the observables in the nonleptonic $B \to \rho(\omega)\pi$ decays.

Channel	Observable	Experiment	QCDF [11]	QCDF, this work
$B^{\pm} \to \rho^0\pi^{\pm}$	$\mathrm{BR}\times 10^6$	8.3 ± 1.2	$11.9^{+7.8}_{-6.1}$	$9.5^{+2.9}_{-1.8}$
	$\mathcal{A}_{CP}$	$0.18^{+0.09}_{-0.17}$	0.04 ± 0.19	0.09 ± 0.17
$B^{\pm} \to \omega^0\pi^{\pm}$	$\mathrm{BR}\times 10^6$	6.9 ± 0.5	$8.8^{+5.4}_{-4.3}$	$8.9^{+2.6}_{-1.6}$
	$\mathcal{A}_{CP}$	-0.04 ± 0.06	-0.02 ± 0.04	-0.06 ± 0.06
$B^0 \to \rho^0\pi^0$	$\mathrm{BR}\times 10^6$	2.0 ± 0.5	$0.4^{+1.1}_{-0.4}$	$0.2^{+0.4}_{-0.1}$
	$\mathcal{A}_{CP}$	…	$-0.16^{+0.26}_{-0.32}$	$0.24^{+0.36}_{-0.31}$
$B^0 \to \omega^0\pi^0$	$\mathrm{BR}\times 10^6$	< 0.5	$0.01^{+0.04}_{-0.01}$	$0.01^{+0.06}_{-0.01}$
	$\mathcal{A}_{CP}$	…	…	$-0.94^{+0.87}_{-0.04}$

VI. HADRONIC DISPERSION RELATIONS

Following Refs. [9,10], the invariant amplitudes $\mathcal{H}^{(u)}(q^2)$ and $\mathcal{H}^{(c)}(q^2)$ are represented in a form of hadronic dispersion relations in the variable q^2, inserting the total set of hadronic intermediate states between the electromagnetic current and the effective operators in the correlation functions (5),

$$\mathcal{H}^{(p)}(q^2)-\mathcal{H}^{(p)}(q_0^2) = (q^2-q_0^2)\left[\sum_{V=\rho,\omega,J/\psi,\psi(2S)}\frac{k_V f_V A^p_{BV\pi}}{(m_V^2-q_0^2)(m_V^2-q^2-im_V\Gamma_V^{\rm tot})} + \int_{s_h}^{\infty} ds\frac{\rho_h^{(p)}(s)}{(s-q_0^2)(s-q^2-i\epsilon)}\right], \quad (p=u,c), \tag{31}$$

where the ground-state vector mesons (except ϕ) are isolated and the integral describes the contribution of excited and continuum contributions starting from $s_h = 4m_\pi^2$, the lowest hadronic threshold.[2] To achieve a better convergence, we implement one subtraction at $q_0^2 = -1.0\ \text{GeV}^2$ in Eq. (31). In the above, the masses and total widths of the vector mesons $V = \rho^0, \omega, J/\psi, \psi(2S)$ are taken from Ref. [19]. Their decay constants are defined as

$$\langle 0|j^{\text{em},\mu}|V(q)\rangle = k_V m_V \epsilon_V^\mu(q) f_V, \tag{32}$$

where the coefficients k_V are determined by the valence-quark content of V and the quark charges: $k_\rho = 1/\sqrt{2}$, $k_\omega = 1/(3\sqrt{2})$ and $k_{J/\psi} = k_{\psi(2S)} = 2/3$. The numerical values of f_V are fixed from the measured [19] leptonic widths $\Gamma(V\to\ell^+\ell^-)$ yielding $f_\rho = 221$ MeV, $f_\omega = 195$ MeV, $f_{J/\psi} = 416$ MeV and $f_{\psi(2S)} = 297$ MeV. The absolute values of the amplitudes $A^u_{BV\pi}$ and $A^c_{BV\pi}$ obtained from the analysis of nonleptonic decays in the previous section are taken from Table II.

At $q^2 < 0$, more specifically, in the region $-4.0\ \text{GeV}^2 \le q^2 \le -1.0\ \text{GeV}^2$, we substitute in the lhs of the relations (31) the result for $H^{(p)}(q^2)$ specified in Eq. (26), calculating simultaneously the subtraction terms at $q_0^2 = -1.0\ \text{GeV}^2$. The task is then to fit the free parameters on the rhs of the hadronic dispersion relations. Importantly, each V-pole residue in Eq. (31) for $p = u$ or $p = c$ has a relative phase with respect to the other vector-meson contributions and to the integral over $\rho_h^{(p)}(s)$. These phases should match the imaginary part of the calculated lhs of the dispersion relation. As explained in Ref. [10], the phases emerge due to the intermediate on-shell hadronic states in the variable $(p+q)^2 = m_B^2$ and are not related to the analytical continuation in the variable q^2.

Note that the relative strong phase between the amplitudes $A^u_{BV\pi}$ and $A^c_{BV\pi}$ contributing to the $B\to V\pi$ nonleptonic amplitude, although of the same origin, is a different quantity, because in each of dispersion relations (31) only one of these amplitudes enter. On the other hand, calculating the phases of nonleptonic amplitudes within a theoretical framework, such as QCDF, it is possible to estimate the relative phase between, say, $A^u_{B\rho\pi}$ and $A^u_{B\omega\pi}$.

[2]Note however that a part of the 2-pion continuum contribution in this region is effectively absorbed in the ρ-meson total width (for more details see, e.g., [27]).

In what follows, we attribute a phase to each V-pole term,

$$A^p_{BV\pi} = |A^p_{BV\pi}|\exp(i\delta^{(p)}_{BV\pi}). \tag{33}$$

To reduce the number of free parameters, we fix the phase differences,

$$\delta^{(u)}_{B^-\rho^0\pi^-} - \delta^{(u)}_{B^-\omega\pi^-} = 0.033, \quad \delta^{(c)}_{B^-\rho^0\pi^-} - \delta^{(c)}_{B^-\omega\pi^-} = -3.65, \tag{34}$$

calculating it from QCDF, as explained in the previous section. Note that for the neutral mode the contribution of the ω meson is neglected and the corresponding difference is irrelevant. The three remaining phases $\delta^{(p)}_\rho$, $\delta^{(p)}_{J/\psi}$ and $\delta^{(p)}_{\psi(2S)}$ for each $p = u, c$ are included into the set of fit parameters. This set will be completed below by the fit parameters of the integrals over $\rho_h^{(p)}(s)$. Furthermore, we adopt the Breit-Wigner form of the vector meson contributions in (31) with an energy-dependent total width for the broad ρ resonance so that it vanishes at $q^2 < 4m_\pi^2$ and adopting constant total widths $\Gamma_V^{\rm tot}$ for the remaining narrow resonances.

To complete the ansatz for the hadronic dispersion relations, we have to specify the integrals over the hadronic spectral densities of excited and continuum states $\rho^{(u,c)}(s)$ in Eq. (31). In the region below the open charm threshold, $q^2 = s \le 4m_D^2$, apart from the two narrow charmonium resonances J/ψ and $\psi(2S)$, only the intermediate states with light quark-antiquark flavor content and spin-parity 1^- contribute. We make extensive use of the standard quark-hadron duality ansatz employed in the QCD sum rules [28] for the vector-meson channels. The integral over the hadronic spectral density $\rho_h^{(p)}(s)$ including $\rho', \omega', \ldots$ and continuum states with the ρ and ω quantum numbers is replaced by the spectral density calculated from OPE,

$$\rho_h^{(p)}(s)\theta(s-s_h) \simeq \frac{1}{\pi}(\text{Im}\mathcal{H}^{(p)}_{\text{fact,LO}\{u,d\}}(s) + \text{Im}\mathcal{H}^{(p)}_{\text{WA}}(s))\theta(s-s_0) + \frac{1}{\pi}\text{Im}\mathcal{H}^{(p)}_{\text{fact,LO}\{s\}}(s)\theta(s-\tilde{s_0}), \quad (p=u,c; s<4m_D^2), \tag{35}$$

where only the LO contributions are taken into account, including the leading-order quark loops and weak annihilation diagrams. The indices $\{u,d\}$ and $\{s\}$ mean that only the diagrams with u, d and s quarks, respectively, are taken into account. The duality threshold $s_0 \simeq 1.5\ \text{GeV}^2$ is chosen in accordance with the analysis of QCD sum rules in the light-vector-meson channels. In the contribution of the intermediate $\bar{s}s$ hadronic states to the spectral density $\rho_h^{(p)}(s)$ [the last term in (35)] we include also the small ϕ-meson pole contribution. This is reflected by the choice of a lower effective threshold parameter $\tilde{s}_0 = 4m_K^2 \simeq 1.0\ \text{GeV}^2$. Taking at $s = (q^2 + i\epsilon)$ the imaginary parts of the loop function (12),

$$\frac{1}{\pi}\mathrm{Im}g(q^2+i\epsilon,m_q^2)=\left(1+\frac{2m_q^2}{q^2}\right)\sqrt{1-\frac{4m_q^2}{q^2}}\theta(q^2-4m_q^2), \tag{36}$$

and of the WA contribution (18),

$$\frac{1}{\pi}\mathrm{Im}\mathcal{H}^{(p)}_{\mathrm{WA}}(q^2+i\epsilon)=\frac{Q_q f_B f_\pi}{2N_c\lambda_B m_B}e^{-q^2/(\lambda_B m_B)}\tilde{C}^p_{\mathrm{WA}}\theta(s), \tag{37}$$

we obtain

$$\begin{aligned}\rho^{(u)}_{LO}(s)=&\left[\frac{1}{24\pi^2}\left(\frac{2}{3}C_1+2C_2+C_3+\frac{C_4}{3}+C_5+\frac{C_6}{3}\right)f^+_{B\pi}(s)\right.\\&+Q_q\frac{f_B f_\pi}{2N_c\lambda_B m_B}e^{-s/(\lambda_B m_B)}(\delta_{qu}(C_2+3C_1)\\&\left.+\delta_{qd}(C_1+3C_2)+C_3+3C_4)\right]\theta(s-s_0)\\&-\frac{1}{24\pi^3}\left(\frac{4}{3}C_3+\frac{4}{3}C_4+C_5+\frac{C_6}{3}\right)\\&\times\mathrm{Im}g(s,m_s^2)f^+_{B\pi}(s)\theta(s-\tilde{s}_0)\end{aligned} \tag{38}$$

and a similar expression

$$\begin{aligned}\rho^{(c)}_{LO}(s)=&\left[\frac{1}{24\pi^2}\left(C_3+\frac{C_4}{3}+C_5+\frac{C_6}{3}\right)f^+_{B\pi}(s)\right.\\&\left.+Q_q\frac{f_B f_\pi}{2N_c\lambda_B m_B}e^{-s/(\lambda_B m_B)}(C_3+3C_4)\right]\theta(s-s_0)\\&-\frac{1}{24\pi^3}\left(\frac{4}{3}C_3+\frac{4}{3}C_4+C_5+\frac{C_6}{3}\right)\\&\times\mathrm{Im}g(s,m_s^2)f^+_{B\pi}(s)\theta(s-\tilde{s}_0).\end{aligned} \tag{39}$$

The two above expressions specify the adopted ansatz (35) at $s_h<s<4m_D^2$. Note that in the LO approximation, the spectral densities $\rho_h^{(p)}(s)$ are real functions. Following Ref. [10] we slightly modify the denominator in the dispersion integral over $s_0<s<4m_D^2$, replacing $s-q^2-i\epsilon\to s-q^2-i\sqrt{s}\Gamma_{\mathrm{eff}}(s,q^2)$ where $\Gamma_{\mathrm{eff}}(s,q^2)=\gamma\sqrt{s}\Theta(q^2-4m_\pi^2)$, $\gamma=0.2$ is the effective energy-dependent width, where the θ function ensures that this width is absent at negative q^2. This modification allows one to transform the smooth duality-driven spectral density towards more realistic series of equidistant vector mesons (cf. the model for the pion timelike form factor used in Ref. [27]). The addition of NLO corrections to the LO approximation for the duality ansatz remains a difficult task for a future improvement, involving a calculation of the spectral densities of the diagrams in Figs. 3 and 5.

The spectral densities $\rho_h^{(p)}(s)$ above the open charm threshold, $s>4m_D^2$, contain a complicated overlap of broad charmonium resonances and open-charm states, together with the light-quark contributions. Moreover, starting from $s=(m_B+m_\pi)^2$ the on-shell intermediate states with b flavor related to the imaginary part of the $B\to\pi$ form factor in the timelike region also contribute. Hence, a duality-based parameterization of the $s>4m_D^2$ part of the integral over $\rho_h^{(p)}(s)$ will not adequately reflect the complicated resonance-continuum structure of the hadronic spectral density. On the other hand, we only need this part of the integral at relatively small $q^2<m^2_{J/\psi}$; hence, following Ref. [10], we use a simple expansion in the powers of $q^2/4m_D^2$, truncating it at the first order,

$$\int_{4m_D^2}^{\infty}ds\frac{\rho^{(p)}(s)}{(s-q_0^2)(s-q^2-i\epsilon)}\simeq a_p+b_p\frac{q^2}{4m_D^2},\qquad p=u,c, \tag{40}$$

where $a_{u,c}=|a_{u,c}|e^{i\phi_a}$ and $b_{u,c}=|b_{u,c}|e^{i\phi_b}$ are two unknown complex parameters. Note that in Ref. [10] other parameterizations of the dispersion integral were also probed, and the results in the large recoil region were numerically close to the ones obtained with Eq. (40); hence, we will only consider this choice.

Finally, the dispersion relations (31) take the following form:

$$\begin{aligned}\mathcal{H}^{(p)}(q^2)-\mathcal{H}^{(p)}(q_0^2)=(q^2-q_0^2)\Bigg[&\sum_{V=\rho,\omega,J/\psi,\psi(2S)}k_V f_V\frac{|A^p_{BV\pi}|\exp(i\delta^{(p)}_{BV\pi})}{(m_V^2-q_0^2)(m_V^2-q^2-im_V\Gamma_V^{\mathrm{tot}})}\\&+\int_{\tilde{s}_0(s_0)}^{4m_D^2}ds\frac{\rho^{(p)}_{LO}(s)}{(s-q_0^2)(s-q^2-i\sqrt{s}\Gamma_{\mathrm{eff}}(s))}+|a_p|\exp(i\phi_a)+|b_p|\exp(i\phi_b)\frac{q^2}{4m_D^2}\Bigg].\end{aligned} \tag{41}$$

These two relations at $p=u$ and $p=c$ are then separately fitted to the OPE result obtained for the lhs at $q^2<0$. After that we can use the dispersion form of $\mathcal{H}^{(p)}(q^2)$ in $q^2>0$ and calculate the correction to the Wilson coefficient $\Delta C_9(q^2)$ defined in (7) in the whole large recoil region, which we specify as

$$4m_\ell^2\le q^2\lesssim m^2_{J/\psi}. \tag{42}$$

The resulting plots are presented in Figs. 9 and 10 for $B^\mp\to\pi^\mp\ell^+\ell^-$ and $B^{\bar{0}0}\to\pi^0\ell^+\ell^-$, respectively. Instead of showing the fit results for $\mathcal{H}^{(p)}$ directly, we present the directly related, but physically more relevant, plots for $\Delta C_9^{(B\pi)}(q^2)$. At q^2 above the J/ψ region our approach ceases to work, mostly because the contribution of the hadronic dispersion integral (40) to the dispersion relation

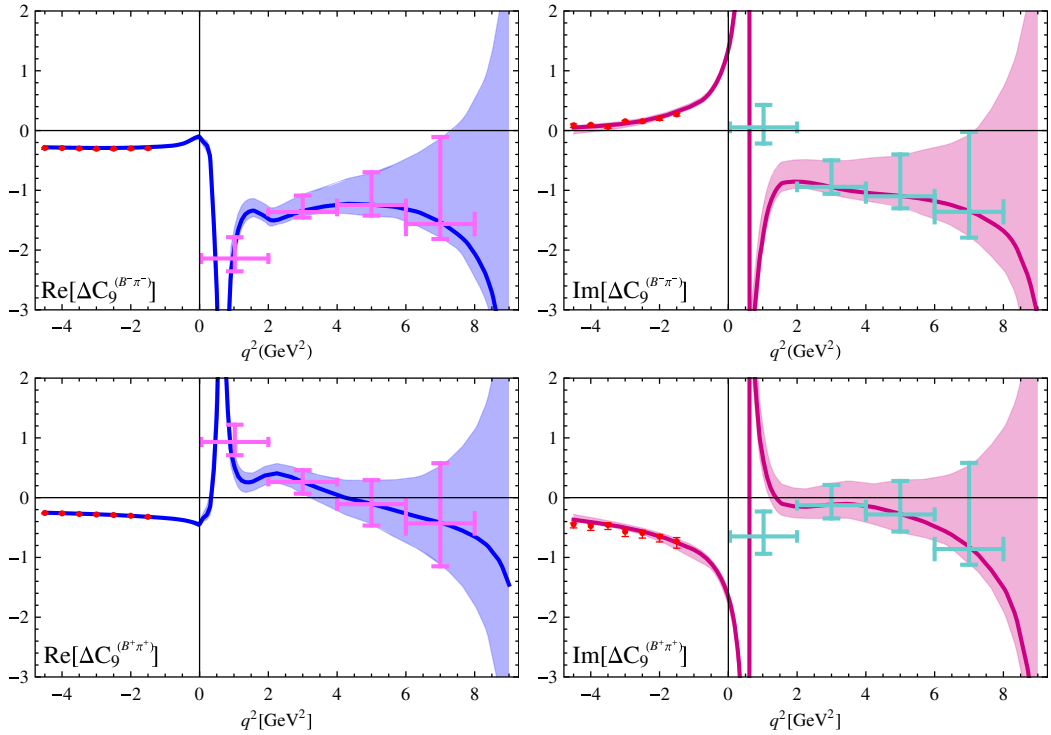

FIG. 9 (color online). The real part (upper left, blue online) and imaginary part (upper right, red online) of $\Delta C_9^{B\pi}(q^2)$ for $B^- \to \pi^- \ell^+ \ell^-$. The solid line is the dispersion relation fitted to the results calculated at $q^2 < 0$ at the central input. The shaded area indicates the estimated 68% C.L. uncertainties obtained in the fit to the "data" points (dots, red online) at $q^2 < 0$. The values of $\Delta C_9^{B\pi}(q^2)$ averaged over the q^2 bins are also shown. The lower panel contains the same plots for $B^+ \to \pi^+ \ell^+ \ell^-$.

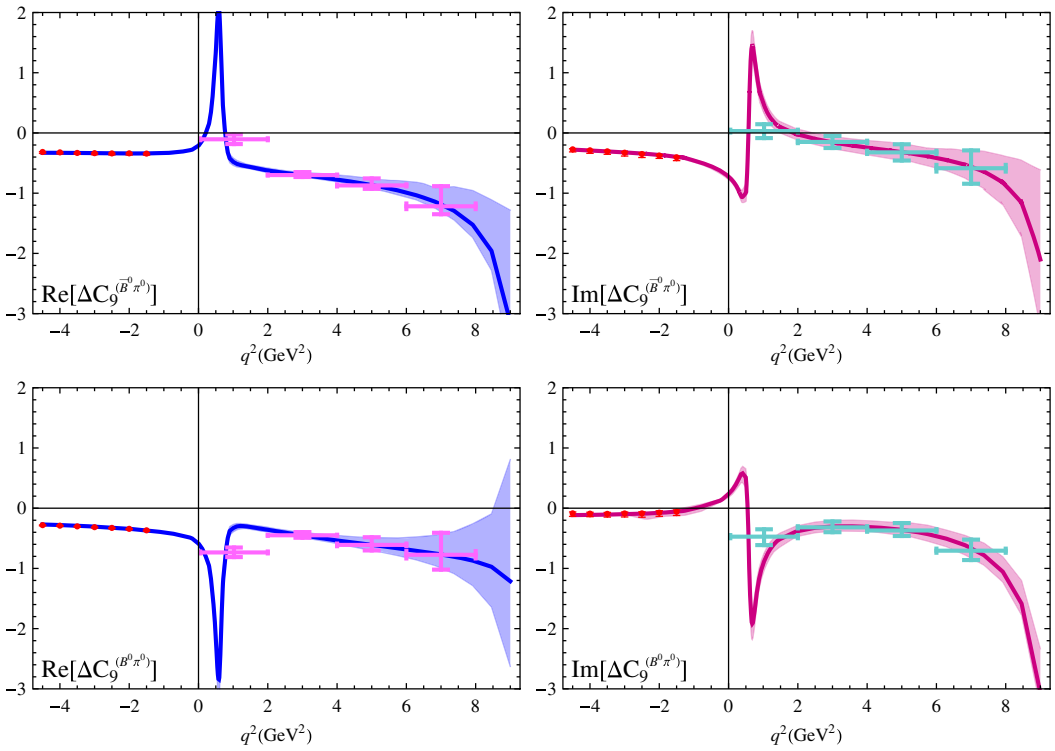

FIG. 10 (color online). The same as in Fig. 9 for $\bar{B^o} \to \pi^0 \ell^+ \ell^-$ (upper panel) and for $B^o \to \pi^0 \ell^+ \ell^-$ (lower panel).

increases and the simple polynomial parametrization cannot be used. This is also reflected by the growth of the uncertainties.

A few comments on the fit procedure of Eq. (41) are in order. Here we only discuss the $B^{\mp} \to \pi^{\mp} + \ell^+\ell^-$ decay, as the case of the neutral B decays is very similar. We represent the results of our calculation at negative q^2 values as "data" points and perform a χ^2 fit for our "model function" (dispersion relation), which is valid in both positive and negative q^2 regions, to the obtained points. A technical remark: The fit is performed by collecting in the "data" all parts of Eq. (41) which contains no fit parameters, i.e. only the resonance contributions (amplitudes and phases) and the polynomial continuum parameters are included in the "model function." Furthermore, we include the error correlation of the respective points at negative q^2, and, in addition, of the parameter $f^+_{B\pi}(q^2 = 0)$. The errors and the correlation coefficients of the "data" are obtained by varying the input parameters within their intervals given in Table I, while assuming no correlation between the parameters themselves. Thus, we include two correlated "data" sets in the fit for both charged B-meson transitions, namely, the real and imaginary parts of $\mathcal{H}^{(u)}$ and $\mathcal{H}^{(c)}$. We assume a Gaussian error interval of the input parameters for this procedure and a maximum error correlation of 80% for the numerical stability, providing also a more conservative estimate. As expected, the error correlation between the "data" points is very large and usually exceeds 80%. In addition, we find a positive correlation of, respectively, ~1%(10%) for the real part and ~40%(1%) for the imaginary part of $H^{(u)}$ ($H^{(c)}$) with $f^+_{B\pi}(q^2 = 0)$. The global minima are acceptable with $\chi^2_{\rm min} = 1.93$ and $\chi^2_{\rm min} = 2.53$ for u and c, respectively. The central values quoted here belong to the global minimum, whereas the 68% C.L. error estimate includes all minima in the $\delta\chi^2 < 1$ region.

VII. OBSERVABLES IN $B \to \pi\ell^+\ell^-$

Having calculated the nonlocal amplitudes in a form of the function $\Delta C_9^{(B\pi)}(q^2)$, we substitute this function in the amplitude (6) of the $B \to \pi\ell^+\ell^-$ decay and predict the observables in the accessible dilepton mass region (42).

The only element in the complete decay amplitude, that was not specified so far, is the ratio (8) of tensor and vector $B \to \pi$ form factors entering the contribution of the $O_{7\gamma}$ operator. To obtain it, we evaluate the ratio of LCSRs for both form factors obtained in Ref. [29]. The q^2 dependence turns out to be negligible in the whole region of validity of the sum rules, which covers the region (42), and we obtain

$$r_T(q^2) \simeq r_T(0) = 0.98 \pm 0.02. \tag{43}$$

The observables in $B \to \pi\ell^+\ell^-$ include the differential branching fraction, direct CP asymmetry and isospin asymmetry. Note that in SM the angular distribution in $B \to \pi\ell^+\ell^-$ at fixed q^2 is reduced to an overall factor $(1 - \cos^2\Theta)$ in the double differential distribution where Θ is the angle between the momentum of the lepton ℓ^- and the momentum of the B-meson in the dilepton center mass frame. In particular, the forward-backward asymmetry in $B \to \pi\ell^+\ell^-$ vanishes in the SM. Hence, it is sufficient to calculate the dilepton invariant mass distribution of the branching fraction,

$$\begin{aligned}\frac{1}{\tau_{B^-}}\frac{dB(B^- \to \pi^-\ell^+\ell^-)}{dq^2} &= \frac{G_F^2\alpha_{\rm em}^2|\lambda_t|^2}{1536\pi^5 m_B^3}|f^+_{B\pi}(q^2)|^2\lambda^{3/2}(m_B^2, m_\pi^2, q^2) \\ &\times\left\{\left|C_9 + \Delta C_9^{B\pi}(q^2) + \frac{2m_b}{m_B + m_\pi}C_7 r^T_{B\pi}(q^2)\right|^2 + |C_{10}|^2\right\}.\end{aligned} \tag{44}$$

For $\bar{B}^0 \to \pi^0\ell^+\ell^-$ the corresponding formula contains τ_{B^0} and an additional factor $1/2$ reflecting the normalization of the $\bar{B}^0 \to \pi^0$ form factor. The resulting plots are presented in Figs. 11 and 12. Averaging the above distribution over $q_1^2 \le q^2 \le q_2^2$ yields the binned branching fraction defined, e.g., for $B^- \to \pi^-\ell^+\ell^-$ as

$$\begin{aligned}&\mathcal{B}(B^- \to \pi^-\ell^+\ell^-[q_1^2, q_2^2]) \\ &\quad\equiv \frac{1}{q_2^2 - q_1^2}\int_{q_1^2}^{q_2^2} dq^2 \frac{dB(B^- \to \pi^-\ell^+\ell^-)}{dq^2}.\end{aligned} \tag{45}$$

The predicted binned branching fractions within the region (42) are presented in Table IV for all four flavor/charge combinations.

The most interesting characteristic of the $B \to \pi\ell^+\ell^-$ decay in SM is the q^2-dependent direct CP asymmetry defined for the charged B-meson modes as

$$\mathcal{A}_{CP}^{(-+)}(q^2) = \frac{dB(B^- \to \pi^-\ell^+\ell^-)/dq^2 - dB(B^+ \to \pi^+\ell^+\ell^-)/dq^2}{dB(B^- \to \pi^-\ell^+\ell^-)/dq^2 + dB(B^+ \to \pi^+\ell^+\ell^-)/dq^2}. \tag{46}$$

The asymmetry for the neutral B-meson modes denoted as $\mathcal{A}_{CP}^{(\bar{0}0)}(q^2)$ has the same expression with $B^- \to \bar{B}^0$, $B^+ \to B^0$. The results obtained for this observable are presented in Fig. 13.

Anticipating the future measurements of the q^2-averaged bins of CP asymmetry, we also calculate

$$\mathcal{A}_{CP}^{(-+)}[q_1^2, q_2^2] = \frac{\mathcal{B}(B^- \to \pi^-\ell^+\ell^-[q_1^2, q_2^2]) - \mathcal{B}(B^+ \to \pi^+\ell^+\ell^-[q_1^2, q_2^2])}{\mathcal{B}(B^- \to \pi^-\ell^+\ell^-[q_1^2, q_2^2]) + \mathcal{B}(B^+ \to \pi^+\ell^+\ell^-[q_1^2, q_2^2])}, \tag{47}$$

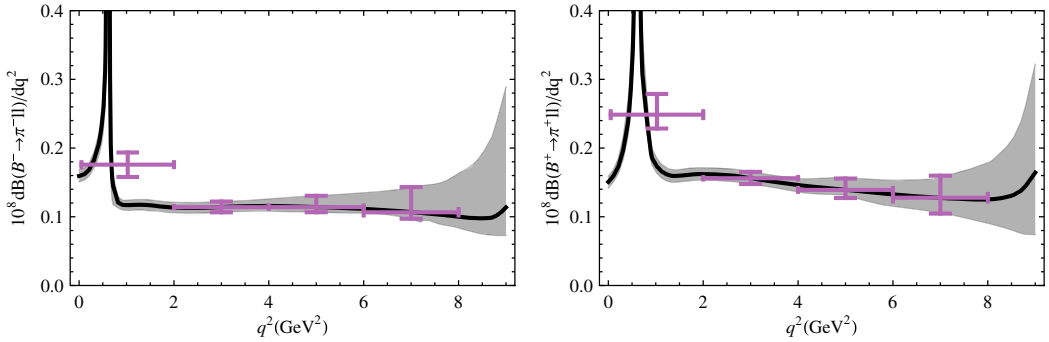

FIG. 11 (color online). Dilepton invariant mass spectrum and binned branching fraction (in GeV^{-2}) for $B^- \to \pi^-\ell^+\ell^-$ (left panel) and $B^+ \to \pi^+\ell^+\ell^-$ (right panel) with 68% C.L. errors (shaded region and error bars).

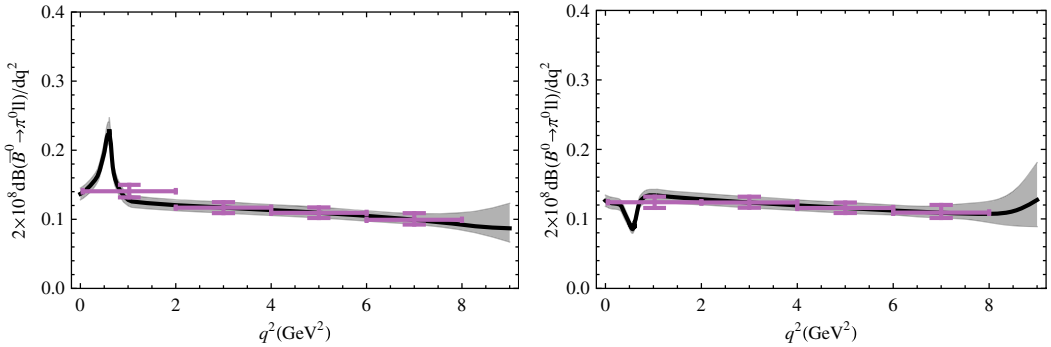

FIG. 12 (color online). The same as in Fig. 11 for $\bar{B}^0 \to \pi^0\ell^+\ell^-$ (left panel) and $B^0 \to \pi^+\ell^+\ell^-$ (right panel).

and the analogous binned asymmetry $\mathcal{A}_{CP}^{\bar{0}0}[q_1^2, q_2^2]$ for the neutral B-meson modes. Our predictions are collected in Table IV.

Finally, an important indicator of the spectator-dependent nonlocal effects, such as weak annihilation, is a nonvanishing differential isospin asymmetry defined as

$$\mathcal{A}_I(q^2) = \frac{2d\Gamma(\bar{B}^0 \to \pi^0\ell^+\ell^-)/dq^2 - d\Gamma(B^- \to \pi^-\ell^+\ell^-)/dq^2}{2d\Gamma(\bar{B}^0 \to \pi^0\ell^+\ell^-)/dq^2 + d\Gamma(B^- \to \pi^-\ell^+\ell^-)/dq^2}, \tag{48}$$

where the differential widths are understood as the CP-averaged ones. Our result is presented in Fig. 14 and the corresponding q^2-bins of isospin asymmetry,

$$\mathcal{A}_I[q_1^2, q_2^2] = \frac{2\Gamma(\bar{B}^0 \to \pi^0\ell^+\ell^-[q_1^2, q_2^2]) - \Gamma(B^- \to \pi^-\ell^+\ell^-[q_1^2, q_2^2])}{2\Gamma(\bar{B}^0 \to \pi^0\ell^+\ell^-[q_1^2, q_2^2]) + \Gamma(B^- \to \pi^-\ell^+\ell^-[q_1^2, q_2^2])}, \tag{49}$$

are given in Table IV.

TABLE IV. Binned branching fractions [in units of 10^{-8} (GeV^{-2})], direct CP asymmetry and isospin asymmetry of $B \to \pi\ell^+\ell^-$.

Bin (GeV^2)	[0.05, 2.0]	[2.0, 4.0]	[4.0, 6.0]	[6.0, 8.0]	[1.0, 6.0]
$\mathcal{B}(B^-)$	$0.176^{+0.018}_{-0.018}$	$0.114^{+0.008}_{-0.007}$	$0.114^{+0.016}_{-0.007}$	$0.107^{+0.036}_{-0.009}$	$0.126^{+0.013}_{-0.010}$
$\mathcal{B}(B^+)$	$0.249^{+0.030}_{-0.020}$	$0.156^{+0.009}_{-0.008}$	$0.139^{+0.016}_{-0.011}$	$0.128^{+0.030}_{-0.023}$	$0.168^{+0.016}_{-0.012}$
$2\times\mathcal{B}(\bar{B}^0)$	$0.140^{+0.009}_{-0.009}$	$0.117^{+0.008}_{-0.008}$	$0.109^{+0.008}_{-0.008}$	$0.099^{+0.010}_{-0.007}$	$0.119^{+0.008}_{-0.008}$
$2\times\mathcal{B}(B^0)$	$0.124^{+0.008}_{-0.008}$	$0.124^{+0.008}_{-0.008}$	$0.116^{+0.008}_{-0.007}$	$0.109^{+0.011}_{-0.008}$	$0.121^{+0.008}_{-0.008}$
$\mathcal{A}_{CP}^{(-+)}$	$-0.171^{+0.027}_{-0.045}$	$-0.156^{+0.027}_{-0.024}$	$-0.099^{+0.047}_{-0.025}$	$-0.091^{+0.093}_{-0.053}$	$-0.143^{+0.035}_{-0.029}$
$\mathcal{A}_{CP}^{(\bar{0}0)}$	$0.063^{+0.014}_{-0.015}$	$-0.028^{+0.010}_{-0.010}$	$-0.028^{+0.015}_{-0.015}$	$-0.047^{+0.023}_{-0.023}$	$-0.008^{+0.013}_{-0.013}$
$\mathcal{A}_I$	$-0.195^{+0.033}_{-0.035}$	$-0.020^{+0.031}_{-0.032}$	$-0.021^{+0.035}_{-0.053}$	$-0.021^{+0.060}_{-0.100}$	$-0.063^{+0.033}_{-0.040}$

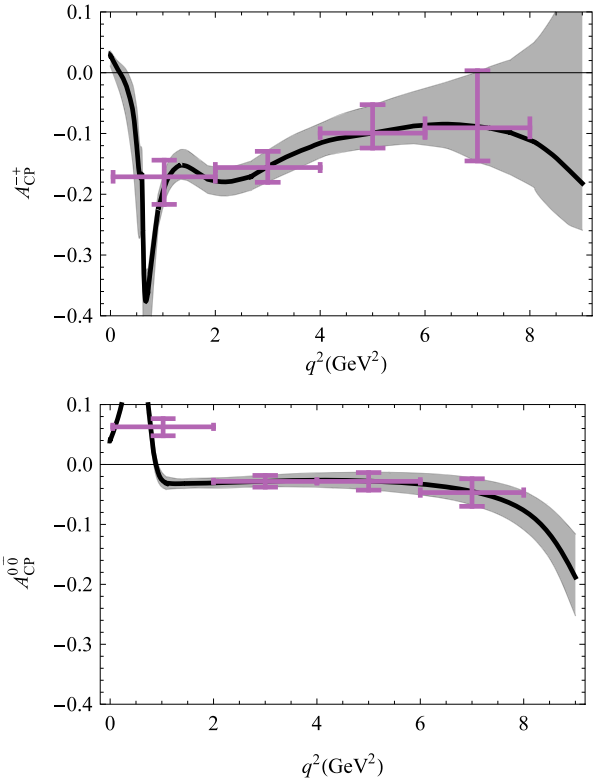

FIG. 13 (color online). Direct CP asymmetry in $B^{\pm} \to \pi^{\pm}\ell^+\ell^-$ (upper panel) and in $B^{\bar{0}0} \to \pi^0\ell^+\ell^-$ (lower panel).

Concluding the analysis of observables in $B \to \pi\ell^+\ell^-$, we notice that the magnitude of the predicted direct CP asymmetry for the charged B-decay modes is quite visible; for the neutral B decays this effect is expected to be small. In this and other observables our analysis generates large uncertainties in the region adjacent to J/ψ, whereas the uncertainties in the ρ and ω region are significantly smaller. This is partly caused by the use of QCDF to fix the relative phase between the nonleptonic amplitudes with ρ and ω, which probably leads to a slight underestimation of the errors in the resonance region.

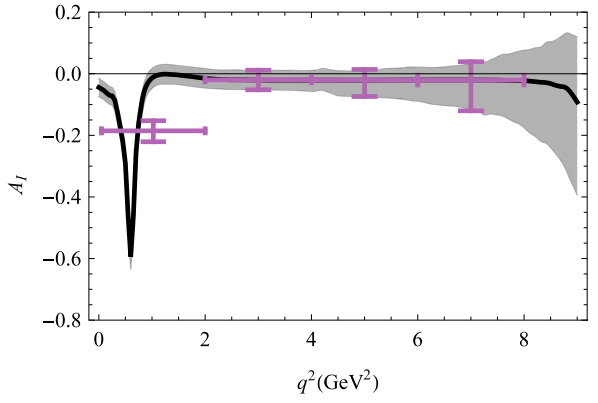

FIG. 14 (color online). Differential isospin asymmetry for $B \to \pi\ell^+\ell^-$ decays.

VIII. THE $B \to \pi\nu\bar{\nu}$ DECAY

The semileptonic FCNC decay $B \to \pi\nu\bar{\nu}$ is closely related to the charged lepton channel. Theoretically, this process is a very clean test of the SM, involving a single effective operator similar to O_{10}, whereas the nonlocal effects studied above are absent. Hence, we are in a position to predict the branching fraction of this decay with a better accuracy than for the $B \to \pi\ell^+\ell^-$. The only hadronic input in $B \to \pi\nu\bar{\nu}$ is the vector $B \to \pi$ form factor. The LCSR form factor [20] given in (27) provides an extrapolation beyond the large recoil region up to the kinematical limit $q^2 = (m_B - m_\pi)^2$, revealing a good agreement with the lattice QCD results in the low recoil region. We use this form factor to predict the total branching fraction of the $B \to \pi\nu\bar{\nu}$ decay.

The effective Hamiltonian encompassing the $b \to d\nu\bar{\nu}$ transition in the SM can be written as

$$\mathcal{H}_{\mathrm{eff}}^{b\to d\nu\bar{\nu}} = -\frac{4G_F}{\sqrt{2}}\lambda_t C_{10\nu}\frac{\alpha_{\mathrm{em}}}{4\pi}(\bar{d}_L\gamma_\mu b_L)(\bar{\nu}\gamma^\mu(1-\gamma_5)\nu), \quad (50)$$

with the (scale-independent) Wilson coefficient

$$C_{10\nu} = -\frac{1}{\sin^2\Theta_W}\left(X_0(x_t) + \frac{\alpha_s}{4\pi}X_1(x_t)\right), \quad (51)$$

where $x_t = m_t^2/m_W^2$ and the functions $X_0(x)$ and $X_1(x)$ can be found in Ref. [13].

The differential branching fraction of the $B^- \to \pi^-\nu\bar{\nu}$ decay summed over neutrino flavors has the form

$$\begin{aligned}\frac{1}{\tau_{B^-}}\frac{d\mathcal{B}(B^- \to \pi^-\nu\bar{\nu})}{dq^2} &\equiv \frac{1}{\tau_{B^-}}\sum_{\ell=e,\mu,\tau}\frac{d\mathcal{B}(B \to \pi\nu_\ell\bar{\nu}_\ell)}{dq^2} \\ &= \frac{G_F^2\alpha_{\mathrm{em}}^2}{256\pi^5 m_B^3}|\lambda_t|^2|C_{10\nu}|^2|f_{B\pi}^+(q^2)|^2\lambda^{3/2}(m_B^2, m_\pi^2, q^2). \quad (52)\end{aligned}$$

Substituting the form factor $f_{B\pi}^+(q^2)$ from Eq. (27), the numerical values of the Wilson coefficient $C_{10\nu} = -6.79$ and other parameters in Eq. (52), we obtain the differential branching fraction shown in Fig. 15. Integrating it over $0 < q^2 < (m_B - m_\pi)^2$ we obtain

$$\mathcal{B}(B^- \to \pi^-\nu\bar{\nu}) = 2\mathcal{B}(B^0 \to \pi^0\nu\bar{\nu}) = (2.39^{+0.30}_{-0.28}) \times 10^{-7}. \quad (53)$$

Despite the fact that this branching fraction is well within the reach of B-physics experiments, a significant problem is the identification of the final state with respect to the background.

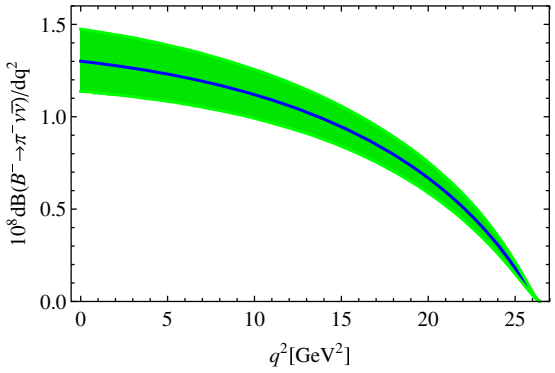

FIG. 15 (color online). The differential branching fraction of the $B^- \to \pi^- \nu\bar{\nu}$ decay.

IX. CONCLUSION

In this paper we calculated the hadronic input for the rare FCNC decay $B \to \pi\ell^+\ell^-$ in the large recoil region of the pion, i.e., at small and intermediate lepton-pair masses up to the J/ψ mass. We focused on the most difficult problem in the theory of these decays: the effects generated by a nonlocal overlap of the pointlike weak transition with the electromagnetic lepton-pair emission. At $q^2 > 0$ the nonlocality involves long distances, including the formation of hadronic resonances—the vector mesons. On the other hand, this part of the decay amplitude is not simply a background for the FCNC $b \to d\ell^+\ell^-$ transition, but provides the strong-interaction phase. The latter, combined with the CKM phase, generates the unique characteristics of the $B \to \pi\ell^+\ell^-$ decay in SM, that is, the q^2-dependent direct CP asymmetry, suppressed in the $b \to s\ell^+\ell^-$ decays.

To avoid the complications related to the long-distance part of the nonlocal effects, we employed the method used earlier in Ref. [10] for $B \to K\ell^+\ell^-$. The nonlocal contributions to $B \to \pi\ell^+\ell^-$ transitions were calculated one by one, combining QCDF and LCSRs at spacelike $q^2 < 0$, where the quark-level diagrams are well defined and the nonlocality is effectively reduced to the distances of $O(1/\sqrt{|q^2|})$. We also used the recently updated [20] $B \to \pi$ form factor from LCSR. The accuracy of our calculation is characterized by taking into account, in addition to the factorizable quark-loop effects and the factorizable NLO corrections, the important nonfactorizable contributions: the soft gluon emission, spectator scattering and weak annihilation. We then combined the quark-level calculation with the hadronic dispersion relation and fitted the parameters of the latter to access the $q^2 > 0$ region. The main result of our calculation is presented in a form of the q^2-dependent and process-specific correction $\Delta C_9^{(B\pi)}(q^2)$ to the Wilson coefficient of the semileptonic operator O_9. Apart from the numerical prediction for $\Delta C_9^{(B\pi)}(q^2)$, we also estimated the uncertainties due to the input parameter variation. We predicted the observables in $B \to \pi\ell^+\ell^-$, including the differential branching fraction, direct CP asymmetry and the isospin asymmetry. The main advantage of the method used in this paper is the possibility to access the ρ, ω resonance region and, simultaneously, to approach the charmonium region from below.

The accuracy of the calculation carried out in this paper can be improved further. On the theory side it is worth calculating the nonlocal contributions using entirely LCSRs instead of the QCDF approximation. This will allow one to assess the missing power corrections. Such analysis is possible at least for the weak annihilation and for the hard-spectator contributions. A more elaborated ansatz for the hadronic dispersion relation, including the radial excitations of light vector mesons, is also desirable. For that, more accurate data on the $B \to V\pi$ nonleptonic decays and a better understanding of the structure of various nonleptonic amplitudes are needed.

Let us compare our results with the two most recent analyses of the $B \to \pi\ell^+\ell^-$ decay. In [30], only the factorizable nonlocal contributions were taken into account, approximated by the quark-level diagrams at positive q^2, embedded in the short-distance coefficients. Only the differential branching fraction was calculated, with no prediction for the CP asymmetry. In [7], the QCDF method was systematically used at positive q^2, therefore the resonance region of q^2 was not accessible. In the region between 2 and 6 GeV^2 the branching fraction obtained in [7] is somewhat smaller than our result, whereas the CP asymmetry is close to our prediction.

We emphasize that our method produces a quantitative estimate of the nonlocal effects in the whole large-recoil region, starting from the kinematical threshold of the lepton-pair production. The price to pay is a model dependence of the ansatz for the dispersion relation, related to the nonleptonic $B \to V\pi$ decays. The function $\Delta C_9^{(B\pi)}(q^2)$ obtained in this paper can be used in further analyses of the $B \to \pi\ell^+\ell^-$ decay, e.g., when adding certain new physics contributions to the decay amplitude in the SM. But, first, it will be very interesting to confront our prediction for the direct CP asymmetry in $B \to \pi\ell^+\ell^-$ with the data. Note that the $b \to d\ell^+\ell^-$ effective interaction is also probed in $B_d \to \mu^+\mu^-$ decay. Its branching fraction measurement by LHCb and CMS Collaborations [31] still leaves some room for new physics, making further studies of $b \to d\ell^+\ell^-$ decays very important.

ACKNOWLEDGMENTS

The work of Ch. H. and A. K. is supported by DFG Research Unit FOR 1873 "Quark Flavour Physics and Effective Theories," Contract No. KH 205/2-1. A. R. acknowledges the support by the Michail-Lomonosov Program of the German Academic Exchange Service (DAAD) and the Ministry of Education and Science of

the Russian Federation (Project No. 11.9197.2014) and the Russian Foundation for Basic Research (Project No. 15-02-06033-a). We are grateful to Thorsten Feldmann, Thomas Mannel, Dirk Seidel, Xavier Virto, Danny van Dyk and Yuming Wang for useful comments. One of us (A. K.) is grateful to Johannes Albrecht for a helpful discussion.

APPENDIX A: OPERATORS AND CKM PARAMETERS

In Table V we list the operators entering the effective Hamiltonian (1), and their Wilson coefficients calculated at LO for three different renormalization scales, where $\alpha_{\rm em} = e^2/(4\pi)$ is the electromagnetic coupling and g_s is the strong coupling. We use the standard conventions for the operators O_i^p $(p = u, c)$ except the labeling of $\mathcal{O}_1^p$ and $\mathcal{O}_2^p$ is interchanged, as in [10]. In the quark-penguin operators $q = u, d, s, c, b$ and the mass of the d quark in $\mathcal{O}_{7\gamma}$ and $\mathcal{O}_{8g}$ is neglected. The sign conventions for covariant derivatives, γ-matrices, and left- and right-handed components of the quark fields are the same as quoted in the appendix of [10]. The electroweak parameters used to calculate the coefficients C_i are [19]

$$\alpha_{\rm em} = \frac{1}{129}, \qquad \sin^2(\Theta_W) = 0.23126,$$
$$m_W = 80.385\ \text{GeV}, \qquad G_F = 1.1663787 \times 10^{-5}\ \text{GeV}^{-2},$$
$$m_z = 91.186\ \text{GeV}, \qquad m_t = 173.3\ \text{GeV}. \tag{A1}$$

We use the CKM mixing matrix in terms of Wolfenstein parameters

$$V_{\rm CKM} = \begin{pmatrix} 1-\lambda^2/2 & \lambda & A\lambda^3(\rho - i\eta) \\ -\lambda & 1-\lambda^2/2 & A\lambda^2 \\ A\lambda^3(1-\rho-i\eta) & -A\lambda^2 & 1 \end{pmatrix},$$

taking into account that $\rho \simeq \bar{\rho}(1+\lambda^2/2)$ and $\eta \simeq \bar{\eta}(1+\lambda^2/2)$ and using the current values [19] obtained from the global CKM fit,

$$\lambda = 0.22537 \pm 0.00061, \qquad A = 0.814^{+0.023}_{-0.024},$$
$$\bar{\rho} = 0.117 \pm 0.021, \qquad \bar{\eta} = 0.353 \pm 0.013. \tag{A2}$$

This results in the following combinations of CKM elements we use:

$$\lambda_u/\lambda_t = -0.0274 - i0.3896, \qquad |\lambda_u/\lambda_t| = 0.3906,$$
$$\arg(\lambda_u/\lambda_t) = -94.02°$$
$$\lambda_c/\lambda_t = -0.9719 + i0.3998, \qquad |\lambda_c/\lambda_t| = 1.0509,$$
$$\arg(\lambda_c/\lambda_t) = 157.64°. \tag{A3}$$

APPENDIX B: AMPLITUDES OF $B \to \rho(\omega)\pi$ IN QCDF

Here we present the expressions of the QCDF amplitudes [11] for the $B^- \to (\rho^0, \omega)\pi^-$ nonleptonic decays. Our operators differs from the ones in [11] by a factor of $1/4$ whereas the labeling of $O_{1,2}$ is the same. The expressions for the parts of $B^- \to \rho^0\pi^-$ and $B^- \to \omega\pi^-$ amplitudes multiplying λ^p $(p = u, c)$ are

$$A^p_{B^-\rho\pi^-} = A_{\pi\rho}(\delta_{pu}[\alpha_2(\pi\rho) - \beta_2(\pi\rho)] - \alpha_4^p(\pi\rho) - \beta_3^p(\pi\rho)) + A_{\rho\pi}(\delta_{pu}[\alpha_1(\rho\pi) + \beta_2(\rho\pi)] + \alpha_4^p(\rho\pi) + \beta_3^p(\rho\pi)), \tag{B1}$$

$$A^p_{B^-\omega\pi^-} = A_{\pi\omega}(\delta_{pu}[\alpha_2(\pi\omega) + \beta_2(\pi\omega)] + 2\alpha_3^p(\pi\omega) + \alpha_4^p(\pi\omega) + \beta_3^p(\pi\omega)) + A_{\omega\pi}(\delta_{pu}[\alpha_1(\omega\pi) + \beta_2(\omega\pi)] + \alpha_4^p(\omega\pi) + \beta_3^p(\omega\pi)), \tag{B2}$$

where the factorized combinations of form factors and decay constants are

$$A_{\pi\rho(\omega)} = \frac{1}{2\sqrt{2}} f^+_{B\pi}(m_\rho^2) f_{\rho(\omega)}, \qquad A_{\rho(\omega)\pi} = \frac{1}{2\sqrt{2}} A^0_{B\rho(\omega)}(0) f_\pi. \tag{B3}$$

TABLE V. Effective operators and Wilson coefficients.

Operator	μ (GeV)	2.5	3.0	4.5
$\mathcal{O}_1^p = (\bar{d}_L\gamma_\mu p_L)(\bar{p}_L\gamma^\mu b_L)$	C_1	1.169	1.148	1.111
$\mathcal{O}_2^p = (\bar{d}^i_L\gamma_\mu p^j_L)(\bar{p}^j_L\gamma^\mu b^i_L)$	C_2	−0.360	−0.324	−0.255
$\mathcal{O}_3 = (\bar{d}_L\gamma_\mu b_L)\sum_q(\bar{q}_L\gamma^\mu q_L)$	$C_3(\times 10^{-2})$	1.700	1.503	1.144
$\mathcal{O}_4 = (\bar{d}^i_L\gamma_\mu b^j_L)\sum_q(\bar{q}^j_L\gamma^\mu q^i_L)$	$C_4(\times 10^{-2})$	−3.602	−3.271	−2.630
$\mathcal{O}_5 = (\bar{d}_L\gamma_\mu b_L)\sum_q(\bar{q}_R\gamma^\mu q_R)$	$C_5(\times 10^{-2})$	0.985	0.910	0.756
$\mathcal{O}_6 = (\bar{d}^i_L\gamma_\mu b^j_L)\sum_q(\bar{q}^j_R\gamma^\mu q^i_R)$	$C_6(\times 10^{-2})$	−4.829	−4.258	−3.236
$\mathcal{O}_{7\gamma} = -\frac{em_b}{16\pi^2}(\bar{d}_L\sigma^{\mu\nu}b_R)F_{\mu\nu}$	$C_7^{\rm eff}$	−0.356	−0.343	−0.316
$\mathcal{O}_{8g} = -\frac{g_s m_b}{16\pi^2}(\bar{d}^i_L\sigma_{\mu\nu}(T^a)^{ij}b^j_R)G^{a\mu\nu}$	$C_8^{\rm eff}$	−0.166	−0.160	−0.150
$\mathcal{O}_9 = \frac{\alpha_{\rm em}}{4\pi}(\bar{d}_L\gamma^\mu b_L)(\bar{\ell}\gamma_\mu\ell)$	C_9	4.514	4.462	4.293
$\mathcal{O}_{10} = \frac{\alpha_{\rm em}}{4\pi}(\bar{d}_L\gamma^\mu b_L)(\bar{\ell}\gamma_\mu\gamma_5\ell)$	C_{10}	−4.493	−4.493	−4.493

TABLE VI. Additional input parameters related to the light vector mesons and used in the QCDF amplitudes of $B \to \rho(\omega)\pi$ decays.

Parameter	References
$(m_u + m_d)(1\ \text{GeV}) = 7.0^{+1.4}_{-0.4}$ MeV	[19]
$f_+^{(B\pi)}(m_\rho^2) = 0.316 \pm 0.021$	[20]
$A_0^{B\rho}(0) = 0.396^{+0.039}_{-0.031}$	[24]
$A_0^{B\omega}(0) \simeq A_0^{B\rho}(0)$	
$f_\rho^\perp(1\ \text{GeV}) = (0.160 \pm 0.010)\ \text{GeV}$	[32]
$f_\omega^\perp(1\ \text{GeV}) = (0.145 \pm 0.010)\ \text{GeV}$	
$a_2^{\rho,\omega}(1\ \text{GeV}) = a_2^{\rho,\omega\perp}(1\ \text{GeV}) = 0.09^{+0.10}_{-0.07}$	

In addition to the already introduced notation, $A^0_{B\rho(\omega)}(0)$ in the above is the relevant $B \to \rho(\omega)$ form factor taken at $q^2 = 0$, neglecting the pion mass squared; for the $B \to \pi$ form factor we approximate $m_\rho^2 = m_\omega^2$. The parameters $\alpha_i^p(M_1M_2)$ are defined as follows [11]:

$$\alpha_i(M_1M_2) = a_i(M_1M_2), \quad i = 1, 2, \tag{B4}$$

$$\alpha_3^p = \begin{cases} a_3^p(M_1M_2) + a_5^p(M_1M_2), & \text{if } M_2 = \rho, \omega, \\ a_3^p(M_1M_2) - a_5^p(M_1M_2), & \text{if } M_2 = \pi, \end{cases} \tag{B5}$$

$$\alpha_4^p = \begin{cases} a_4^p(M_1M_2) + r_\chi^{M_2} a_6^p(M_1M_2), & \text{if } M_2 = \rho, \omega, \\ a_4^p(M_1M_2) - r_\chi^{M_2} a_6^p(M_1M_2), & \text{if } M_2 = \pi, \end{cases} \tag{B6}$$

where

$$r_\chi^\pi = \frac{2m_\pi^2}{m_b(m_u + m_d)}, \qquad r_\chi^{\rho,\omega} = \frac{2m_{\rho,\omega}}{m_b}\frac{f_{\rho,\omega}^\perp}{f_{\rho,\omega}}, \tag{B7}$$

and $f_{\rho(\omega)}^\perp$ is the vector-meson transverse decay constant, defined as

$$\langle 0|\bar{q}\sigma^{\mu\nu}q|V(q)\rangle = ik^\perp(\varepsilon_V^\mu q^\nu - \varepsilon_V^\nu q^\mu) f_V^\perp \tag{B8}$$

with $k^\perp = 1/\sqrt{2}$ for $q = u$, $V = \rho^0, \omega$.

The quantities $a_i^p(M_1M_2)$ have the form [2]

$$a_i^p(M_1M_2) = \left(C_i + \frac{C_{i\pm1}}{N_c}\right)N_i(M_2) + \frac{C_{i\pm1}}{N_c}\frac{C_F\alpha_s}{4\pi}\left[V_i(M_2) + \frac{4\pi^2}{N_c}H_i(M_1M_2)\right] + P_i^p(M_2), \tag{B9}$$

where the upper (lower) signs apply when i is odd (even); $N_i(M_2) = 0$ for $i = 6$ and $M_2 = \rho, \omega$ and $N_i(M_2) = 1$ in all other cases. The parameters $\beta_i^p(M_1M_2)$ involve the weak annihilation contributions

$$\beta_i^p(M_1M_2) \equiv \frac{-f_B f_{M_1} f_{M_2}}{2\sqrt{2}m_B^2 A_{M_1M_2}} b_i^p(M_1M_2). \tag{B10}$$

The expressions used for the separate contributions in Eqs. (B9), (B10) [$V_i(M_2)$ (one-loop vertex correction), $H_i(M_1M_2)$ (hard-spectator scattering), $P_i^p(M_1M_2)$ (penguin contractions) and $b_i^{(p)}(M_1M_2)$ (weak annihilation)] can be found in [2,11]. They were calculated in QCDF in terms of the perturbative kernels convoluted with the DAs of the B meson, pion and $\rho(\omega)$ meson. The latter DAs include the Gegenbauer moments $a_2^{\rho(\omega)}$ and $a_2^{\rho,\perp}$, similar to the ones that are contained in the pion twist-2 DA (25).

For the numerical analysis of the $B^- \to \rho(\omega)\pi$ amplitudes we need additional input parameters listed in Table VI, where, in order to decrease the uncertainty, the $A_0^{B\omega}(0)$ form factor is calculated multiplying the ratio $A_0^{B\omega}(0)/f_+^{(B\pi)}(0)$ obtained from the LCSRs with the B-meson DAs [24] with the form factor $f_+^{(B\pi)}(0)$ taken from the most accurate LCSR with pion DAs [20].

[1] R. Aaij *et al.* (LHCb Collaboration), J. High Energy Phys. 12 (2012) 125.
[2] M. Beneke, G. Buchalla, M. Neubert, and C. T. Sachrajda, Phys. Rev. Lett. **83**, 1914 (1999); Nucl. Phys. **B606**, 245 (2001).
[3] M. Beneke, T. Feldmann, and D. Seidel, Nucl. Phys. **B612**, 25 (2001).
[4] M. Beneke, T. Feldmann, and D. Seidel, Eur. Phys. J. C **41**, 173 (2005).
[5] M. Bartsch, M. Beylich, G. Buchalla, and D.-N. Gao, J. High Energy Phys. 11 (2009) 011.
[6] C. Bobeth, G. Hiller, and G. Piranishvili, J. High Energy Phys. 12 (2007) 040.
[7] W. S. Hou, M. Kohda, and F. Xu, Phys. Rev. D **90**, 013002 (2014).
[8] J. Lyon and R. Zwicky, Phys. Rev. D **88**, 094004 (2013).
[9] A. Khodjamirian, T. Mannel, A. A. Pivovarov, and Y.-M. Wang, J. High Energy Phys. 09 (2010) 089.
[10] A. Khodjamirian, T. Mannel, and Y. M. Wang, J. High Energy Phys. 02 (2013) 010.
[11] M. Beneke and M. Neubert, Nucl. Phys. **B675**, 333 (2003).

[12] B. Grinstein, M. J. Savage, and M. B. Wise, Nucl. Phys. **B319**, 271 (1989); M. Misiak, Nucl. Phys. **B393**, 23 (1993); A. J. Buras and M. Munz, Phys. Rev. D **52**, 186 (1995).
[13] G. Buchalla, A. J. Buras, and M. E. Lautenbacher, Rev. Mod. Phys. **68**, 1125 (1996).
[14] A. G. Grozin and M. Neubert, Phys. Rev. D **55**, 272 (1997).
[15] M. Beneke and T. Feldmann, Nucl. Phys. **B592**, 3 (2001).
[16] H. H. Asatryan, H. M. Asatrian, C. Greub, and M. Walker, Phys. Rev. D **65**, 074004 (2002).
[17] H. M. Asatrian, K. Bieri, C. Greub, and M. Walker, Phys. Rev. D **69**, 074007 (2004).
[18] D. Seidel, Phys. Rev. D **70**, 094038 (2004).
[19] K. A. Olive *et al.* (Particle Data Group Collaboration), Chin. Phys. C **38**, 090001 (2014).
[20] I. Sentitemsu Imsong, A. Khodjamirian, T. Mannel, and D. van Dyk, J. High Energy Phys. 02 (2015) 126.
[21] P. Gelhausen, A. Khodjamirian, A. A. Pivovarov, and D. Rosenthal, Phys. Rev. D **88**, 014015 (2013); **89**, 099901(E) (2014); **91**, 099901(E) (2015).
[22] V. M. Braun, D. Y. Ivanov, and G. P. Korchemsky, Phys. Rev. D **69**, 034014 (2004).
[23] A. Khodjamirian, T. Mannel, N. Offen, and Y.-M. Wang, Phys. Rev. D **83**, 094031 (2011).
[24] A. Khodjamirian, T. Mannel, and N. Offen, Phys. Rev. D **75**, 054013 (2007).
[25] H. Boos, T. Mannel, and J. Reuter, Phys. Rev. D **70**, 036006 (2004).
[26] P. Frings, U. Nierste, and M. Wiebusch, Phys. Rev. Lett. **115**, 061802 (2015).
[27] C. Bruch, A. Khodjamirian, and J. H. Kuhn, Eur. Phys. J. C **39**, 41 (2005).
[28] M. A. Shifman, A. I. Vainshtein, and V. I. Zakharov, Nucl. Phys. **B147**, 385 (1979); **B147**, 448 (1979).
[29] G. Duplancic, A. Khodjamirian, T. Mannel, B. Melic, and N. Offen, J. High Energy Phys. 04 (2008) 014.
[30] A. Ali, A. Y. Parkhomenko, and A. V. Rusov, Phys. Rev. D **89**, 094021 (2014).
[31] V. Khachatryan *et al.* (CMS and LHCb Collaborations), Nature (London) **522**, 68 (2015).
[32] P. Ball and R. Zwicky, Phys. Rev. D **71**, 014029 (2005).

Chapter 3

Higher-twist effects in light-cone sum rules for $B \to \pi$ form factor

Published as an article in:
A.V. Rusov, Eur.Phys.J. **C77** (2017) 442.

Contributions of the authors to the article.
A.V. Rusov is the only author of this article.

Eur. Phys. J. C (2017) 77:442
DOI 10.1140/epjc/s10052-017-5000-9

THE EUROPEAN PHYSICAL JOURNAL C

Regular Article - Theoretical Physics

Higher-twist effects in light-cone sum rule for the $B \to \pi$ form factor

Aleksey V. Rusov[1,2,a]

[1] Theoretische Physik 1, Naturwissenschaftlich-Technische Fakultät, Universität Siegen, 57068 Siegen, Germany
[2] Department of Theoretical Physics, P.G. Demidov Yaroslavl State University, Yaroslavl 150000, Russia

Received: 12 May 2017 / Accepted: 17 June 2017

Abstract We calculate the higher-twist corrections to the QCD light-cone sum rule for the $B \to \pi$ transition form factor. The light-cone expansion of the massive quark propagator in the external gluonic field is extended to include new terms containing the derivatives of the gluon-field strength. The resulting analytical expressions for the twist-5 and twist-6 contributions to the correlation function are obtained in a factorized approximation, expressed via the product of the lower-twist pion distribution amplitudes and the quark-condensate density. The numerical analysis reveals that new higher-twist effects for the $B \to \pi$ form factor are strongly suppressed. This result justifies the conventional truncation of the operator product expansion in the light-cone sum rules up to twist-4 terms.

1 Introduction

Accurate calculation of the $B \to \pi$ transition form factors in QCD plays an important role, since, for instance, the vector form factor is used for the determination of the Cabibbo–Kobayashi–Maskawa (CKM) matrix element V_{ub} from the experimental data on the exclusive $B \to \pi \ell \nu_\ell$ decays. The $B \to \pi$ transition form factors are nonpertubative quantities accounting for the complicated quark–gluon dynamics inside the meson states and can be calculated using different QCD-based approaches. Among them, the method of light-cone sum rules (LCSRs) [1,2] is applicable at large hadronic recoil [3,4]. The main advantage of this method is the possibility to perform a calculation in full QCD, with finite b-quark mass. The starting object of the calculation is a properly designed correlation function of the quark currents for which the operator product expansion (OPE) near the light cone is applicable. Within OPE, the correlation function is decomposed into a series of the hard-scattering kernels convoluted with the pion light-cone distribution amplitudes (DAs) of the growing twist. The result of the OPE for correlation function is related to the $B \to \pi$ form factor employing the hadronic dispersion relation and quark–hadron duality.

At present, the accuracy of the LCSR calculation of heavy-to-light transition form factors is limited by the contributions of the operators up to twist 4. The results for the relevant partial contributions of the twist-2, -3 and -4 terms to the LCSR as well as radiative gluon corrections to the corresponding hard-scattering kernels of the twist-2 and twist-3 terms can be found in [3–8]. Moreover, a β_0 estimation for the twist-2 $O(\alpha_s^2)$ contributions can be found in [9]. It is important to note that the contributions of even- and odd-twist terms in the OPE form two separate hierarchies with respect to the lowest twist-2 and twist-3 terms, respectively. Note also that the twist-3 term, despite power suppression, contains a "chirally enhanced" parameter $\mu_\pi = m_\pi^2/(m_u + m_d)$, which renders the twist-3 contribution to the same order of magnitude as the twist-2 one. The contribution of twist-4 term was found to be significantly suppressed in comparison with the corresponding twist-2 one [5]. Such a comparison in the odd-twist hierarchy is still not possible due to missing estimate of twist-5 effects. Moreover, an estimate of the twist-6 term contribution to LCSR will allow us to confirm the expected power suppression of the higher twists in the even-twist hierarchy. The main purpose of this work is to evaluate the twist-5 and twist-6 contributions to the LCSR for the $B \to \pi$ form factors.

The calculation of the higher twist effects in the OPE near the light cone is interesting for several reasons. As mentioned in Ref. [11], the twist-3 and twist-4 operators cannot be factorized as a product of the gauge-invariant operators of lower twist. There are several operators of twist 5 and twist 6 which can be factorized as a product of the gauge-invariant operators of lower twist. Sandwiched between the vacuum and one-pion state, such operators generally produce two types

[a] e-mail: rusov@physik.uni-siegen.de

Published online: 04 July 2017

of contributions: factorizable ones in terms of a lower-twist two-particle distribution amplitude times quark-condensate and nonfactorizable ones, which give rise to genuine twist-5 and twist-6 multiparton pion distribution amplitudes. As argued in [11], in the context of conformal symmetry the contributions of higher Fock states are strongly suppressed and their contributions to the sum rules are probably negligible. Factorizable contributions, on the other hand, can be comparatively large. Hence their calculation practically solves the problem of investigating the OPE beyond the twist-4 level.

In [11] and [12] the factorizable twist-6 contributions in LCSRs for the pion electromagnetic and $\pi\gamma^*\gamma$ form factors, respectively, were computed. In fact, in these sum rules the twist-6 contributions are the only ones which arise in the presence of virtual massless (u- or d)-quarks in the correlation function, hence, only the even twists are relevant there. Here we extend the analogous calculation to the correlation function with a massive virtual quark. In this case both factorizable twist-5 and twist-6 terms contribute to LCSR. In order to obtain these contributions one needs the massive quark propagator expanded near the light cone up to the terms including the derivatives of the gluon-field strength. The analytical expression for this propagator as well as the factorizable twist-5 and twist-6 contributions to LCSR represent new results obtained here.

The paper is organised as follows. Section 2 is devoted to the derivation of the new terms in the expansion of the massive quark propagating in the external gluonic field near the light cone. In Sect. 3 the detailed calculation of the diagrams corresponding to the factorizable twist-5 and twist-6 contributions to the LCSR for the vector $B \to \pi$ form factor is presented. Section 4 contains the relevant numerical estimates and Sect. 5 the concluding discussion. Some useful formulae are collected in the appendix.

2 Light-cone expansion of the massive quark propagator in the external gluon field

For our purpose we need the light-cone (LC) expansion of the quark propagator in the external gluon field. The corresponding expression including the terms with the covariant derivatives of the gluon-field strength is known only in the case of massless quark and was derived for instance in [10] (see also [11]). For a *massive* quark propagator the corresponding result is known only at leading order of the LC-expansion in the gluon field. To estimate the higher twist effects in the $B \to \pi$ form factors we need also to include the higher order terms in LC-expansion which are proportional to the covariant derivatives of the gluon-field strength. This task is technically more involved due to a presence of the quark mass m.

In order to get the LC-expansion of the massive quark propagator up to the needed accuracy we start from the definition of the quark propagator:

$$S(x,x') = -i\langle 0|T\{\psi(x),\bar{\psi}(x')\}|0\rangle, \tag{1}$$

where $\psi(x)$ denotes the massive quark field operator. Hereafter we choose $x' = 0$ for simplicity. The propagator satisfies the usual Green-function equation,

$$(i\gamma^\mu\partial_\mu + g_s\gamma^\mu A_\mu(x) - m)S(x,0) = \delta^{(4)}(x), \tag{2}$$

where $A_\mu = A^a_\mu\lambda^a/2$ is the four-potential of the gluon field, and λ^a are the Gell-Mann matrices ($a = 1,\dots 8$). The solution of (2) can be presented in the form of a pertubative series in the power of the strong coupling g_s:

$$iS(x,0) = iS^{(0)}(x) + iS^{(1)}(x) + \cdots \tag{3}$$

where

$$iS^{(1)}(x) = g_s\int d^4y\, iS^{(0)}(x-y)\, i\not{A}(y)\, iS^{(0)}(y), \tag{4}$$

and $S^{(0)}$ denotes the free quark propagator. The four-potential of the gluon field is taken in the Fock–Schwinger (of fixed point) gauge, so that $(x_\mu - x'_\mu)A^\mu(x) = 0$ and $x' = 0$. For further calculation it is convenient to use the free quark propagator $S^{(0)}(x-y)$ in the form of the so-called α-representation

$$S^{(0)}(x-y) = -i\int\limits_0^\infty \frac{\mathrm{d}\alpha}{16\pi^2\alpha^2}\left(m + i\frac{\not{x}-\not{y}}{2\alpha}\right)e^{-m^2\alpha+\frac{(x-y)^2}{4\alpha}}, \tag{5}$$

which allows us to rewrite the first order correction $S^{(1)}(x,0)$ to the propagator as follows:

$$S^{(1)}(x,0) = \frac{g_s}{(16\pi^2)^2}\int\limits_0^\infty\frac{\mathrm{d}\alpha}{\alpha^2}\int\limits_0^\infty\frac{\mathrm{d}\beta}{\beta^2}\int d^4y\left(m + i\frac{\not{x}-\not{y}}{2\alpha}\right) \times \not{A}(y)\left(m + i\frac{\not{y}}{2\beta}\right)e^{-m^2(\alpha+\beta)}e^{\frac{(x-y)^2}{4\alpha}+\frac{y^2}{4\beta}}. \tag{6}$$

Transforming the integration variable β as

$$\beta = \frac{\alpha u}{1-u}, \quad 0 < \beta < \infty \quad \text{so that} \quad 0 < u < 1, \tag{7}$$

we introduce a new variable:

$$y' = y - ux. \tag{8}$$

Taking into account the replacements (7) and (8) one can represent Eq. (6) in the form (hereafter we redefine $y' \to y$):

$$
\begin{aligned}
S^{(1)}(x,0) &= \frac{g_s}{(16\pi^2)^2}\int\limits_0^1 \frac{\mathrm{d}u}{u^2}\int\limits_0^\infty \frac{\mathrm{d}\alpha}{\alpha^3}\\
&\times \int d^4y\, e^{-m^2\alpha/\bar u} e^{[y^2+x^2u\bar u]/(4\alpha u)}\\
&\times \Big\{ m^2 \not{A}(y+ux) + \frac{im}{2\alpha u}\big[2u\bar u(x\cdot A(y+ux))\\
&- 2u(y\cdot A(y+ux)) + \not{A}(y+ux)\not{y}\big]\\
&- \frac{\bar u}{4\alpha^2 u}\big[u\bar u \not{x}\not{A}(y+ux)\not{x} - u\not{y}\not{A}(y+ux)\not{x}\\
&+ \bar u\not{x}\not{A}(y+ux)\not{y} - \not{y}\not{A}(y+ux)\not{y}\big]\Big\},
\end{aligned}
\tag{9}
$$

where $\bar u = 1-u$, $(x(y)\cdot A) \equiv x_\mu(y_\mu)A^\mu$. After that we expand the field $A_\alpha(y+ux)$ in powers of the deviation y_μ from the point ux near the light cone ($x^2 \simeq 0$):

$$
\begin{aligned}
A_\alpha(y+ux) = A_\alpha(ux) &+ \partial_\mu A_\alpha(ux)y^\mu + \frac{1}{2}\partial_\mu\partial_\nu A_\alpha(ux)y^\mu y^\nu\\
&+ \frac{1}{6}\partial_\mu\partial_\nu\partial_\rho A_\alpha(ux)y^\mu y^\nu y^\rho + \cdots,
\end{aligned}
\tag{10}
$$

with the following shorthand notation: $\partial_\mu A_\alpha(ux) \equiv \frac{\partial A_\alpha(z)}{\partial z^\mu}\Big|_{z=ux}$. Substituting the expansion (10) in (9) allows one to calculate $S^{(1)}(x,0)$ order by order. Performing the Wick rotation $y_0 \to -iy_4$, one reduces the integrals over d^4y to the standard Gaussian integrals. After integration over d^4y, one calculates the integrals over α introducing the modified Bessel function of the second kind, $K_n(z)$:

$$
\begin{aligned}
&\int\limits_0^\infty \frac{\mathrm{d}\alpha}{\alpha^n}\exp\left[-\frac{m^2\alpha}{1-u} + \frac{x^2(1-u)}{4\alpha}\right] = 2\left(\frac{2m}{\sqrt{-x^2}(1-u)}\right)^{\frac{n-1}{2}}\\
&\times K_{n-1}(m\sqrt{-x^2}), \quad x^2 < 0.
\end{aligned}
\tag{11}
$$

Then we perform some transformations in order to relate the derivatives of $A_\rho(xu)$ with $G^{\mu\nu}(ux)$ and its derivatives. The first term in the expansion (10) yields the scalar product $(x\cdot A)$, which vanishes in the Fock–Schwinger gauge. Since $S^{(1)}(x,0)$ has $\mathcal{O}(g_s)$ accuracy, the partial derivatives ∂_μ can be replaced by the covariant ones D_μ. Taking into account the definition of the gluon-field strength tensor $G_{\mu\nu} = G^a_{\mu\nu}\lambda^a/2 = D_\mu A_\nu - D_\nu A_\mu$, one relates then the covariant derivatives of A_μ with $G_{\mu\nu}$ and its derivatives. We found that the terms proportional to $D^\mu A_\mu$ vanish after integration by parts in the variable u, allowing one to present the final result for the propagator in terms of the gluon-field strength only.

After a lengthy but straightforward calculation we arrive at the following expression for the massive quark propagator expanded near the light cone, including terms up to the second derivative of the gluon-field strength:[1]

$$
\begin{aligned}
S(x,0) = &-\frac{im^2}{4\pi^2}\left[\frac{K_1\big(m\sqrt{-x^2}\big)}{\sqrt{-x^2}} + i\frac{\not{x}}{-x^2}K_2\big(m\sqrt{-x^2}\big)\right]\\
&- \frac{ig_s}{16\pi^2}\int\limits_0^1 \mathrm{d}u\Bigg[mK_0(m\sqrt{-x^2})(G(ux)\cdot\sigma)\\
&+ \frac{im}{\sqrt{-x^2}}K_1(m\sqrt{-x^2})[\bar u\not{x}(G(ux)\cdot\sigma) + u(G(ux)\cdot\sigma)\not{x}]\\
&- 2u\bar u\Bigg(imK_0\big(m\sqrt{-x^2}\big)\\
&- \frac{m\not{x}}{\sqrt{-x^2}}K_1(m\sqrt{-x^2})\Bigg)x_\mu D_\nu G^{\nu\mu}(ux)\\
&+ K_0\big(m\sqrt{-x^2}\big)(2u\bar u - 1)\gamma_\mu D_\nu G^{\nu\mu}(ux)\\
&- u\bar u(1-2u)K_0\big(m\sqrt{-x^2}\big)x_\mu \not{D} D_\nu G^{\nu\mu}(ux)\\
&- iu\bar u K_0\big(m\sqrt{-x^2}\big)\epsilon_{\sigma\mu\nu\rho}x^\sigma\gamma^\mu\gamma_5 D^\nu D_\alpha G^{\alpha\rho}(ux)\\
&+ u\bar u\sqrt{-x^2}K_1\big(m\sqrt{-x^2}\big)\sigma_\rho{}^\nu D_\nu D_\mu G^{\mu\rho}(ux)\Bigg] + \cdots
\end{aligned}
\tag{12}
$$

where $(G\cdot\sigma) \equiv G_{\mu\nu}\sigma^{\mu\nu}$, $\sigma^{\mu\nu} = (i/2)[\gamma^\mu,\gamma^\nu]$, and dots denote the higher powers of the light-cone expansion of $G_{\mu\nu}$ and corrections with two and more gluons, which are beyond the approximation we need. Taking into account the asymptotics of the Bessel functions,

$$
\begin{aligned}
&K_0(m\sqrt{-x^2})\Big|_{m\to 0} \sim -\gamma_E - \ln\left(\frac{m}{2}\right) - \frac{1}{2}\ln(-x^2),\\
&\sqrt{-x^2}K_1\big(m\sqrt{-x^2}\big)\Big|_{m\to 0} \sim \frac{1}{m},
\end{aligned}
\tag{13}
$$

one reproduces the corresponding result in the case of the massless quark given in [10,11].

We also found that the resulting expression, Eq. (12), can be rewritten in an equivalent Fourier-transformed form:

$$
\begin{aligned}
S(x,0) = \int \frac{d^4p}{(2\pi)^4}e^{-ipx}\Bigg\{&\frac{\not{p}+m}{p^2-m^2} - \frac{g_s}{(p^2-m^2)^3}\\
&\times\int\limits_0^1 \mathrm{d}u\Bigg[\frac{1}{2}m(p^2-m^2)(G(ux)\cdot\sigma)\\
&+ \frac{1}{2}(p^2-m^2)(\bar u\not{p}(G(ux)\cdot\sigma) + u(G(ux)\cdot\sigma)\not{p})
\end{aligned}
$$

[1] This form of the propagator has been derived in the space-like region of x^2. Performing similar calculations for positive x^2 one can demonstrate that the propagator is expressed via the Hankel functions of the second kind $H_n^{(2)}(z)$. Nevertheless, the representation (12) can also be used for positive x^2 having in mind the following relation between these special functions:

$$K_n(iz) = \frac{\pi}{2}(-i)^{n+1}H_n^{(2)}(z), \quad z>0,$$

allowing one to continue Bessel functions $K_n(m\sqrt{-x^2})$ to the positive x^2-domain.

$$
\begin{aligned}
&- 4u\bar{u}(\not{p}+m)p_\mu D_\nu G^{\nu\mu}(ux)\\
&-\frac{1}{2}(p^2-m^2)\gamma_\mu D_\nu G^{\nu\mu}(ux)\\
&- 2iu\bar{u}(1-2u)p_\mu \not{p} D_\nu G^{\nu\mu}(ux)\\
&+ 2u\bar{u}\epsilon_{\sigma\mu\nu\rho}p^\sigma \gamma^\mu\gamma_5 D^\nu D_\alpha G^{\alpha\rho}(ux)\\
&- 2mu\bar{u}\sigma_\rho{}^\nu D_\nu D_\mu G^{\mu\rho}(ux)+\cdots\Big]\Big\}. \qquad (14)
\end{aligned}
$$

The first terms of this expression are in full agreement with the LC-expansion of the massive quark propagator given in [4], and the terms with the covariant derivative of the gluon-field strength represent a new result of this paper.

3 Factorizable twist-5 and twist-6 contributions to the $B \to \pi$ form factor

The starting object for a calculation of the $B \to \pi$ form factors in the framework of the LCSR approach is the following correlation function of the B-meson interpolating and the $b \to u$ weak transition currents:

$$
\begin{aligned}
F_\mu(p,q) &= i\int d^4x\, e^{iqx}\langle\pi(p)|T\{\bar{u}(x)\gamma_\mu b(x),\\
&\qquad m_b\bar{b}(0)i\gamma_5 d(0)\}|0\rangle\\
&= F(q^2,(p+q)^2)p_\mu + \tilde{F}(q^2,(p+q)^2)q_\mu, \qquad (15)
\end{aligned}
$$

where p is the four-momentum of the pion, q is the outgoing four-momentum, and m_b is the b-quark mass. For definiteness, we consider the $\bar{B}_d^0 \to \pi^+$ flavour configuration. The Lorentz-invariant amplitudes $F(q^2,(p+q)^2)$ and $\tilde{F}(q^2,(p+q)^2)$ are used for the calculation of the vector and scalar form factors. In this paper we focus on an estimate of the higher twist effects for the vector form factor, hence, we need to consider only the amplitude $F(q^2,(p+q)^2)$. In the framework of LCSR approach one considers the correlation function (15) in the kinematic domain $q^2 \ll m_b^2$ and $(p+q)^2 \ll m_b^2$, far from the b-flavour threshold. In this domain the separations near the light cone dominate and one can expand the integrand in (15) near $x^2 = 0$ (see e.g. [5]). Contracting the virtual b-quark fields one rewrites (15) in the form

$$
\begin{aligned}
&F_\mu(p,q) = -m_b\\
&\times\int d^4x\, e^{iqx}\langle\pi(p)|\bar{u}(x)\gamma_\mu i S_b(x,0)\gamma_5 d(0)|0\rangle, \qquad (16)
\end{aligned}
$$

where $S_b(x,0)$ denotes the b-quark propagator expanded near the light cone.

Currently, the accuracy of the OPE for the correlation function at leading order in α_s is limited by contributions up to twist-4 terms. In our paper, we focus on a derivation of the factorizable twist-5 and twist-6 contributions. To this end, we substitute the LC-expansion of the b-quark propagator calculated in the previous section (see Eq. (12)) and take only terms proportional to the derivative $D_\mu G^{\mu\nu}$ of the gluon-field strength. The latter are transformed by applying the equation of motion for the gluon-field strength:

$$
D_\mu G^{\mu\nu}(ux) = -g_s\sum_q\left(\bar{q}(ux)\gamma^\nu\frac{\lambda^a}{2}q(ux)\right)\frac{\lambda^a}{2}. \qquad (17)
$$

In the above, due to the quark content of the final state pion, only the terms with u- and d-quark contribute. Applying the equation of motion (17) yields the matrix elements of two quark–antiquark operators sandwiched between pion and vacuum states. These matrix elements generate two different types of contributions. The first ones related to the four-particle DAs are expected to be negligible [11]. On the other hand, the contributions of the second type (factorizable) could have a larger numerical impact on LCSR for the form factor. In this paper following the same approach as in [11,12] we restrict ourselves to the factorization approximation and present the matrix elements of the two quark–antiquark operators as a product of the dimension-three quark condensate $\langle\bar{q}q\rangle$ and the bilocal vacuum-pion matrix element containing pion twist-2 and twist-3 light-cone distribution amplitudes (LCDAs). The latter matrix element can be presented in the form [5]

$$
\begin{aligned}
&\langle\pi(p)|\bar{u}^i_\alpha(x_1)d^j_\beta(x_2)|0\rangle\Big|_{(x_1-x_2)^2\to 0}\\
&= \frac{i\delta^{ij}f_\pi}{12}\int_0^1 \mathrm{d}v\, e^{iv(px_1)+i\bar{v}(px_2)}\Big([\not{p}\gamma_5]_{\beta\alpha}\,\varphi(v)\\
&\quad -[\gamma_5]_{\beta\alpha}\,\mu_\pi\varphi_p(v)\\
&\quad +\frac{1}{6}[\sigma_{\mu\nu}\gamma_5]_{\beta\alpha}\,p^\mu(x_1-x_2)^\nu\mu_\pi\varphi_\sigma(v)\Big), \qquad (18)
\end{aligned}
$$

where the upper i, j and lower α, β indices are the colour and bispinor indices of the quark fields, respectively, $\bar{v} = 1-v$, f_π is the pion decay constant, and $\varphi(v)$ and $\varphi_{p,\sigma}(v)$ denote the twist-2 and twist-3 pion light-cone DAs, respectively.

The matrix elements of the two quark fields sandwiched between the vacuum states can be expressed via the quark vacuum condensate in the local limit $|x_1-x_2| \to 0$. Expanding the light quark field $q(x) = u(x)$ or $d(x)$ near the point $x = 0$ one can demonstrate that [13]

$$
\langle 0|\bar{q}^i_\alpha(x)q^j_\beta(0)|0\rangle \simeq \frac{\delta^{ij}\delta_{\alpha\beta}}{12}\langle\bar{q}q\rangle, \qquad (19)
$$

where $\langle\bar{q}q\rangle$ denotes the dimension-three light quark condensate, and we assume isospin symmetry, therefore $\langle\bar{q}q\rangle \equiv \langle\bar{u}u\rangle = \langle\bar{d}d\rangle$. The corresponding contributions of the factorizable twist-5 and twist-6 terms to the OPE for the correlation function are described by diagrams shown in Fig. 1.

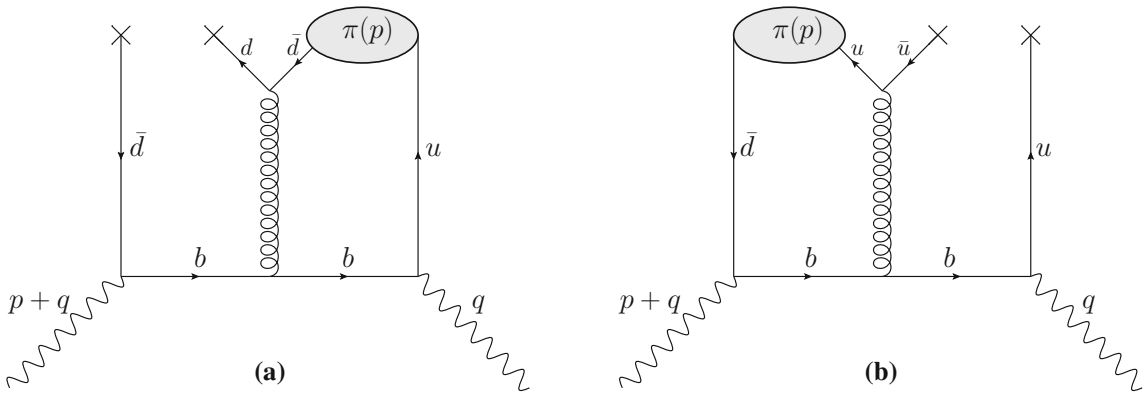

Fig. 1 *Diagrams* representing the factorizable twist-5 and twist-6 contributions to the correlation function (15)

They are formed only by the gluon emitted from the virtual b-quark. Gluons emitted from the light $\bar{d}$ and u quarks and converted to the quark–antiquark pair represent a genuine long-distance effect which is by default included in the DAs. Such an implicit separation of long- and short-distance effects takes place also in the diagrams with three-particle quark–antiquark–gluon DAs of twist 3, 4.

After factorization the further calculation is straightforward, albeit lengthy. The final result of the OPE for the correlation function reads

$$
\begin{aligned}
F^{(\mathrm{OPE})}_{\mathrm{tw5,6}}(q^2,(p+q)^2) &= \alpha_s\langle\bar{q}q\rangle\frac{C_F}{N_c}\pi m_b f_\pi \int_0^1 \mathrm{d}u \int_0^1 \mathrm{d}v \\
&\times \Bigg\{\varphi(v)\Bigg[\frac{1}{[m_b^2-(q+uvp)^2]^2}+\frac{2(1-2u\bar{u})}{[m_b^2-(q+(u+v-uv)p)^2]^2} \\
&+\frac{4u\bar{u}\,q^2}{[m_b^2-(q+uvp)^2]^3}+\frac{4u\bar{u}\,m_b^2}{[m_b^2-(q+(u+v-uv)p)^2]^3}\Bigg] \\
&-4\mu_\pi m_b\,\varphi_p(v)\Bigg[\frac{u^2\bar{u}v}{[m_b^2-(q+uvp)^2]^3} \\
&+\frac{u\bar{u}(uv-u-v)}{[m_b^2-(q+(u+v-uv)p)^2]^3}\Bigg] \\
&+2\mu_\pi m_b\,\varphi_\sigma(v)\Bigg[\frac{u^2\bar{u}(m_b^2+q^2)}{[m_b^2-(q+uvp)^2]^4} \\
&+\frac{u\bar{u}^2(m_b^2+q^2)}{[m_b^2-(q+(u+v-uv)p)^2]^4}\Bigg]\Bigg\},
\end{aligned}
\tag{20}
$$

where the contributions of factorizable twist-5 and twist-6 terms are separated. Note that in the above the masses of the pion and light quarks are neglected, $m_\pi = 0$ and $m_{u,d} = 0$, everywhere except in the parameter $\mu_\pi = m_\pi^2/(m_u + m_d)$.

In order to estimate the corresponding correction to the vector $B \to \pi$ form factor one follows the standard procedure of the LCSR derivation. First of all, one needs to perform the change of the integration variables in (20) in order to present the OPE result for the invariant amplitude $F(q^2,(p+q)^2)$ as a quasi-dispersion integral in the variable $(p+q)^2$. One obtains

$$
\begin{aligned}
F^{(\mathrm{OPE})}_{\mathrm{tw5,6}}(q^2,(p+q)^2) &= \alpha_s\langle\bar{q}q\rangle\frac{C_F}{N_c}\pi m_b f_\pi \\
&\times \int_{m_b^2}^\infty \mathrm{d}s \sum_{n=2,3,4}\frac{g_n(q^2,s)}{(s-(p+q)^2)^n},
\end{aligned}
\tag{21}
$$

where the details of derivation and the explicit expressions of functions $g_n(q^2,s)$ are given in the appendix.

To access the vector $B \to \pi$ form factor, one writes down the hadronic dispersion relation for the invariant amplitude $F(q^2,(p+q)^2)$ in the channel of the $\bar{b}\gamma_5 d$ current with the four-momentum squared $(p+q)^2$. Inserting a full set of the hadronic states with quantum numbers of B-meson between the currents in (15) one isolates the ground state B-meson contribution in the dispersion integral. To this end, we need to define the hadronic matrix elements:

$$
i m_b\langle B|\bar{b}\gamma_5 d|0\rangle = m_B^2 f_B, \tag{22}
$$

$$
\begin{aligned}
&\langle\pi(p)|\bar{q}\gamma^\mu b|B(p+q)\rangle \\
&\quad= f^+_{B\pi}(q^2)\left[2p^\mu+\left(1-\frac{m_B^2-m_\pi^2}{q^2}\right)q^\mu\right] \\
&\qquad+ f^0_{B\pi}(q^2)\,\frac{m_B^2-m_\pi^2}{q^2}\,q^\mu,
\end{aligned}
\tag{23}
$$

where f_B is the B-meson decay constant and $f^+_{B\pi}(q^2)$ and $f^0_{B\pi}(q^2)$ are the standard $B \to \pi$ vector and scalar form factors. One presents then the amplitude $F(q^2,(p+q)^2)$ as follows:

$$
F(q^2,(p+q)^2) = \frac{2f^+_{B\pi}(q^2)m_B^2 f_B}{m_B^2-(p+q)^2} + \int_{s_0^B}^\infty \mathrm{d}s\,\frac{\rho^h(q^2,s)}{s-(p+q)^2}. \tag{24}
$$

In the above, the contribution of the excited states and continuum of hadrons with the same quantum numbers as B-meson is presented in the form of the integral over the spectral density $\rho^h(q^2, s)$. Its contribution can be related with the OPE result by means of the quark–hadron duality

$$\rho^h(q^2, s) = \frac{1}{\pi}\mathrm{Im}F^{(\mathrm{OPE})}(q^2, s)\,\Theta(s - s_0^B), \tag{25}$$

introducing the effective continuum threshold s_0^B. The imaginary part of the invariant amplitude $\mathrm{Im}F^{(\mathrm{OPE})}(q^2, (p+q)^2)$ in the variable $(p+q)^2$ is easily extracted from (21). In order to suppress the contribution of the excited states one applies the Borel transformation, replacing the variable $(p+q)^2$ by the Borel parameter M^2. Finally, after subtraction of the continuum contribution the corresponding twist-5 and twist-6 corrections for the vector $B \to \pi$ form factor can be presented in the following compact form:

$$\left[f_{B\pi}^+(q^2)\right]_{\mathrm{tw5,6}} = \left(\frac{e^{m_B^2/M^2}}{2m_B^2 f_B}\right)\alpha_s\langle\bar{q}q\rangle\frac{C_F}{N_c}\pi m_b f_\pi$$
$$\times\int_{m_b^2}^{\infty} \mathrm{d}s \sum_{n=2,3,4}\rho_n(q^2, s; s_0^B, M^2) \tag{26}$$

with the auxiliary functions $\rho_n(q^2, s; s_0^B, M^2)$ taking the form

$$\rho_n(q^2, s; s_0^B, M^2) = \frac{(-1)^{n-1}}{(n-1)!}\,g_n(q^2, s)\frac{d^{n-1}}{\mathrm{d}s^{n-1}}\left[\theta(s_0^B - s)e^{-s/M^2}\right], \tag{27}$$

where the derivatives in s emerge due to the higher power of the denominator in (21), yielding the surface terms in the LCSR at $s = s_0^B$.

4 Numerical analysis

In order to estimate the numerical impact of the factorizable twist-5 and twist-6 terms on the vector $B \to \pi$ form factor we need to specify the input used in the LCSR. First of all, the values of the B-mesons mass $m_{B^0} = 5.27931\,\mathrm{GeV}$ and the pion decay constant $f_\pi = 130.4\,\mathrm{MeV}$ are taken from [14]. The mass of b-quark is used in $\overline{MS}$-scheme and we adopt the interval $\overline{m}_b(\overline{m}_b) = 4.18 \pm 0.03$ GeV [14]. The value of the quark-condensate density $\langle\bar{q}q\rangle(2\,\mathrm{GeV}) = -(277^{+12}_{-10}\,\mathrm{MeV})^3$ is taken from [15]. The normalization parameter of the twist-3 DAs μ_π is determined by means of ChPT relations and we use $\mu_\pi(2\,\mathrm{GeV}) = 2.50\,\mathrm{GeV}$ following [16]. For the renormalization scale we use the value $\mu = 3\,\mathrm{GeV}$. The B-meson decay constant can be extracted from the QCD sum rules and we apply the value $f_B = 202\,\mathrm{MeV}$ corresponding to the NLO accuracy of the corresponding sum rules [15]. Furthermore, the Borel parameter M^2 and the continuum threshold s_0^B are taken at their typical values $M^2 = 16\,\mathrm{GeV}^2$ and $s_0^B = 37.2\,\mathrm{GeV}^2$ used as central values in the most recent paper [17].

Concerning the choice of the twist-2 and twist-3 pion DAs, we restrict ourselves by the asymptotic form $\varphi(v) = 6v\bar{v}$, $\varphi_p(v) = 1$ and $\varphi_\sigma(v) = 6v\bar{v}$, sufficient for our accuracy having in mind that the nonasymptotic corrections to these DAs are relatively small. Implementing the explicit forms for the DAs allows one to perform an integration over u in (34)–(36) and to determine the auxiliary functions $g_n(q^2, s)$ entering the LCSR for the vector $B \to \pi$ form factor (26).

The numerical results for $f_{B\pi}^+(q^2)$ corresponding to the above described input are presented in Fig. 2, where the q^2-dependence of the factorizable twist-5 and twist-6 corrections is plotted. Note that the corrections grow at large q^2 as they should, reflecting the growth of the higher twists effects in the region of low recoil, where OPE starts to diverge. In Table 1 we present separate contributions to the LCSR for the vector $B \to \pi$ form factor at two typical values $q^2 = 0$

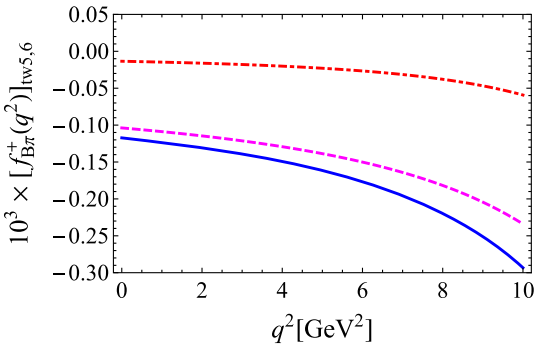

Fig. 2 The factorizable twist-5 and twist-6 corrections to the vector $B \to \pi$ form factor. The dot-dashed (*red*) curve is the twist 6. The dashed (*magenta*) one is the twist 5 and the *solid* (*blue*) *curve* is the sum of the two

Table 1 The values of the $B \to \pi$ form factor at two typical values $q^2 = 0$ and $q^2 = 10\,\mathrm{GeV}^2$ and the partial contributions to the LCSR (in %)

	$q^2 = 0$	$q^2 = 10\,\mathrm{GeV}^2$
$f_{B\pi}^+(q^2)$	0.301	0.562
Tw2 LO	47.5	48.2
Tw2 NLO	6.9	5.9
Tw3 LO	50.0	54.2
Tw3 NLO	−4.6	−7.5
Tw4 LO	0.2	−0.8
Tw5 LO, fact	−0.034	−0.042
Tw6 LO, fact	−0.004	−0.011

and $q^2 = 10\,\text{GeV}^2$ in order to demonstrate the magnitude of the factorizable higher twist corrections to the vector $B \to \pi$ form factor. We found that in the whole domain of q^2 of the LCSR applicability the relative contributions of the higher twist effects do not exceed 0.05% revealing their strong suppression. The obtained result justifies a standard truncation of the OPE in LCSR up to the twist-4 terms. It is important to note that one of the sources of such a suppression is the magnitude of the b-quark mass. We also extended the analysis for the LCSRs for other, $B \to K$ and $B_s \to K$ transition vector form factors. We found that in all these cases, the factorizable higher twist effects are also significantly suppressed. The corresponding corrections could have more sizeable effects in the case of $D \to \pi$ and $D \to K$ from factor due to a smaller value of the c-quark mass. We plan to perform such analysis in the future.

5 Conclusion

In this paper we estimate the higher twist effects in the LCSR for the $B \to \pi$ vector form factor in the framework of the factorization approximation. To this end, the light-cone expansion of the massive quark propagator including the higher derivatives of the gluon-field strength is derived. The corresponding expression is in agreement with the leading order expansion of the massive propagator [4] and in the massless quark limit reproduces the propagator obtained in [10]. Our result has a more general relevance since it can be used in any other application of LCSR where one needs the LC-expansion of the massive quark propagator. We derive the analytical expressions for the factorizable twist-5 and twist-6 contributions to the LCSR for the vector $B \to \pi$ form factor. The relevant numerical analysis reveals that these effects are extremely suppressed. This justifies the conventional truncation of the operator product expansion in the light-cone sum rules up to twist-4 terms adopted in the previous LCSR analyses.

Acknowledgements I am grateful to Alexander Khodjamirian for encouraging to carry out this project and for the helpful discussions and careful reading of the manuscript. I appreciate the helpful discussion with Vladimir Braun. The work is supported by the Nikolai-Uraltsev Fellowship of Siegen University and by the DFG Research Unit FOR 1873 "Quark Flavour Physics and Effective Theories", contract No. KH 205/2-2, and partially by the Russian Foundation for Basic Research (project No. 15-02-06033-a).

Appendix

In order to present the OPE result for the correlation function in the form of dispersion integral we need to perform some transformations. The integrals

$$I_n = \int_0^1 \int_0^1 \mathrm{d}v\,\mathrm{d}u\,\frac{f_n(q^2,u,v)}{[m_b^2-(q+uvp)^2]^n}, \quad n=2,3,4, \tag{28}$$

result from the diagram (a) of Fig. 1, and

$$J_n = \int_0^1 \int_0^1 \mathrm{d}v\,\mathrm{d}u\,\frac{\bar{f}_n(q^2,u,v)}{[m_b^2-(q+(u+v-uv)p)^2]^n}, \quad n=2,3,4, \tag{29}$$

from diagram (b). The functions $f_n(q^2,u,v)$ and $\bar{f}_n(q^2,u,v)$ can easily be read off from Eq. (20). Our task is to present both I_n and J_n in the form of dispersion integral. To this end, in the integrals I_n of the first type we replace the variable v by $\alpha = uv$, and change then the integration order

$$\int_0^1 \mathrm{d}u \int_0^u \mathrm{d}\alpha\,(\ldots) = \int_0^1 \mathrm{d}\alpha \int_\alpha^1 \mathrm{d}u\,(\ldots).$$

Afterwards, we introduce a new variable s as follows:

$$\alpha = \frac{m_b^2-q^2}{s-q^2} \equiv u_1(s,q^2). \tag{30}$$

Finally, the integrals I_n transform to

$$I_n = \int_{m_b^2}^\infty \mathrm{d}s \int_{u_1(s,q^2)}^1 \frac{\mathrm{d}u}{u}\,\frac{(s-q^2)^{n-2}}{(m_b^2-q^2)^{n-1}}\,\frac{f_n\left(q^2,u,\dfrac{m_b^2-q^2}{u(s-q^2)}\right)}{(s-(p+q)^2)^n}. \tag{31}$$

For the integrals of the second type J_n we perform the replacements $u \to 1-u = \bar{u}$ and $v \to 1-v = \bar{v}$. The next steps are similar to the previous case and the integrals J_n finally transform to

$$J_n = \int_{m_b^2}^\infty \mathrm{d}s \int_{u_2(s,q^2)}^1 \frac{\mathrm{d}\bar{u}}{\bar{u}}\,\frac{(s-q^2)^{n-2}}{(m_b^2-q^2)^{n-1}}\,\frac{\bar{f}_n\left(q^2,\bar{u},\dfrac{s-m_b^2}{\bar{u}(s-q^2)}\right)}{(s-(p+q)^2)^n}, \tag{32}$$

with $u_2(s, q^2)$ defined as

$$u_2(s, q^2) = \frac{s - m_b^2}{s - q^2}. \tag{33}$$

Note that in the above integrals the dependence on the variable $(p + q)^2$ is reduced to the denominator in the form $(s - (p + q)^2)^n$. This significantly simplifies the derivation of the LCSR for the correlation function. With the help of (31) and (32), the OPE result for the correlation function transforms into the quasi-dispersion form (21) with the functions $g_n(q^2, s)$ listed below:

$$g_2(q^2, s) = \frac{1}{m_b^2 - q^2} \int_{u_1}^{1} \frac{\mathrm{d}u}{u} \varphi(u_1/u) + \frac{2}{m_b^2 - q^2} \int_{u_2}^{1} \frac{\mathrm{d}u}{u} (1 - 2u\bar{u}) \varphi(u_2/u), \tag{34}$$

$$\begin{aligned} g_3(q^2, s) = {} & \frac{4q^2(s - q^2)}{(m_b^2 - q^2)^2} \int_{u_1}^{1} \mathrm{d}u\, \bar{u}\, \varphi(u_1/u) \\ & - \frac{4\mu_\pi m_b}{m_b^2 - q^2} \int_{u_1}^{1} \mathrm{d}u\, \bar{u}\, \varphi_p(u_1/u) \\ & + \frac{4m_b^2(s - q^2)}{(m_b^2 - q^2)^2} \int_{u_2}^{1} \mathrm{d}u\, \bar{u}\, \varphi(u_2/u) \\ & + \frac{4\mu_\pi m_b}{m_b^2 - q^2} \int_{u_2}^{1} \mathrm{d}u\, \bar{u}\, \varphi_p(u_2/u), \end{aligned} \tag{35}$$

$$\begin{aligned} g_4(q^2, s) = {} & 2\mu_\pi m_b \frac{(s - q^2)^2 (m_b^2 + q^2)}{(m_b^2 - q^2)^3} \int_{u_1}^{1} \mathrm{d}u u\bar{u}\, \varphi_\sigma(u_1/u) \\ & + 2\mu_\pi m_b \frac{(s - q^2)^2 (m_b^2 + q^2)}{(m_b^2 - q^2)^3} \int_{u_2}^{1} \mathrm{d}u u\bar{u}\, \varphi_\sigma(u_2/u), \end{aligned} \tag{36}$$

where $u_{1,2} = u_{1,2}(s, q^2)$ are already defined in (30) and (33). Inserting the explicit expressions for the pion LCDAs $\varphi(v)$, $\varphi_p(v)$ and $\varphi_\sigma(v)$ allows one to perform an integration over variable u in (34), (35) and (36).

References

1. I.I. Balitsky, V.M. Braun, A.V. Kolesnichenko, Sov. J. Nucl. Phys. **44**, 1028 (1986) [Yad. Fiz. **44** (1986) 1582]
2. V.L. Chernyak, I.R. Zhitnitsky, Nucl. Phys. B **345**, 137 (1990)
3. V.M. Belyaev, A. Khodjamirian, R. Ruckl, Z. Phys. C **60**, 349 (1993). arXiv:hep-ph/9305348
4. V.M. Belyaev, V.M. Braun, A. Khodjamirian, R. Ruckl, Phys. Rev. D **51**, 6177 (1995). arXiv:hep-ph/9410280
5. G. Duplancic, A. Khodjamirian, T. Mannel, B. Melic, N. Offen, JHEP **0804**, 014 (2008). arXiv:0801.1796 [hep-ph]
6. A. Khodjamirian, R. Ruckl, S. Weinzierl, O.I. Yakovlev, Phys. Lett. B **410**, 275 (1997). arXiv:hep-ph/9706303
7. E. Bagan, P. Ball, V.M. Braun, Phys. Lett. B **417**, 154 (1998). arXiv:hep-ph/9709243
8. P. Ball, R. Zwicky, JHEP **0110**, 019 (2001). arXiv:hep-ph/0110115
9. A. Bharucha, JHEP **1205**, 092 (2012). arXiv:1203.1359 [hep-ph]
10. I.I. Balitsky, V.M. Braun, Nucl. Phys. B **311**, 541 (1989)
11. V.M. Braun, A. Khodjamirian, M. Maul, Phys. Rev. D **61**, 073004 (2000). arXiv:hep-ph/9907495
12. S.S. Agaev, V.M. Braun, N. Offen, F.A. Porkert, Phys. Rev. D **83**, 054020 (2011). arXiv:1012.4671 [hep-ph]
13. P. Colangelo, A. Khodjamirian, in *At the Frontier of Particle Physics*, ed. by M. *Shifman, vol. 3*, pp. 1495–1576. arXiv:hep-ph/0010175
14. C. Patrignani et al. [Particle Data Group], Chin. Phys. C **40**, 100001 (2016)
15. P. Gelhausen, A. Khodjamirian, A.A. Pivovarov, D. Rosenthal, Phys. Rev. D **88**, 014015 (2013). Erratum: [Phys. Rev. D **89** (2014) 099901]. Erratum: [Phys. Rev. D **91** (2015) 099901]. arXiv:1305.5432 [hep-ph]
16. A. Khodjamirian, C. Klein, T. Mannel, N. Offen, Phys. Rev. D **80**, 114005 (2009). arXiv:0907.2842 [hep-ph]
17. A. Khodjamirian, A.V. Rusov, arXiv:1703.04765 [hep-ph]

Chapter 4

$B_s \to K\ell\bar{\nu}_\ell$ and $B_{(s)} \to \pi(K)\ell^+\ell^-$ at large recoil and CKM matrix elements

Published as an article in:
A. Khodjamirian and A.V. Rusov, JHEP **1708** (2017) 112

Contributions of the authors to the article.
A.V. Rusov performed the analytical derivation of expressions and numerical calculation of all results presented in the paper. Additionally, A.V. Rusov prepared the draft of the manuscript. Prof. Dr. A. Khodjamirian suggested the outline of this project and the idea of sect. 2 in Chapter 4, supervised the work and discussed the results, and worked on the final version of the manuscript.

Published for SISSA by Springer

Received: *March 24, 2017*
Revised: *August 1, 2017*
Accepted: *August 6, 2017*
Published: *August 25, 2017*

$B_s \to K\ell\nu_\ell$ and $B_{(s)} \to \pi(K)\ell^+\ell^-$ decays at large recoil and CKM matrix elements

Alexander Khodjamirian[a] **and Aleksey V. Rusov**[a,b]

[a] *Theoretische Physik 1, Naturwissenschaftlich-Technische Fakultät, Universität Siegen, D-57068 Siegen, Germany*

[b] *Department of Theoretical Physics, P.G. Demidov Yaroslavl State University, 150000, Yaroslavl, Russia*

E-mail: khodjamirian@physik.uni-siegen.de, rusov@physik.uni-siegen.de

Abstract: We provide hadronic input for the B-meson semileptonic transitions to a light pseudoscalar meson at large recoil. The $B_s \to K$ form factor calculated from QCD light-cone sum rule is updated, to be used for a $|V_{ub}|$ determination from the $B_s \to K\ell\nu$ width. Furthermore, we calculate the hadronic input for the binned observables of $B \to \pi\ell^+\ell^-$ and $B \to K\ell^+\ell^-$. In addition to the form factors, the nonlocal hadronic matrix elements are obtained, combining QCD factorization and light-cone sum rules with hadronic dispersion relations. We emphasize that, due to nonlocal effects, the ratio of branching fractions of these decays is not sufficient for an accurate extraction of the $|V_{td}/V_{ts}|$ ratio. Instead, we suggest to determine the Wolfenstein parameters A, ρ, η of the CKM matrix, combining the branching fractions of $B \to K\ell^+\ell^-$ and $B \to \pi\ell^+\ell^-$ with the direct CP-asymmetry in the latter decay. We also obtain the hadronic matrix elements for a yet unexplored channel $B_s \to K\ell^+\ell^-$.

Keywords: Heavy Quark Physics, CP violation

ArXiv ePrint: 1703.04765

https://doi.org/10.1007/JHEP08(2017)112

JHEP08(2017)112

Contents

JHEP08(2017)112

1 Introduction

Determination of CKM matrix elements from the semileptonic decays of B meson remains a topical problem. Most importantly, one has to clarify the origin of the tension between the $|V_{ub}|$ values extracted from the exclusive $B \to \pi\ell\nu_\ell$ and inclusive $B \to X_u\ell\nu_\ell$ decays (see e.g., the review [1]). The $B \to \pi$ vector form factor $f^+_{B\pi}(q^2)$ is the only theory input sufficient for the $|V_{ub}|$ determination from $B \to \pi\ell\nu_\ell$. This hadronic matrix element is calculated in the lattice QCD at small recoil of the pion (at large q^2) or from QCD light-cone sum rules (LCSRs) at large recoil of the pion (at small and intermediate q^2).

Apart from increasing the accuracy of the form factor calculation, it is important to extend the set of "standard" exclusive processes used for $|V_{ub}|$ determination. The $B_s \to K^*(\to K\pi)\ell\nu_\ell$ decay, as one possibility, was discussed in [2]. A simpler process is the $B_s \to K\ell\nu_\ell$ decay, where the data are anticipated from LHCb collaboration. Our first goal in this paper is to provide this decay mode with a hadronic input, updating the calculation of the $B_s \to K$ form factors from LCSRs. This method [3–5] is based on the operator-product expansion (OPE) of a correlation function expressed in terms of light-meson distribution amplitudes (DAs) with growing twist. The violation of the $\mathrm{SU}(3)_{fl}$ symmetry in $B_s \to K$ with respect to $B \to \pi$ transition emerges in LCSRs due to the s-quark mass effects in the correlation function, including the asymmetry between the s- and $\{u, d\}$-partons in the kaon DAs. Earlier LCSR results on the $B_s \to K$ form factors can be found in [6], where the NLO corrections to the correlation function computed in [7] were taken into account. In this paper we update the LCSRs for $f^+_{B_sK}(q^2)$ and also for the tensor form factor $f^T_{B_sK}(q^2)$. In particular, we correct certain terms in the subleading twist-3,4 contributions to LCSRs for both vector and tensor form factors. In parallel, we recalculate the $B \to K$ and $B \to \pi$ form factors using a common set of input parameters, e.g., the updated [8] 2-point QCD sum rule for the decay constants f_B and f_{B_s}. Importantly, the twist-5,6 corrections to the LCSRs estimated by one of us [9] are negligibly small, ensuring the reliability of the adopted twist ≤ 4 approximation.

The calculated form factors are then used to address the second goal of this paper: determination of CKM parameters from the flavour-changing neutral current (FCNC) decays $B \to K\ell^+\ell^-$, $B \to \pi\ell^+\ell^-$ and $B_s \to K\ell^+\ell^-$. Recently, $|V_{td}|$, $|V_{ts}|$ and their ratio were determined by LHCb collaboration [10] from the measured $B \to \pi\ell^+\ell^-$ and $B \to K\ell^+\ell^-$ partial widths. We suggest to make the extraction of CKM parameters from these decays more accurate and comprehensive. As well known, in addition to the semileptonic form factors, the hadronic input in FCNC decays includes also nonlocal hadronic matrix elements emerging due to the electromagnetic lepton-pair emission combined with the weak transitions. These hadronic matrix elements in the $B \to \pi\ell^+\ell^-$ decay amplitude are multiplied by the CKM parameters other than V_{td}, making the determination of the latter not straightforward. We take into account the nonlocal hadronic effects in $B \to K\ell^+\ell^-$ and $B \to \pi\ell^+\ell^-$, employing the methods used in [12, 13] and originally suggested in [11]. The nonlocal hadronic matrix elements are calculated at spacelike q^2, using OPE, QCD factorization [14] and LCSRs, and are then matched to their values at timelike q^2 via hadronic dispersion relations. The results of this calculation are reliable at large hadronic recoil, below the charmonium region, that is, at $q^2 < m^2_{J/\psi}$. Here we also extend the calculation of nonlocal effects to the previously unexplored channel $B_s \to K\ell^+\ell^-$.

The binned widths and direct CP-asymmetries of FCNC semileptonic decays are then expressed in a form combining the CKM parameters with the quantities determined by the calculated hadronic input. Here we find it more convenient to switch to the Wolfenstein parametrization of the CKM matrix. In this form, three observables: the width of $B \to K\ell^+\ell^-$, the ratio of $B \to \pi\ell^+\ell^-$ and $B \to K\ell^+\ell^-$ widths and the direct CP-asymmetry in $B \to \pi\ell^+\ell^-$, are sufficient to extract the three Wolfenstein parameters A, η and ρ from experimental data, provided the parameter λ is known quite precisely. Two additional observables for the same determination are given by the yet unobserved $B_s \to K\ell^+\ell^-$ decay. The current data on the $B \to K\ell^+\ell^-$ and $B \to \pi\ell^+\ell^-$ decays are not yet precise enough to yield the CKM parameters with an accuracy comparable to the other determinations. Hence, here we limit ourselves with the Wolfenstein parameters taken from the global CKM fit and predict the binned observables of all three FCNC decays in the optimal interval $1.0\ \text{GeV}^2 < q^2 < 6.0\ \text{GeV}^2$ of the large recoil region.

In what follows, in section 2 we specify and discuss the hadronic input and observables in the exclusive semileptonic $B_{(s)}$ decays. In section 3 we present the numerical results and section 4 is devoted to the final discussion. In the appendices, we briefly recapitulate the calculation A of the form factors from LCSRs and B of the nonlocal hadronic matrix elements.

2 Observables in semileptonic $B_{(s)}$ decays and CKM parameters

The form factors of semileptonic transitions of B-meson to a light pseudoscalar meson $P = \pi, K$ are defined in a standard way:

$$\langle P(p)|\bar{q}\gamma^\mu b|B(p+q)\rangle = f^+_{BP}(q^2)\left[2p^\mu + \left(1 - \frac{m_B^2 - m_P^2}{q^2}\right)q^\mu\right] + f^0_{BP}(q^2)\,\frac{m_B^2 - m_P^2}{q^2}\,q^\mu, \quad (2.1)$$

$$\langle P(p)|\bar{q}\sigma^{\mu\nu}q_\nu b|B(p+q)\rangle = \frac{i f^T_{BP}(q^2)}{m_B + m_P}\left[2q^2 p^\mu + \left(q^2 - m_B^2 - m_P^2\right)q^\mu\right], \quad (2.2)$$

JHEP08(2017)112

where p^μ and q^μ are the four-momenta of the P-meson and lepton pair, respectively, and the vector and scalar form factors coincide at $q^2 = 0$, that is, $f^+_{BP}(0) = f^0_{BP}(0)$.

We start from the weak semileptonic decay $\bar{B}_s \to K^+\ell\bar{\nu}_\ell$, where the hadronic input for $\ell = e, \mu$ in the $m_\ell = 0$ approximation is given by the vector form factor $f^+_{B_sK}$. We use the following quantity related to the differential width integrated over an interval $0 \le q^2 \le q^2_0$:

$$\Delta\zeta_{B_sK}\,[0, q^2_0] \equiv \frac{G_F^2}{24\pi^3}\int\limits_0^{q^2_0} dq^2 p^3_{B_sK}|f^+_{B_sK}(q^2)|^2 = \frac{1}{|V_{ub}|^2\tau_{B_s}}\int\limits_0^{q^2_0} dq^2\frac{dB(\bar{B}_s \to K^+\ell\bar{\nu}_\ell)}{dq^2}\,, \quad (2.3)$$

where the q^2-dependent kinematical factor $p_{BP} = [(m_B^2 + m_P^2 - q^2)^2/(4m_B^2) - m_P^2]^{1/2}$ is the 3-momentum of P meson in the rest frame of B meson. Our choice for the integration interval is $q^2_0 = 12.0$ GeV^2, covering the region where the LCSRs used for the calculation of the form factors (see appendix A) are valid. The same interval was adopted for the analogous quantity $\Delta\zeta_{B\pi}[0, q^2_0]$ for $B \to \pi\ell\nu_\ell$ calculated in [15, 16]. The numerical estimate of $\Delta\zeta_{B_sK}\,[0, q^2_0]$ presented in the next section can be directly used for $|V_{ub}|$ determination, provided the integrated branching fraction on the r.h.s. of eq. (2.3) is measured.

Turning to semileptonic decays generated by the $b \to s(d)\ell^+\ell^-$ transitions ($\ell = e, \mu$), we use a generic notation $\bar{B} \to P\ell^+\ell^-$ for the three channels: $B^- \to K^-\ell^+\ell^-$, $B^- \to \pi^-\ell^+\ell^-$ and $\bar{B}_s \to K^0\ell^+\ell^-$,[1] denoting the CP conjugated channels by $B \to \bar{P}\ell^+\ell^-$. The decay amplitude can be represented in the following form:

$$A(\bar{B} \to P\ell^+\ell^-) = \frac{G_F}{\sqrt{2}}\frac{\alpha_{\rm em}}{\pi}\Bigg\{\Big[\lambda_t^{(q)} f^+_{BP}(q^2)c_{BP}(q^2) + \lambda_u^{(q)} d_{BP}(q^2)\Big]\ \ \bar{\ell}\gamma^\mu\ell\big)\, p_\mu$$
$$+\ \lambda_t^{(q)} C_{10} f^+_{BP}(q^2)\ \ \bar{\ell}\gamma^\mu\gamma_5\ell\big)\, p_\mu\Bigg\}\,, \quad (2.4)$$

where $\lambda_p^{(q)} = V_{pb}V^*_{pq}$ ($p = u, c, t$; $q = d, s$), $m_\ell = 0$, and we use unitarity of the CKM matrix, fixing hereafter $\lambda_c^{(q)} = -(\lambda_t^{(q)} + \lambda_u^{(q)})$. In eq. (2.4) we introduce a compact notation:

$$c_{BP}(q^2) = C_9 + \frac{2(m_b + m_q)}{m_B + m_P}C_7^{\rm eff}\frac{f^T_{BP}(q^2)}{f^+_{BP}(q^2)} + 16\pi^2\frac{\mathcal{H}^{(c)}_{BP}(q^2)}{f^+_{BP}(q^2)}\,, \quad (2.5)$$

where m_q is the mass of d or s-quark and

$$d_{BP}(q^2) = 16\pi^2\Big(\mathcal{H}^{(c)}_{BP}(q^2) - \mathcal{H}^{(u)}_{BP}(q^2)\Big)\,. \quad (2.6)$$

In addition, we introduce the phase difference of the hadronic amplitudes defined above:

$$\delta_{BP}(q^2) = {\rm Arg}(d_{BP}(q^2)) - {\rm Arg}(c_{BP}(q^2)). \quad (2.7)$$

In eq. (2.4) the dominant contributions of the operators $O_{9,10}$ and $O_{7\gamma}$ of the effective Hamiltonian (see appendix B) are expressed in terms of the vector and tensor $B \to P$

[1] For simplicity we consider a transition into the fixed flavour state K^0 which is easy to convert to K_s if needed.

JHEP08(2017)112

form factors, $f_{BP}^{+}(q^2)$ and $f_{BP}^{T}(q^2)$, respectively, defined in eqs. (2.1) and (2.2). The amplitudes $\mathcal{H}_{BP}^{(c,u)}(q^2)$ parametrize the nonlocal contributions to $B \to P\ell^+\ell^-$, generated by the current-current, quark-penguin and chromomagnetic operators in the effective Hamiltonian, combined with an electromagnetically produced lepton pair. The definition of nonlocal amplitudes is given in appendix B, where also the method of their calculation is briefly explained. In refs. [11, 12], this part of hadronic input was cast in the form of an effective (process- and q^2-dependent) addition $\Delta C_9^{BP}(q^2)$ to the Wilson coefficient C_9. Here, as in ref. [13], we find it more convenient to separate the parts proportional to $\lambda_u^{(q)}$ and $\lambda_c^{(q)} = -(\lambda_t^{(q)} + \lambda_u^{(q)})$.

Squaring the amplitude (2.4) and integrating over the phase space, one obtains for the q^2-binned branching fraction, defined as:

$$\mathcal{B}(\bar{B} \to P\ell^+\ell^-[q_1^2, q_2^2]) \equiv \frac{1}{q_2^2 - q_1^2} \int\limits_{q_1^2}^{q_2^2} dq^2 \frac{dB(\bar{B} \to P\ell^+\ell^-)}{dq^2}\,, \tag{2.8}$$

the following expression:

$$\begin{aligned}\mathcal{B}(\bar{B} \to P\ell^+\ell^-[q_1^2, q_2^2]) = \frac{G_F^2 \alpha_{\rm em}^2 |\lambda_t^{(q)}|^2}{192\pi^5} \Big\{ & \mathcal{F}_{BP}[q_1^2, q_2^2] + \kappa_q^2 \mathcal{D}_{BP}[q_1^2, q_2^2] \\ & + 2\kappa_q \Big(\cos\xi_q \, \mathcal{C}_{BP}[q_1^2, q_2^2] - \sin\xi_q \, \mathcal{S}_{BP}[q_1^2, q_2^2] \Big) \Big\} \tau_B\,,\end{aligned} \tag{2.9}$$

where the ratio of CKM matrix elements is parametrized in terms of its module and phase:

$$\frac{\lambda_u^{(q)}}{\lambda_t^{(q)}} = \frac{V_{ub} V_{uq}^*}{V_{tb} V_{tq}^*} \equiv \kappa_q \, e^{i\xi_q}, \quad (q = d, s)\,, \tag{2.10}$$

and we use the following notation for the phase-space weighted and integrated parts of the decay amplitude squared:

$$\mathcal{F}_{BP}[q_1^2, q_2^2] = \frac{1}{q_2^2 - q_1^2} \int\limits_{q_1^2}^{q_2^2} dq^2 \, p_{BP}^3 |f_{BP}^{+}(q^2)|^2 \Big(\big|c_{BP}(q^2)\big|^2 + |C_{10}|^2 \Big)\,, \tag{2.11}$$

$$\mathcal{D}_{BP}[q_1^2, q_2^2] = \frac{1}{q_2^2 - q_1^2} \int\limits_{q_1^2}^{q_2^2} dq^2 \, p_{BP}^3 \big|d_{BP}(q^2)\big|^2\,, \tag{2.12}$$

$$\mathcal{C}_{BP}[q_1^2, q_2^2] = \frac{1}{q_2^2 - q_1^2} \int\limits_{q_1^2}^{q_2^2} dq^2 \, p_{BP}^3 \big|f_{BP}^{+}(q^2) c_{BP}(q^2) d_{BP}(q^2)\big| \cos\delta_{BP}(q^2)\,, \tag{2.13}$$

$$\mathcal{S}_{BP}[q_1^2, q_2^2] = \frac{1}{q_2^2 - q_1^2} \int\limits_{q_1^2}^{q_2^2} dq^2 \, p_{BP}^3 \big|f_{BP}^{+}(q^2) c_{BP}(q^2) d_{BP}(q^2)\big| \sin\delta_{BP}(q^2)\,. \tag{2.14}$$

JHEP08(2017)112

The binned branching fraction for the CP-conjugated mode $B \to \bar{P}\ell^+\ell^-$ is obtained from eq. (2.9) by changing the sign at the term proportional to $\sin\xi_q$.

Furthermore, we consider two binned observables: the CP-averaged branching fraction:

$$\begin{aligned}\mathcal{B}_{BP}\left[q_1^2, q_2^2\right] &\equiv \frac{1}{2}\ \mathcal{B}\ \bar{B} \to P\ell^+\ell^-\left[q_1^2, q_2^2\right]) + \mathcal{B}\ B \to \bar{P}\ell^+\ell^-\left[q_1^2, q_2^2\right])) \\ &= \frac{G_F^2\alpha_{\rm em}^2|\lambda_t^{(q)}|^2}{192\pi^5}\left\{\mathcal{F}_{BP}\left[q_1^2, q_2^2\right] + \kappa_q^2\,\mathcal{D}_{BP}\left[q_1^2, q_2^2\right] + 2\kappa_q\cos\xi_q\,\mathcal{C}_{BP}\left[q_1^2, q_2^2\right]\right\}\tau_B,\end{aligned} \tag{2.15}$$

and the corresponding direct CP-asymmetry:

$$\begin{aligned}\mathcal{A}_{BP}[q_1^2, q_2^2] &= \frac{\mathcal{B}(\bar{B} \to P\ell^+\ell^-[q_1^2, q_2^2]) - \mathcal{B}(B \to \bar{P}\ell^+\ell^-[q_1^2, q_2^2])}{\mathcal{B}(\bar{B} \to P\ell^+\ell^-[q_1^2, q_2^2]) + \mathcal{B}(B \to \bar{P}\ell^+\ell^-[q_1^2, q_2^2])} \\ &= \frac{-2\kappa_q\sin\xi_q\,\mathcal{S}_{BP}[q_1^2, q_2^2]}{\mathcal{F}_{BP}[q_1^2, q_2^2] + \kappa_q^2\,\mathcal{D}_{BP}[q_1^2, q_2^2] + 2\kappa_q\cos\xi_q\,\mathcal{C}_{BP}[q_1^2, q_2^2]}\,.\end{aligned} \tag{2.16}$$

In eqs. (2.15) and (2.16) the CKM-dependent coefficients are conveniently separated from the quantities $\mathcal{F}_{BP}$, $\mathcal{D}_{BP}$, $\mathcal{C}_{BP}$, $\mathcal{S}_{BP}$, which contain the calculable hadronic matrix elements, Wilson coefficients and kinematical factors. In the next section we present numerical results for these quantities for a definite q^2-bin in the large-recoil region.

Turning to the observables for the specific decay channels, we neglect $\lambda_u^{(s)}$, hence, put $\kappa_s = 0$ and obtain for $B \to K\ell^+\ell^-$:

$$\mathcal{B}_{BK}[q_1^2, q_2^2] = \frac{G_F^2\alpha_{\rm em}^2|\lambda_t^{(s)}|^2}{192\pi^5}\mathcal{F}_{BK}[q_1^2, q_2^2]\tau_B, \tag{2.17}$$

with vanishing CP asymmetry. For $B^- \to \pi^-\ell^+\ell^-$ and its CP-conjugated process both observables,

$$\mathcal{B}_{B\pi}[q_1^2, q_2^2] = \frac{G_F^2\alpha_{\rm em}^2|\lambda_t^{(d)}|^2}{192\pi^5}\left\{\mathcal{F}_{B\pi}[q_1^2, q_2^2] + \kappa_d^2\,\mathcal{D}_{B\pi}[q_1^2, q_2^2] + 2\kappa_d\cos\xi_d\,\mathcal{C}_{B\pi}[q_1^2, q_2^2]\right\}\tau_B\,, \tag{2.18}$$

and

$$\mathcal{A}_{B\pi}[q_1^2, q_2^2] = \frac{-2\kappa_d\,\sin\xi_d\,\mathcal{S}_{B\pi}[q_1^2, q_2^2]}{\mathcal{F}_{B\pi}[q_1^2, q_2^2] + \kappa_d^2\,\mathcal{D}_{B\pi}[q_1^2, q_2^2] + 2\kappa_d\,\cos\xi_d\,\mathcal{C}_{B\pi}[q_1^2, q_2^2]}\,, \tag{2.19}$$

are relevant. The corresponding observables $\mathcal{B}_{B_sK}[q_1^2, q_2^2]$ and $\mathcal{A}_{B_sK}[q_1^2, q_2^2]$ for $\bar{B}_s \to K^0\ell^+\ell^-$ and its CP-conjugated mode are given by the expressions similar to eqs. (2.18), (2.19), with $B\pi$ replaced by B_sK. Here we do not consider the decays $\bar{B}^0 \to \bar{K}^0\ell^+\ell^-$ and $\bar{B}^0 \to \pi^0\ell^+\ell^-$, which are the isospin counterparts of, respectively, $B^- \to K^-\ell^+\ell^-$ and $B^- \to \pi^-\ell^+\ell^-$ and can be treated in a similar way (see [12, 13]). We also postpone to a future study the time-dependent CP-asymmetry in the $\bar{B}_s \to K^0\ell^+\ell^-$ decay.

Dividing eq. (2.18) by eq. (2.17), we notice that an accurate extraction of the ratio $|V_{td}/V_{ts}|$ from the ratio of branching fractions $\mathcal{B}_{B\pi}[q_1^2, q_2^2]/\mathcal{B}_{B\pi}[q_1^2, q_2^2]$ can only be achieved

JHEP08(2017)112

if the contributions of process-dependent nonlocal effects are taken into account for both decay modes. Moreover, this ratio depends also on the other CKM parameters, most importantly, on the V_{ub} value.[2]

Here we suggest a different, more systematic way to extract the parameters of CKM matrix from the observables (2.17)–(2.19). First of all, we find it more convenient to switch to the four standard Wolfenstein parameters λ, A, ρ and η defined as in [17]. The relevant CKM factors can be represented as follows:

$$\lambda_t^{(s)} = -A\lambda^2\,, \tag{2.20}$$

$$\left|\frac{\lambda_t^{(d)}}{\lambda_t^{(s)}}\right| = \left|\frac{V_{td}}{V_{ts}}\right| = \lambda\sqrt{(1-\rho)^2+\eta^2}, \tag{2.21}$$

$$\frac{\lambda_u^{(d)}}{\lambda_t^{(d)}} = \frac{V_{ub}V_{ud}^*}{V_{tb}V_{td}^*} \equiv \kappa_d e^{i\xi_d} = \left(1-\frac{\lambda^2}{2}\right)\frac{\rho(1-\rho)-\eta^2-i\eta}{(1-\rho)^2+\eta^2}, \tag{2.22}$$

so that

$$\kappa_d = \left(1-\frac{\lambda^2}{2}\right)\frac{\sqrt{(\rho(1-\rho)-\eta^2)^2+\eta^2}}{(1-\rho)^2+\eta^2}, \tag{2.23}$$

$$\sin\xi_d = \frac{-\eta}{\sqrt{(\rho(1-\rho)-\eta^2)^2+\eta^2}}, \quad \cos\xi_d = \frac{\rho(1-\rho)-\eta^2}{\sqrt{(\rho(1-\rho)-\eta^2)^2+\eta^2}}, \tag{2.24}$$

where we neglect very small $O(\lambda^4)$ corrections to these expressions.[3]

Hereafter, we suppose, that the parameter λ, precisely determined from the global CKM fit [17], is used as an input. Then, it is possible to extract all three remaining Wolfenstein parameters combining the three observables (2.17)–(2.19) for semileptonic FCNC decays. First, the parameter A is determined from the binned branching fraction of $B\to K\ell^+\ell^-$, as follows after substituting eq. (2.20) in eq. (2.17):

$$A = \frac{(192\pi^5)^{1/2}}{G_F\alpha_{em}\lambda^2}\left(\frac{1}{\mathcal{F}_{BK}[q_1^2,q_2^2]}\right)^{1/2}\left(\frac{\mathcal{B}_{BK}[q_1^2,q_2^2]}{\tau_B}\right)^{1/2}. \tag{2.25}$$

Then, combining the ratio of the $B\to\pi\ell^+\ell^-$ and $B\to K\ell^+\ell^-$ binned branching fractions with the CP-asymmetry of the pion mode, and employing eqs. (2.21), (2.23) and (2.24), we obtain for the parameter η the following relation:

$$\eta = \frac{1}{2\lambda^2\,(1-\lambda^2/2)}\left(\frac{\mathcal{F}_{BK}\left[q_1^2,q_2^2\right]}{\mathcal{S}_{B\pi}\left[q_1^2,q_2^2\right]}\right)\left(\mathcal{A}_{B\pi}\left[q_1^2,q_2^2\right]\frac{\mathcal{B}_{B\pi}\left[q_1^2,q_2^2\right]}{\mathcal{B}_{BK}\left[q_1^2,q_2^2\right]}\right). \tag{2.26}$$

[2]Note that in the analysis of $B\to\pi\ell^+\ell^-$ and $B\to K\ell^+\ell^-$ presented in [10] these effects are not explicitly specified.

[3]This is consisent with neglecting the $O(\lambda_u^{(s)})\sim O(\lambda^4)$ terms in the $B\to K\ell^+\ell^-$ amplitude. These terms contain nonlocal effects generated by the u-quark loops and calculable within our approach. Hence, achieving the $O(\lambda^4)$ precision is possible in future.

JHEP08(2017)112

Parameter	Ref.
$G_F = 1.1664 \times 10^{-5}$ GeV^2; $\alpha_{em} = 1/129$ $\alpha_s(m_Z) = 0.1185 \pm 0.0006$; $\alpha_s(3\text{ GeV}) = 0.252$ $\overline{m}_b(\overline{m}_b) = 4.18 \pm 0.03$ GeV; $\overline{m}_c(\overline{m}_c) = 1.275 \pm 0.025$ GeV $\overline{m}_s(2\text{ GeV}) = 95 \pm 10$ MeV	[17]
$\mu = 3.0^{+1.5}_{-0.5}$ GeV	
$f_\pi = 130.4$ MeV; $f_K = 159.8$ MeV	[17]
$a_2^\pi(1\text{GeV}) = 0.17 \pm 0.08$; $a_4^\pi(1\text{GeV}) = 0.06 \pm 0.10$	[15]
$a_1^K(1\text{GeV}) = 0.10 \pm 0.04$; $a_2^K(1\text{GeV}) = 0.25 \pm 0.15$	[18, 19]
$\mu_\pi(2\text{ GeV}) = 2.50 \pm 0.30$ GeV; $\mu_K(2\text{ GeV}) = 2.49 \pm 0.26$ GeV	[18, 20]
$M^2 = 16 \pm 4$ GeV^2 ($M^2 = 17 \pm 4$ GeV^2) [in $B(B_s)$-channel]	[15]
$\lambda_B = 460 \pm 110$ MeV	[30]
$M^2 = 1.0 \pm 0.5$ GeV^2; $s_0^\pi = 0.7$ GeV^2; $s_0^K = 1.05$ GeV^2	[11]

Table 1. Input parameters used in the numerical analysis.

Finally, after η is determined, the parameter ρ can be extracted from the ratio of branching fractions (2.18) and (2.17) written explicitly in terms of η and ρ:

$$\frac{\mathcal{B}_{B\pi}[q_1^2,q_2^2]}{\mathcal{B}_{BK}[q_1^2,q_2^2]} = \frac{\lambda^2}{\mathcal{F}_{BK}[q_1^2,q_2^2]}\left(\left[(1-\rho)^2+\eta^2\right]\mathcal{F}_{B\pi}\left[q_1^2,q_2^2\right]\right.$$
$$+\frac{\left[\rho(1-\rho)-\eta^2\right]^2+\eta^2}{(1-\rho)^2+\eta^2}\left(1-\frac{\lambda^2}{2}\right)^2\mathcal{D}_{B\pi}\left[q_1^2,q_2^2\right]$$
$$\left.+2\left[\rho(1-\rho)-\eta^2\right]\left(1-\frac{\lambda^2}{2}\right)\mathcal{C}_{B\pi}[q_1^2,q_2^2]\right). \qquad (2.27)$$

Similar relations for the $B_s \to K\ell^+\ell^-$ decay, obtained by replacing $B\pi \to B_sK$ in eqs. (2.26) and (2.27), provide an additional source of these parameters.

3 Numerical results

The most important input parameters used in our numerical analysis are listed in table 1. In particular, the electroweak parameters, the strong coupling and the meson masses are taken from [17]. For the quark masses in $\overline{MS}$ scheme, entering the correlation functions for QCD sum rules, we adopt, following, e.g., [8], the intervals covering the non-lattice determinations in [17]. We put $m_{u,d} = 0$, except in the combination $\mu_{\pi(K)} = m^2_{\pi(K)}/(m_u + m_{d(s)})$ entering the pion and kaon DAs. In LCSRs, parameters of the pion and kaon twist-2 DA's include the decay constants, and the Gegenbauer moments $a^\pi_{2,4}$ and $a^K_{1,2}$. Normalization of the twist-3 DAs is determined by $\mu_{\pi,K}$, where the ChPT relations [20] between light-quark masses are used (see e.g., [18]). The remaining parameters of the

JHEP08(2017)112

Transition	$f^+_{BP}(0)$	$b^+_{1\,(BP)}$	Correlation
$B_s \to K$	0.336 ± 0.023	-2.53 ± 1.17	0.79
$B \to K$	0.395 ± 0.033	-1.42 ± 1.52	0.72
$B \to \pi$	0.301 ± 0.023	-1.72 ± 1.14	0.74
Transition	$f^T_{BP}(0)$	$b^T_{1\,(BP)}$	Correlation
$B_s \to K$	0.320 ± 0.019	-1.08 ± 1.53	0.74
$B \to K$	0.381 ± 0.027	-0.87 ± 1.72	0.75
$B \to \pi$	0.273 ± 0.021	-1.54 ± 1.42	0.78

Table 2. The fitted parameters of the z-expansion (3.1) for the vector (upper panel) and tensor (lower panel) $B \to P$ form factors at $0 < q^2 < 12.0\,\text{GeV}^2$ calculated from LCSRs.

twist-3 and twist-4 DAs, not shown in table 1 for brevity, are taken from [21], they were also used in [11, 15, 18]. Furthermore, in LCSRs the renormalization scale μ and the Borel parameters M for the sum rules with B (B_s) interpolating current quoted in table 1 are chosen, largely following [15]. The effective quark-hadron duality threshold is determined calculating the $B_{(s)}$-meson mass from the differentiated LCSR. The decay constants f_B and f_{B_s} entering LCRSs are replaced by the two-point sum rules in NLO, their expressions and input parameters (in particular, the vacuum condensate densities) are the same as in [8]. The intervals obtained from these sum rules in NLO are $f_B = (202^{+35}_{-21})\,\text{MeV}$, $f_{B_s} = (222^{+38}_{-24})\,\text{MeV}$. Note that the above uncertainties are effectively smaller in LCSRs (eq. (A.4) in appendix A) due to the correlations of common parameters.

Using the input described above, we obtain the updated prediction for the $B_s \to K$ vector and tensor form factors in the region $0 \le q^2 \le 12.0\,\text{GeV}^2$ where the OPE for LCSRs in the adopted approximation is reliable (see appendix A). In parallel, we also recalculate the $B \to K$ and $B \to \pi$ form factors. For convenience, we fit the LCSR predictions for the $B \to P$ form factors in this region to the two-parameter BCL-version of z-expansion [22] in the form adopted in [18]:

$$f^{+,T}_{BP}(q^2) = \frac{f^{+,T}_{BP}(0)}{1 - q^2/m^2_{B^*_{(s)}}} \left\{ 1 + b^{+,T}_{1(BP)} \left[z(q^2) - z(0) + \frac{1}{2}\Big(z(q^2)^2 - z(0)^2 \Big) \right] \right\}, \tag{3.1}$$

where

$$z(q^2) = \frac{\sqrt{t_+ - q^2} - \sqrt{t_+ - t_0}}{\sqrt{t_+ - q^2} + \sqrt{t_+ - t_0}}\,, \tag{3.2}$$

$$t_\pm = (m_B \pm m_P)^2, \qquad t_0 = (m_B + m_P) \cdot (\sqrt{m_B} - \sqrt{m_P})^2\,, \tag{3.3}$$

and the pole mass in eq. (3.1) for $B_s \to K$, $B \to \pi$ ($B \to K$) form factors is equal to m_{B^*} ($m_{B^*_s}$). The fitted parameters of the vector and tensor form factors and their correlations are presented in table 2. Note that, adopting a more complicated z-expansion with more slope parameters, only insignificantly changes the quality of the fit, and reveals strong

JHEP08(2017)112

correlations between these parameters. In any case the actual form of parametrization does not play a role as soon as we stay within the q^2-region where the form factors are directly calculated from LCSRs. Our results for the form factors are also plotted in figure 1, where the error bands correspond to the uncertainties of the fitted parameters shown in table 2. For comparison, we also show in the same figures the extrapolations of the recent lattice QCD results obtained at large q^2 (low hadronic recoil) and continued to the small q^2 region using the z-series parametrization. For the vector $B_s \to K$ form factor this extrapolation was obtained by HPQCD Collaboration [23]. The same form factor was also calculated by ALPHA Collaboration [24] at a single large-q^2 value. For the vector and tensor $B \to K$ form factors we compare our results with the extrapolations obtained from Fermilab Lattice and MILC Collaboration results [25], to which the HPQCD Collaboration results [26] are very close (not shown here). Finally, the low-q^2 extrapolations of the lattice $B \to \pi$ vector and tensor form factors are taken from [27] and [28], respectively.

The knowledge of the $B_s \to K$ vector form factor at large recoil enables us to calculate the quantity defined in eq. (2.3). The result

$$\Delta\zeta_{B_sK}\,[0, 12\,\mathrm{GeV}^2] = 7.03^{+0.73}_{-0.69}\,\mathrm{ps}^{-1} \tag{3.4}$$

can be directly used for $|V_{ub}|$ determination, provided the differential width of $B_s \to K\ell\nu_\ell$ integrated over the same bin is measured. For comparison we recalculate the same quantity for $B \to \pi\ell\nu_\ell$:

$$\Delta\zeta_{B\pi}\,[0, 12\,\mathrm{GeV}^2] = 5.30^{+0.67}_{-0.63}\,\mathrm{ps}^{-1}\,, \tag{3.5}$$

which is, as it should be, very close to the interval predicted in [16]. The latter interval is somewhat narrower than (3.5), reflecting the statistical (Bayesian) treatment applied in [16] which generally produces less conservative errors. In the future, when sufficiently accurate data on $B_s \to K\ell\nu_\ell$ become available, a global statistical treatment of all $B \to P$ form factors is desirable.

Comparing our results in table 2 with the earlier LCSR calculation [6] of the $B \to K$ and $B_s \to K$ form factors, we emphasize that, albeit the numerical results look close to ours, there are differences in the subleading twist-3,4 terms. We follow ref. [18] where these terms have already been discussed and corrected. Also, as compared to [6], we use slightly different $B_{(s)}$ decay constants and twist-3 normalization parameter μ_K.

Furthermore, the interval for our updated result for the $B \to K$ vector form factor in table 2 lies somewhat above the previous LCSR prediction [11], $f_{BK}^+(0) = 0.34^{+0.05}_{-0.02}$, mainly due to the smaller value of f_B from the two-point sum rule used here and due to the slightly smaller value of the effective threshold in LCSR used in [11]. On the other hand, in the LCSR for $f_{BK}^T(q^2)$ some minor corrections, implemented here in the subleading twist-4 terms, largely compensate the shift caused by the B-decay constant, so that our result in table 2 is close to $f_{BK}^T(0) = 0.39^{+0.05}_{-0.03}$ obtained in [11].

Turning finally to the LCSR result for the vector $B \to \pi$ form factor, which was updated several times in past, let us mention that although we use the same analytical expressions as in ref. [7], the input parameters such as μ_π (determined by the light quark masses) and Gegenbauer moments a_2^π, a_4^π became more accurate, leading to a narrower

JHEP08(2017)112

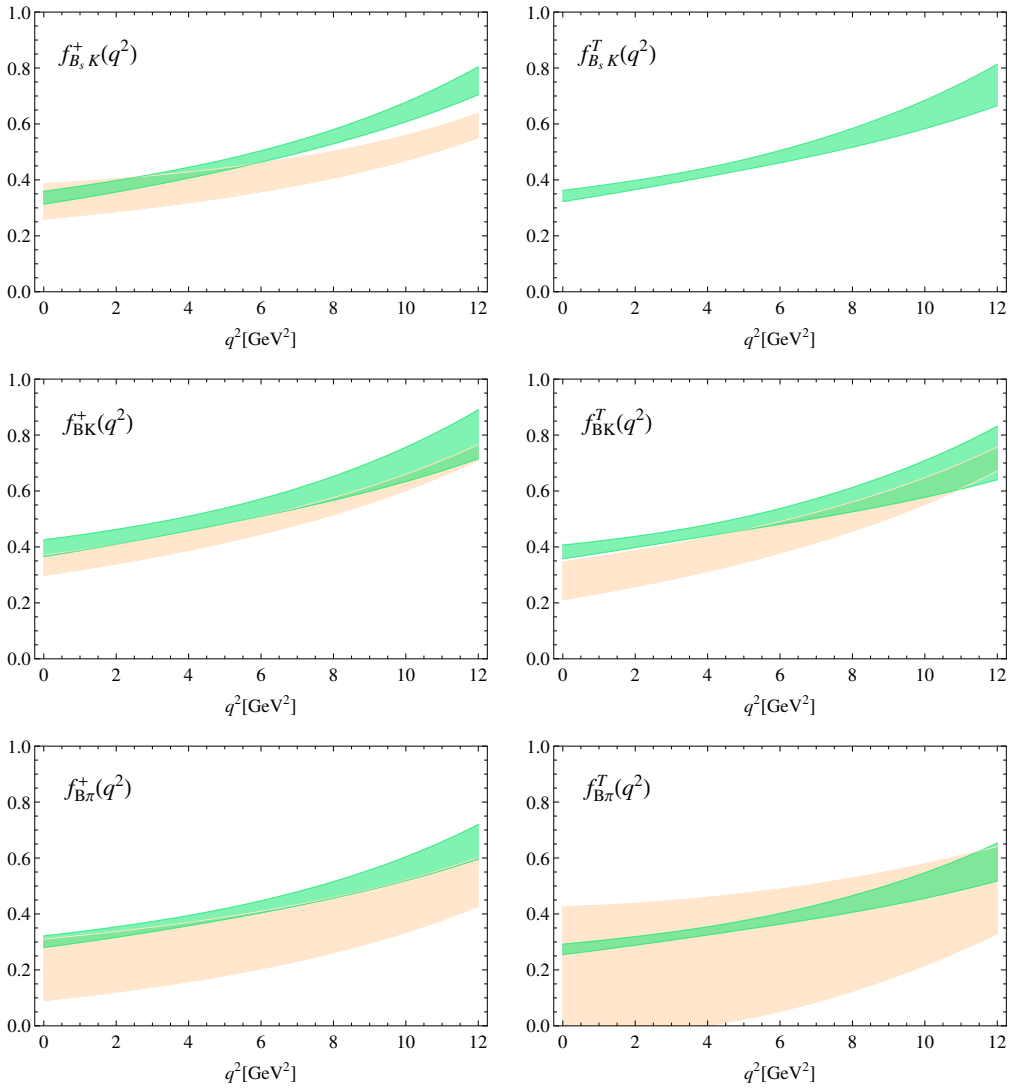

Figure 1. The vector (tensor) form factors of $B_s \to K$, $B \to K$ and $B \to \pi$ transitions calculated from LCSRs including estimated parametrical uncertainties are shown on the upper, middle and lower left (right) panels, respectively, with the dark-shaded (green) bands. Extrapolations of the lattice QCD results for $B_s \to K$ [23], $B \to K$ [25] and $B \to \pi$ [27, 28] form factors are shown with the light-shaded (orange) bands.

interval of our prediction, compared to the interval $f^+_{B\pi}(0) = 0.26^{+0.04}_{-0.03}$ obtained in ref. [7]. The central value of the latter is somewhat below the one we present in table 2, since we use a smaller (larger) central input value of f_B (of μ_π). In ref. [7] one can also find a detailed comparison with the LCSR $B \to \pi$ form factor obtained earlier in ref. [29].

We turn to the numerical analysis of $B \to P\ell^+\ell^-$ observables, where the $B \to P$ form factors obtained above are used. We recalculate the nonlocal amplitudes, following [12, 13]. In appendix B a brief outline of the calculational method is given. Here we need some additional input parameters. The most important are: the inverse moment λ_B of the B-meson DA (we assume $\lambda_{B_s} = \lambda_B$) and the Borel and threshold parameters in π, K channel

JHEP08(2017)112

Coefficent	$\mu = 2.5\,\text{GeV}$	$\mu = 3.0\,\text{GeV}$	$\mu = 4.5\,\text{GeV}$
C_7^{eff}	-0.332	-0.321	-0.304
	(-0.356)	(-0.343)	(-0.316)
C_9	4.070	4.076	4.115
	(4.514)	(4.462)	(4.293)
C_{10}	-4.122	-4.122	-4.122
	(-4.493)	(-4.493)	(-4.493)

Table 3. Wilson coefficients of the FCNC operators at next-to-leading (leading) order in α_s used in our numerical analysis at various scales.

Decay mode	$\mathcal{F}_{BP}[1.0, 6.0]$	$\mathcal{D}_{BP}[1.0, 6.0]$	$\mathcal{C}_{BP}[1.0, 6.0]$	$\mathcal{S}_{BP}[1.0, 6.0]$
$B^- \to K^-\ell^+\ell^-$	$75.0^{+10.5}_{-9.7}$	—	—	—
$B^- \to \pi^-\ell^+\ell^-$	$47.7^{+6.4}_{-5.9}$	$16.1^{+2.8}_{-10.1}$	$14.3^{+7.8}_{-5.8}$	$-9.8^{+7.1}_{-7.2}$
$\bar{B}_s \to K^0\ell^+\ell^-$	$61.0^{+7.0}_{-6.8}$	$7.8^{+3.4}_{-2.5}$	$-12.9^{+2.4}_{-2.2}$	$-3.4^{+1.1}_{-2.6}$

Table 4. The parts of the $B \to P\ell^+\ell^-$ amplitudes squared, as defined in eqs. (2.11)–(2.14), in the units [GeV^3], for the bin $[1.0\ \text{GeV}^2, 6.0\ \text{GeV}^2]$.

in the LCSRs for the soft-gluon emission contributions. They are displayed in table 1. The same input parameters for the pion, kaon and B-meson DAs as the ones given in table 1 serve as an input in the hard-gluon contributions for which we use the QCD factorization expressions [14] at spacelike q^2.

The effective FCNC Hamiltonian (see eq. (B.1) in appendix B) is chosen as in [13] (see table V there), with all Wilson coefficients C_i taken at leading order in α_s. This accuracy is sufficient for $C_{1-6}, C_8^{\text{eff}}$ entering the nonlocal hadronic amplitudes, having in mind the overall accuracy of our method for these amplitudes. At the same time, the numerically large Wilson coefficients C_9, C_{10} and C_7^{eff} of the FCNC operators multiplying the factorizable parts of the decay amplitudes, have a noticeable impact on the observables. Therefore, we adopt here the values of these coefficients at the next-to-leading order in α_s (see table 3).

For completeness and future use, in appendix B the numerical results for the separate nonlocal amplitudes $\mathcal{H}_{BP}^{(u)}$ and $\mathcal{H}_{BP}^{(c)}$ defined as in eq. (B.2) are presented in figures 2, 3, 4. Combining these results with the form factors, we compute the quantities defined in eq. (2.9) for a single bin $[q_1^2, q_2^2] = [1.0\ \text{GeV}^2, 6.0\ \text{GeV}^2]$ which optimally covers the part of the large-recoil region. The results are collected in table 4, where the (uncorrelated) uncertainties are obtained by adding in quadrature the individual variations due to changes of input parameters.

Note that the binned quantities $\mathcal{F}_{BP}$ are not much sensitive to the magnitude of the nonlocal amplitudes $\mathcal{H}_{BP}^{(c)}(q^2)$, which enter the numerically subleading contributions to the coefficients $c_{BP}(q^2)$. Hence, the differences between $\mathcal{F}_{BK}$, $\mathcal{F}_{B\pi}$ and $\mathcal{F}_{B_sK}$ in table 4 roughly

JHEP08(2017)112

Decay mode	$B^- \to K^- \ell^+ \ell^-$	$B^- \to \pi^- \ell^+ \ell^-$	$\bar{B}_s \to K^0 \ell^+ \ell^-$
Measurement or calculation	$\mathcal{B}_{BK}[1.0\,, 6.0]$	$\mathcal{B}_{B\pi}[1.0\,, 6.0]$	$\mathcal{B}_{B_sK}[1.0, 6.0]$
Belle [31]	$2.72\,^{+0.46}_{-0.42} \pm 0.16$	—	—
CDF [32]	$2.58 \pm 0.36 \pm 0.16$	—	—
BaBar [33]	$2.72\,^{+0.54}_{-0.48} \pm 0.06$	—	—
LHCb [10, 34]	$2.42 \pm 0.7 \pm 0.12$	$0.091^{+0.021}_{-0.020} \pm 0.003$	—
HPQCD [38]	3.62 ± 1.22	—	—
Fermilab/MILC [28, 39]	3.49 ± 0.62	0.096 ± 0.013	—
This work	$4.38^{+0.62}_{-0.57} \pm 0.28$	$0.131^{+0.023}_{-0.022} \pm 0.010$	$0.154^{+0.018}_{-0.017} \pm 0.011$

Table 5. Binned branching fractions in the units of 10^{-8} GeV^{-2} defined in eq. (2.15) for the bin $[q_1^2, q_2^2] = [1.0\ \text{GeV}^2 - 6.0\ \text{GeV}^2]$. The first (second) error in our predictions is due to the uncertainty of the input (only of the CKM parameters).

reflect the ratios of the corresponding form factors. On the other hand, the remaining binned quantities $\mathcal{D}_{BP}$, $\mathcal{C}_{BP}$ and $\mathcal{S}_{BP}$ are essentially determined by the nonlocal effects in $B \to P\ell^+\ell^-$. In particular, the large differences between $\mathcal{D}_{B\pi}$, $\mathcal{C}_{B\pi}$, $\mathcal{S}_{B\pi}$ and $\mathcal{D}_{B_sK}$, $\mathcal{C}_{B_sK}$, $\mathcal{S}_{B_sK}$ emerge mainly due to the enhancement of the weak annihilation mechanism in the nonlocal amplitude $\mathcal{H}^{(u)}_{B\pi}(q^2)$ for $B^- \to \pi^-\ell^+\ell^-$ [13]. The same mechanism does not play a role in the amplitude $\mathcal{H}^{(u)}_{B_sK}(q^2)$ contributing to $\bar{B}_s \to K^0\ell^+\ell^-$, due to a different quark content of the initial B_s meson, and due to a suppressed combination of Wilson coefficients.

As shown in the previous section, the binned quantities $\mathcal{F}_{BP}$, $\mathcal{D}_{BP}$, $\mathcal{C}_{BP}$, $\mathcal{S}_{BP}$ can in principle be used for an independent determination of the Wolfenstein parameters A, η and ρ from the combination of observables measured in $B \to P\ell^+\ell^-$ decays. The important role in this determination is played by the direct CP-asymmetry in $B \to \pi\ell^+\ell^-$ which is not available yet in the large-recoil region bins. Hence, here we limit ourselves by an inverse procedure. Taking the values of all Wolfenstein parameters

$$\begin{aligned} &\lambda = 0.22506 \pm 0.00050, && A = 0.811 \pm 0.026, \\ &\bar{\rho} = \rho\left(1 - \frac{\lambda^2}{2}\right) = 0.124^{+0.019}_{-0.018}, && \bar{\eta} = \eta\left(1 - \frac{\lambda^2}{2}\right) = 0.356 \pm 0.011\,, \end{aligned} \tag{3.6}$$

from the global fit of CKM matrix [17] and using the calculated hadronic input from table 4, we predict the values of the binned branching fractions presented in table 5 and the binned direct CP-asymmetries:

$$\mathcal{A}_{B\pi}[1.0, 6.0] = -0.15^{+0.11}_{-0.11}\,, \qquad \mathcal{A}_{B_sK}[1.0, 6.0] = -0.04^{+0.01}_{-0.03}\,. \tag{3.7}$$

The numerical results for the $B \to K\ell^+\ell^-$ and $B \to \pi\ell^+\ell^-$ decays presented here update the previous ones obtained, respectively, in [12][4] and [13].

[4]Note that the branching fractions given in the literature are adjusted to our definition, which implies division by the width $(q_2^2 - q_1^2)$ of the bin.

JHEP08(2017)112

4 Discussion

In this paper we updated the LCSR predictions for the $B_s \to K$ form factors in the large recoil region of the kaon. We predicted the ratio of the integrated $B_s \to K\ell\nu_\ell$ decay width and $|V_{ub}|^2$. Our result can be used to determine this CKM matrix element from the future data on $B_s \to K\ell\nu_\ell$ in the kinematically dominant large recoil region.

We also calculated the hadronic input for the branching fractions and direct CP-asymmetries of $B \to P\ell^+\ell^-$ FCNC decays in the large recoil bin $1.0 \leq q^2 \leq 6.0\,\text{GeV}^2$. Our results include the $B \to P$ form factors and nonlocal hadronic matrix elements, all obtained in the same framework and with a uniform input. The LCSRs used in this calculation take into account the soft-overlap nonfactorizable contributions to the form factors and nonlocal amplitudes. Extending the application of LCSRs to other nonlocal contributions represents an important task for the future. For example, as discussed in more detail in [13], the weak annihilation contribution which is important in the $B \to \pi\ell^+\ell^-$ decay can be obtained from LCSRs with B-meson DAs, alternative to QCD factorization and potentially including subleading effects.

Furthermore, we suggested a systematic way to extract the CKM matrix elements, cast in a form of the Wolfenstein parameters, from the combination of observables in $B \to P\ell^+\ell^-$ decays, independent of the other methods involving the nonleptonic B-decays and/or $B - \bar{B}$ mixing.

Note that an independent extraction of CKM parameters is also possible from other modes of FCNC exclusive B-decays, such as $B_{(s)} \to V\gamma$ or $B_{(s)} \to V\ell^+\ell^-$, where $V = K^*, \rho$. The corresponding combinations of observables demand, apart from $B \to V$ form factors, a dedicated calculation of all relevant nonlocal hadronic matrix elements. For this not yet accomplished task, a variety of methods combining QCD factorization with various versions of LCSRs may prove to be useful. In case of radiative decays the sum rules with photon and vector-meson DAs and heavy-meson interpolating currents can be also of use (for previous works in this direction see [35–37]).

In table 5 we compare our results for the binned branching fractions[4] with the experimental measurements and lattice QCD predictions [28, 38, 39]. In the lattice QCD studies of $B \to P\ell^+\ell^-$ decays, as explained in detail in [39], the nonlocal contributions cannot be calculated in a fully model-independent way. Instead, the (continuum) QCD-factorization [14] in the timelike region of q^2 is employed. Let us also mention in this context the earlier estimates of $B \to K\ell\ell$ [40, 41] and $B \to \pi\ell\ell$ [42] where the QCD-factorization approach was used combined with various inputs and extrapolations for the form factors.

As seen from table 5, the theory predictions for the $B \to K\ell^+\ell^-$ branching fraction reveal some tension with the experimentally measured values, making this observable an important ingredient of the global fits of rare B decays (see e.g., [43]). Adding the characteristics of $B \to \pi\ell^+\ell^-$ and $B_s \to K\ell^+\ell^-$ decays to the set of fitted observables will further extend the possibilities to test the Standard Model in the quark-flavour sector. The fact that these very rare B-decay modes are within the reach of LHCb experiment, makes this task realistic.

JHEP08(2017)112

Acknowledgments

We thank Danny van Dyk and Yu-Ming Wang for useful discussions. This work is supported by the DFG Research Unit FOR 1873 "Quark Flavour Physics and Effective Theories", contract No KH 205/2-2. AK is grateful for support to the Munich Institute for Astro- and Particle Physics (MIAPP) of the DFG cluster of excellence "Origin and Structure of the Universe" where the part of this work was done. AR acknowledges the Nikolai-Uraltsev Fellowship of Siegen University and the partial support of the Russian Foundation for Basic Research (project No. 15-02-06033-a).

A LCSR calculation of the $B \to P$ form factors

The LCSRs for $B \to P$ ($P = \pi, K$) form factors at large recoil of P (parametrically, at $q^2 \ll m_b^2$) are derived from the correlation function of the weak flavour-changing current and B-interpolating quark current, sandwiched between the vacuum and on-shell P-state:

$$\begin{aligned} F^{\mu}_{BP}(p,q) &= i \int d^4x e^{iqx} \langle P(p)|T\{\bar{q}_1(x) \ \ ^{\mu} b(x), (m_b + m_{q_2})\bar{b}(0) i\gamma_5 q_2(0)\}|0\rangle \\ &= \begin{cases} F_{BP}(q^2,(p+q)^2)p^{\mu} + \tilde{F}_{BP}(q^2,(p+q)^2)q^{\mu}, & ^{\mu} = \gamma^{\mu}\,, \\ F^T_{BP}(q^2,(p+q)^2)\left[q^2 p^{\mu} - (q\cdot p)q^{\mu}\right], & ^{\mu} = -i\sigma^{\mu\nu}q_{\nu}\,, \end{cases} \end{aligned} \tag{A.1}$$

where the quark-flavour combination $q_1 = u$, $q_2 = s$ corresponds to the $\bar{B}_s \to K^+$ weak transition; $q_1 = s$, $q_2 = u$ and $q_1 = d$ and $q_2 = u$ ($q_2 = s$) correspond, respectively to the $B^- \to K^-$ and $B^- \to \pi^-$ ($\bar{B}_s \to K^0$) FCNC transitions.

The invariant amplitudes $F_{BP}(q^2,(p+q)^2)$ and $F^T_{BP}(q^2,(p+q)^2)$ in (A.1) are used to derive the LCSRs for the vector $f^+_{BP}(q^2)$ and tensor $f^T_{BP}(q^2)$ form factors, respectively. At $q^2 \ll m_b^2$ and $(p+q)^2 \ll m_b^2$ the OPE near the light-cone $x^2 \simeq 0$ is applied for the correlation function (A.1) and the result is cast in a form of convolution, e.g.,:

$$F^{(\mathrm{OPE})}_{BP}(q^2,(p+q)^2) = \sum_{t=2,3,4,\ldots} \int \mathcal{D}u \sum_{k=0,1,\ldots} \left(\frac{\alpha_s(\mu)}{\pi}\right)^k T^{(t)}_k(q^2,(p+q)^2,\{u_i\})\varphi^{(t)}_P(\{u_i\},\mu), \tag{A.2}$$

where $T^{(t)}_k$ are the perturbatively calculable hard-scattering amplitudes and $\varphi^{(t)}_P(u_i)$ are the P-meson light-cone distribution amplitudes (DAs) of the twist $t \geq 2$. The variables $\{u_i\} = \{u_1, u_2, \ldots\}$ are the fractions of the P-meson momentum carried by the constituents of DAs and $\mathcal{D}u = \delta(1 - \sum_i u_i)\prod_i du_i$. In eq. (A.2) the same renormalization scale μ is used for DAs and for the QCD running parameters in the adopted $\overline{MS}$ scheme.

The terms in the eq. (A.2) that correspond to higher-twist light meson DAs are suppressed by inverse powers of the b-quark virtuality $\sim ((p+q)^2 - m_b^2) \sim \bar{\Lambda} m_b$, where $\bar{\Lambda} \gg \Lambda_{\mathrm{QCD}}$ does not scale with m_b. The adopted approximation for the correlation function includes LO contributions of the twist 2,3,4 quark-antiquark and quark-antiquark-gluon DAs. For the kaon DAs the $O(m_K^2) \sim O(m_s)$ accuracy is adopted. The factorizable parts of twist-5,6 contributions to LCSRs for $B \to P$ form factors were calculated by one of us [9] and their numerical impact on the total invariant amplitude was found negligible,

JHEP08(2017)112

$< 0.1\%$ of the total. This strengthens the argument for using a truncated twist expansion to the accuracy $t = 4$.

The NLO $O(\alpha_s)$ corrections to the twist-2 and (two-particle) twist-3 hard-scattering amplitudes $T_1^{(2,3)}$ are taken into account. In the latter we neglect the s-quark mass, hence, the double suppressed $O(\alpha_s m_s/\bar{\Lambda})$ effects. We use the expressions for OPE derived in [7] extending them to the $B \to K$ and $B_s \to K$ cases (see also [18]). We do not include the $O(\beta_0)$ estimate of the twist-2 $O(\alpha_s^2)$ contribution to the twist-2 hard-scattering amplitude calculated in [44], since the resulting effect in LSCR is very small and does not yet represent a complete NNLO computation of $T_1^{(2)}$.

The analytic result for $F_{BP}^{(\mathrm{OPE})}(q^2,(p+q)^2)$ and $F_{BP}^{T(\mathrm{OPE})}(q^2,(p+q)^2)$ is matched to the hadronic dispersion relation for the correlation function (A.1) in the variable $(p+q)^2$. To apply quark-hadron duality one needs to transform the calculated invariant amplitudes to the form of dispersion integral,

$$F_{BP}^{(T)(\mathrm{OPE})}(q^2,(p+q)^2) = \frac{1}{\pi}\int\limits_{m_b^2}^{\infty} ds \frac{\mathrm{Im}F_{BP}^{(T)(\mathrm{OPE})}(q^2,s)}{s-(p+q)^2}\,. \tag{A.3}$$

We equate the contribution of the excited and continuum B-states in the hadronic dispersion relation to the part of the above integral at $s > s_0^B$, where s_0^B is the effective, process-dependent threshold. The integral at $s \le s_0^B$ is then equated to the contribution of the ground-state of B-meson. The subsequent Borel transformation with respect to the variable $(p+q)^2$ exponentiates denominators, so that, e.g., $1/[s-(p+q)^2] \to e^{-s/M^2}$. Here M^2 is the Borel parameter chosen so that $M^2 \sim \overline{\Lambda} m_b \sim \mu^2$ guarantees a power suppression of higher-twist contributions. One finally obtains the LCSRs for the $B \to P$ form factors:

$$\begin{aligned} f_{BP}^{+}(q^2) &= \frac{e^{m_B^2/M^2}}{2m_B^2 f_B}\frac{1}{\pi}\int\limits_{m_b^2}^{s_0^B} ds\ \mathrm{Im}F_{BP}^{(\mathrm{OPE})}(q^2,s)e^{-s/M^2}\,, \\ f_{BP}^{T}(q^2) &= \frac{(m_B+m_P)e^{m_B^2/M^2}}{2m_B^2 f_B}\frac{1}{\pi}\int\limits_{m_b^2}^{s_0^B} ds\ \mathrm{Im}F_{BP}^{T(\mathrm{OPE})}(q^2,s)e^{-s/M^2}\,. \end{aligned} \tag{A.4}$$

B Nonlocal contributions to $B \to P\ell^+\ell^-$

The effective weak Hamiltonian of the $b \to q\ell^+\ell^-$ transitions ($q = d, s$) generating the $B \to P\ell^+\ell^-$ decays has the following form in the Standard Model (see e.g., the review [45]):

$$H_{\mathrm{eff}}^{b\to q} = \frac{4G_F}{\sqrt{2}}\left(\lambda_u^{(q)}\sum_{i=1}^{2} C_i\,\mathcal{O}_i^u + \lambda_c^{(q)}\sum_{i=1}^{2} C_i\,\mathcal{O}_i^c - \lambda_t^{(q)}\sum_{i=3}^{10} C_i\,\mathcal{O}_i\right) + h.c.\,, \tag{B.1}$$

where $\lambda_p^{(q)} = V_{pb}V_{pq}^*$, $(p = u, c, t)$ are the products of CKM matrix elements. For the $B \to K\ell^+\ell^-$ transitions, the part of the decay amplitude proportional to $\lambda_u^{(s)} \sim \lambda^4$ is neglected. The operators $\mathcal{O}_i$ in (B.1) and the numerical values of their Wilson coefficients C_i

JHEP08(2017)112

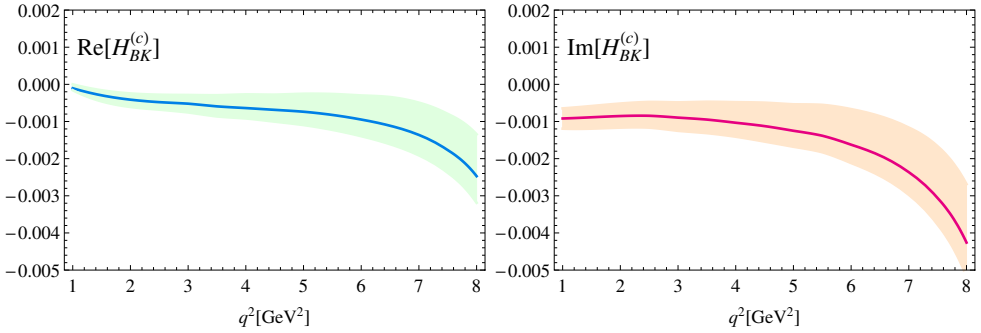

Figure 2. Hadronic nonlocal amplitude $\mathcal{H}_{BK}^{(c)}(q^2)$ in $B^- \to K^-\ell^+\ell^-$ in the large recoil region. On the left (right) panel the real (imaginary) part is plotted for the central input (solid) and including uncertainties (dashed band).

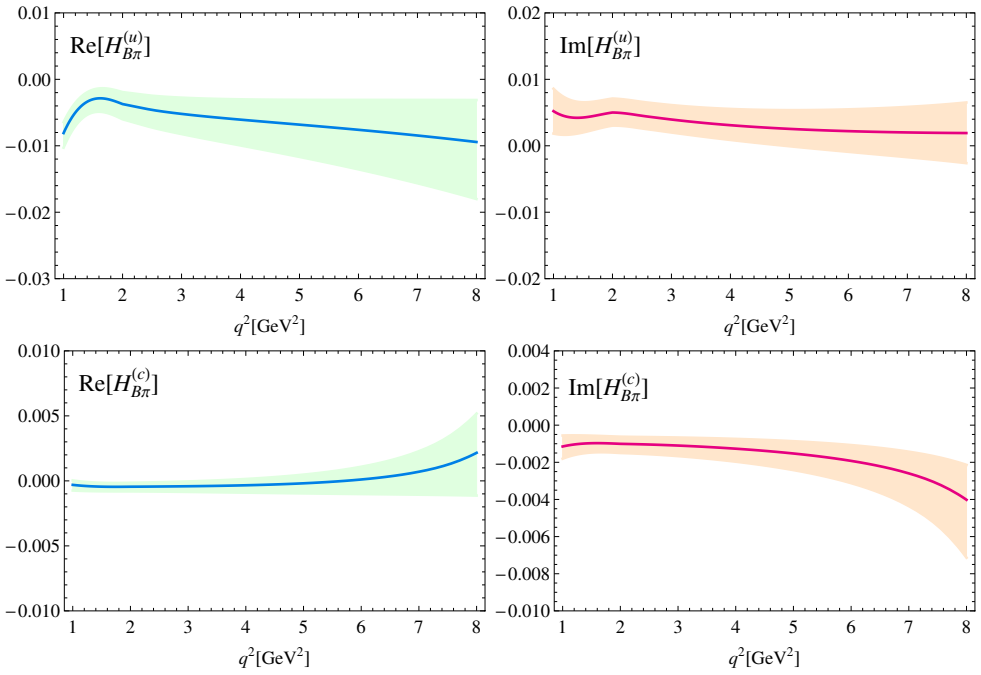

Figure 3. The same as in figure 2 for the amplitudes $\mathcal{H}_{B\pi}^{(u)}(q^2)$ and $\mathcal{H}_{B\pi}^{(c)}(q^2)$ in $B^- \to \pi^-\ell^+\ell^-$.

used in this paper are listed in the appendix A of ref. [13] and in table 3 above. In the decay amplitude (2.4) the dominant contributions of the operators $\mathcal{O}_{9,10}$ and $\mathcal{O}_7$ are factorized to the $B \to P$ form factors. The additional amplitudes denoted as $\mathcal{H}_{BP}^{(c)}(q^2), \mathcal{H}_{BP}^{(u)}(q^2)$ in eqs. (2.5), (2.6) accumulate the nonlocal effects generated by the all remaining effective operators combined with the electromagnetic emission of the lepton pair. They can be represented as a correlation function of the time-ordered product of effective operators with

JHEP08(2017)112

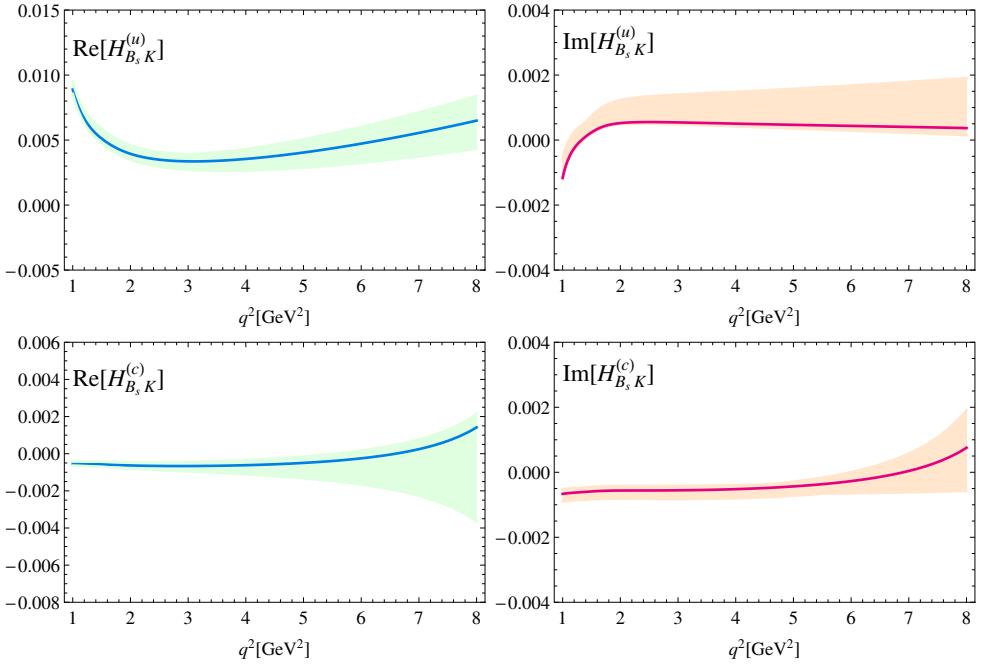

Figure 4. The same as in figure 2 for the amplitudes $\mathcal{H}^{(u)}_{B_s K}(q^2)$ and $\mathcal{H}^{(c)}_{B_s K}(q^2)$ in $\bar{B}_s \to K^0 \ell^+ \ell^-$.

the quark e.m. current, $j^{\rm em}_\mu = \sum_{q=u,d,s,c,b} Q_q \bar{q}\gamma_\mu q$, sandwiched between B and P states:

$$\mathcal{H}^{(p)}_{(BP)\mu} = i\int d^4x e^{iqx}\langle P(p)|\mathrm{T}\left\{j^{\rm em}_\mu(x), \left[C_1\mathcal{O}^p_1(0)+C_2\mathcal{O}^p_2(0)+\sum_{k=3-6,8g} C_k\mathcal{O}_k(0)\right]\right\}|B(p+q)\rangle$$
$$= \left[(p\cdot q)q_\mu - q^2 p_\mu\right]\mathcal{H}^{(p)}_{BP}(q^2), \quad (p=u,c). \tag{B.2}$$

In the case of the $B \to K\ell^+\ell^-$ decay only the amplitude $\mathcal{H}^{(c)}_{BK}(q^2)$ contributes. The calculation of the nonlocal amplitudes following the method suggested in [11] proceeds in two stages. First, the amplitudes $\mathcal{H}^{(c,u)}_{BP}(q^2)$ are splitted in the contributions with different topologies, including c or u quark emission in LO, NLO factorizable corrections, nonfactorizable effects of soft gluon emission, hard-spectator and annihilation contributions. They are calculated one by one at spacelike $q^2 < 0$ where the light-cone OPE for the correlation function (B.2) is valid. For the hard-gluon NLO and spectator contributions we apply the QCD factorization and for the soft gluon emission the dedicated LCSRs. A detailed account of this calculation can be found in refs. [12] and [13]. After that, the resulting functions $\mathcal{H}^{(c,u)}_{BP}(q^2 < 0)$ are fitted to the hadronic dispersion relations in the q^2 variable where the contributions from the lowest vector mesons $V = \rho, \omega, \phi, J/\psi, \psi(2S)$ are isolated and the excited states and continuum contributions are modeled, employing the quark-hadron duality. Here we employ as an additional input the experimental data on branching fractions of the nonleptonic $B \to VP$ decays determining together with the vector meson decay constants the moduli of the residues in the pole terms of the dispersion relation. The phases of these contributions are included in the set of fit parameters. Since in this paper we are interested only in the large recoil (low q^2) region, the integral over

JHEP08(2017)112

hadronic spectral density at $q^2 > 4m_D^2$ with no singularities in the large recoil region is modeled by a polynomial with complex parameters (see refs. [12, 13] for details). Indeed, for our purposes it is not necessary to use a more detailed hadronic representation, like the ansatz suggested in [46] and used in [47], where the broad charmonium resonances located above the open charm threshold are resolved with separate relative phases.

Having fitted the parameters of dispersion relations, we continue them to the positive values of q^2 in the large recoil region, where there is a minor influence of the model-dependent contributions. Finally, we note that in our approach the differences between the $B_s \to K$, $B \to K$ and $B \to \pi$ nonlocal amplitudes originate from the $\mathrm{SU}(3)_{fl}$ -violating differences between the decay constants, parameters of light-meson DAs and nonleptonic amplitudes, as well as from the different spectator-quark flavours, determining the diagram content of these amplitudes.

References

[1] T. Mannel and R. Kowalewski, *Semileptonic bottom hadron decays and the determination of V_{cb} and V_{ub}*, in Particle Data Group collaboration, C. Patrignani et al., *Review of Particle Physics*, *Chin. Phys.* **C 40** (2016) 100001 [INSPIRE].

[2] T. Feldmann, B. Müller and D. van Dyk, *Analyzing $b \to u$ transitions in semileptonic $\bar{B}_s \to K^{*+}(\to K\pi)\ell^-\bar{\nu}_\ell$ decays*, *Phys. Rev.* **D 92** (2015) 034013 [arXiv:1503.09063] [INSPIRE].

[3] I.I. Balitsky, V.M. Braun and A.V. Kolesnichenko, $\Sigma^+ \to P\gamma$ *Decay in QCD* (in Russian), *Sov. J. Nucl. Phys.* **44** (1986) 1028 [*Yad. Fiz.* **44** (1986) 1582] [INSPIRE].

[4] I.I. Balitsky, V.M. Braun and A.V. Kolesnichenko, *Radiative Decay $\Sigma^+ \to p\gamma$ in Quantum Chromodynamics*, *Nucl. Phys.* **B 312** (1989) 509 [INSPIRE].

[5] V.L. Chernyak and I.R. Zhitnitsky, *B meson exclusive decays into baryons*, *Nucl. Phys.* **B 345** (1990) 137 [INSPIRE].

[6] G. Duplancic and B. Melic, *$B, B(s) \to K$ form factors: An update of light-cone sum rule results*, *Phys. Rev.* **D 78** (2008) 054015 [arXiv:0805.4170] [INSPIRE].

[7] G. Duplancic, A. Khodjamirian, T. Mannel, B. Melic and N. Offen, *Light-cone sum rules for $B \to \pi$ form factors revisited*, *JHEP* **04** (2008) 014 [arXiv:0801.1796] [INSPIRE].

[8] P. Gelhausen, A. Khodjamirian, A.A. Pivovarov and D. Rosenthal, *Decay constants of heavy-light vector mesons from QCD sum rules*, *Phys. Rev.* **D 88** (2013) 014015 [*Erratum ibid.* **D 89** (2014) 099901] [*Erratum ibid.* **D 91** (2015) 099901] [arXiv:1305.5432] [INSPIRE].

[9] A.V. Rusov, *Higher-twist effects in light-cone sum rule for the $B \to \pi$ form factor*, *Eur. Phys. J.* **C 77** (2017) 442 [arXiv:1705.01929] [INSPIRE].

[10] LHCb collaboration, *First measurement of the differential branching fraction and CP asymmetry of the $B^\pm \to \pi^\pm\mu^+\mu^-$ decay*, *JHEP* **10** (2015) 034 [arXiv:1509.00414] [INSPIRE].

JHEP08(2017)112

[11] A. Khodjamirian, T. Mannel, A.A. Pivovarov and Y.M. Wang, *Charm-loop effect in $B \to K^{(*)}\ell^+\ell^-$ and $B \to K^*\gamma$*, *JHEP* **09** (2010) 089 [arXiv:1006.4945] [INSPIRE].

[12] A. Khodjamirian, T. Mannel and Y.M. Wang, *$B \to K\ell^+\ell^-$ decay at large hadronic recoil*, *JHEP* **02** (2013) 010 [arXiv:1211.0234] [INSPIRE].

[13] C. Hambrock, A. Khodjamirian and A. Rusov, *Hadronic effects and observables in $B \to \pi\ell^+\ell^-$ decay at large recoil*, *Phys. Rev.* **D 92** (2015) 074020 [arXiv:1506.07760] [INSPIRE].

[14] M. Beneke, T. Feldmann and D. Seidel, *Systematic approach to exclusive $B \to Vl^+l^-$, $V\gamma$ decays*, *Nucl. Phys.* **B 612** (2001) 25 [hep-ph/0106067] [INSPIRE].

[15] A. Khodjamirian, T. Mannel, N. Offen and Y.M. Wang, *$B \to \pi\ell\nu_l$ Width and $|V_{ub}|$ from QCD Light-Cone Sum Rules*, *Phys. Rev.* **D 83** (2011) 094031 [arXiv:1103.2655] [INSPIRE].

[16] I. Sentitemsu Imsong, A. Khodjamirian, T. Mannel and D. van Dyk, *Extrapolation and unitarity bounds for the $B \to \pi$ form factor*, *JHEP* **02** (2015) 126 [arXiv:1409.7816] [INSPIRE].

[17] Particle Data Group collaboration, C. Patrignani et al., *Review of Particle Physics*, *Chin. Phys.* **C 40** (2016) 100001 [INSPIRE] also http://pdg.lbl.gov.

[18] A. Khodjamirian, C. Klein, T. Mannel and N. Offen, *Semileptonic charm decays $D \to \pi\ell\nu_\ell$ and $D \to K\ell\nu_\ell$ from QCD Light-Cone Sum Rules*, *Phys. Rev.* **D 80** (2009) 114005 [arXiv:0907.2842] [INSPIRE].

[19] K.G. Chetyrkin, A. Khodjamirian and A.A. Pivovarov, *Towards NNLO Accuracy in the QCD Sum Rule for the Kaon Distribution Amplitude*, *Phys. Lett.* **B 661** (2008) 250 [arXiv:0712.2999] [INSPIRE].

[20] H. Leutwyler, *The ratios of the light quark masses*, *Phys. Lett.* **B 378** (1996) 313 [hep-ph/9602366] [INSPIRE].

[21] P. Ball, V.M. Braun and A. Lenz, *Higher-twist distribution amplitudes of the K meson in QCD*, *JHEP* **05** (2006) 004 [hep-ph/0603063] [INSPIRE].

[22] C. Bourrely, I. Caprini and L. Lellouch, *Model-independent description of $B \to \pi l\nu$ decays and a determination of $|V_{ub}|$*, *Phys. Rev.* **D 79** (2009) 013008 [*Erratum ibid.* **D 82** (2010) 099902] [arXiv:0807.2722] [INSPIRE].

[23] C.M. Bouchard, G.P. Lepage, C. Monahan, H. Na and J. Shigemitsu, *$B_s \to K\ell\nu$ form factors from lattice QCD*, *Phys. Rev.* **D 90** (2014) 054506 [arXiv:1406.2279] [INSPIRE].

[24] ALPHA collaboration, F. Bahr et al., *Continuum limit of the leading-order HQET form factor in $B_s \to K\ell\nu$ decays*, *Phys. Lett.* **B 757** (2016) 473 [arXiv:1601.04277] [INSPIRE].

[25] J.A. Bailey et al., *$B \to Kl^+l^-$ decay form factors from three-flavor lattice QCD*, *Phys. Rev.* **D 93** (2016) 025026 [arXiv:1509.06235] [INSPIRE].

[26] HPQCD collaboration, C. Bouchard, G.P. Lepage, C. Monahan, H. Na and J. Shigemitsu, *Rare decay $B \to K\ell^+\ell^-$ form factors from lattice QCD*, *Phys. Rev.* **D 88** (2013) 054509 [*Erratum ibid.* **D 88** (2013) 079901] [arXiv:1306.2384] [INSPIRE].

[27] Fermilab Lattice and MILC collaborations, J.A. Bailey et al., *$|V_{ub}|$ from $B \to \pi\ell\nu$ decays and (2+1)-flavor lattice QCD*, *Phys. Rev.* **D 92** (2015) 014024 [arXiv:1503.07839] [INSPIRE].

[28] Fermilab Lattice and MILC collaborations, J.A. Bailey et al., *$B \to \pi\ell\ell$ form factors for new-physics searches from lattice QCD*, *Phys. Rev. Lett.* **115** (2015) 152002 [arXiv:1507.01618] [INSPIRE].

JHEP08(2017)112

[29] P. Ball and R. Zwicky, *New results on $B \to \pi, K, \eta$ decay formfactors from light-cone sum rules*, *Phys. Rev.* **D 71** (2005) 014015 [hep-ph/0406232] [INSPIRE].

[30] V.M. Braun, D. Yu. Ivanov and G.P. Korchemsky, *The B meson distribution amplitude in QCD*, *Phys. Rev.* **D 69** (2004) 034014 [hep-ph/0309330] [INSPIRE].

[31] BELLE collaboration, J.T. Wei et al., *Measurement of the Differential Branching Fraction and Forward-Backword Asymmetry for $B \to K^{(*)}\ell^+\ell^-$*, *Phys. Rev. Lett.* **103** (2009) 171801 [arXiv:0904.0770] [INSPIRE].

[32] CDF collaboration, T. Aaltonen et al., *Observation of the Baryonic Flavor-Changing Neutral Current Decay $\Lambda_b \to \Lambda\mu^+\mu^-$*, *Phys. Rev. Lett.* **107** (2011) 201802 [arXiv:1107.3753] [INSPIRE].

[33] BABAR collaboration, J.P. Lees et al., *Measurement of Branching Fractions and Rate Asymmetries in the Rare Decays $B \to K^{(*)}l^+l^-$*, *Phys. Rev.* **D 86** (2012) 032012 [arXiv:1204.3933] [INSPIRE].

[34] LHCb collaboration, *Differential branching fractions and isospin asymmetries of $B \to K^{(*)}\mu^+\mu^-$ decays*, *JHEP* **06** (2014) 133 [arXiv:1403.8044] [INSPIRE].

[35] A. Khodjamirian, G. Stoll and D. Wyler, *Calculation of long distance effects in exclusive weak radiative decays of B meson*, *Phys. Lett.* **B 358** (1995) 129 [hep-ph/9506242] [INSPIRE].

[36] A. Ali and V.M. Braun, *Estimates of the weak annihilation contributions to the decays $B \to \rho + \gamma$ and $B \to \omega + \gamma$*, *Phys. Lett.* **B 359** (1995) 223 [hep-ph/9506248] [INSPIRE].

[37] J. Lyon and R. Zwicky, *Isospin asymmetries in $B \to (K^*, \rho)\gamma/l^+l^-$ and $B \to Kl^+l^-$ in and beyond the standard model*, *Phys. Rev.* **D 88** (2013) 094004 [arXiv:1305.4797] [INSPIRE].

[38] HPQCD collaboration, C. Bouchard, G.P. Lepage, C. Monahan, H. Na and J. Shigemitsu, *Standard Model Predictions for $B \to K\ell^+\ell^-$ with Form Factors from Lattice QCD*, *Phys. Rev. Lett.* **111** (2013) 162002 [arXiv:1306.0434] [INSPIRE].

[39] D. Du et al., *Phenomenology of semileptonic B-meson decays with form factors from lattice QCD*, *Phys. Rev.* **D 93** (2016) 034005 [arXiv:1510.02349] [INSPIRE].

[40] C. Bobeth, G. Hiller and D. van Dyk, *General analysis of $\bar{B} \to \bar{K}^{(*)}\ell^+\ell^-$ decays at low recoil*, *Phys. Rev.* **D 87** (2013) 034016 [arXiv:1212.2321] [INSPIRE].

[41] W. Altmannshofer and D.M. Straub, *Cornering New Physics in $b \to s$ Transitions*, *JHEP* **08** (2012) 121 [arXiv:1206.0273] [INSPIRE].

[42] A. Ali, A. Ya. Parkhomenko and A.V. Rusov, *Precise Calculation of the Dilepton Invariant-Mass Spectrum and the Decay Rate in $B^\pm \to \pi^\pm\mu^+\mu^-$ in the SM*, *Phys. Rev.* **D 89** (2014) 094021 [arXiv:1312.2523] [INSPIRE].

[43] S. Descotes-Genon, L. Hofer, J. Matias and J. Virto, *Global analysis of $b \to s\ell\ell$ anomalies*, *JHEP* **06** (2016) 092 [arXiv:1510.04239] [INSPIRE].

[44] A. Bharucha, *Two-loop Corrections to the Btoπ Form Factor from QCD Sum Rules on the Light-Cone and $|V_{ub}|$*, *JHEP* **05** (2012) 092 [arXiv:1203.1359] [INSPIRE].

[45] G. Buchalla, A.J. Buras and M.E. Lautenbacher, *Weak decays beyond leading logarithms*, *Rev. Mod. Phys.* **68** (1996) 1125 [hep-ph/9512380] [INSPIRE].

[46] J. Lyon and R. Zwicky, *Resonances gone topsy turvy - the charm of QCD or new physics in $b \to s\ell^+\ell^-$?*, arXiv:1406.0566 [INSPIRE].

[47] LHCb collaboration, *Measurement of the phase difference between short- and long-distance amplitudes in the $B^+ \to K^+\mu^+\mu^-$ decay*, *Eur. Phys. J.* **C 77** (2017) 161 [arXiv:1612.06764] [INSPIRE].

JHEP08(2017)112

Chapter 5

Inclusive semitauonic B decays to order $\mathcal{O}(\Lambda_{QCD}^3/m_b^3)$

Published in:
T. Mannel, A.V. Rusov, and F. Shahriaran, Nucl.Phys. **B921** (2017) 211-224.

Contributions of the authors to the article.
A.V. Rusov performed analytical derivation and numerical calculation of all results presented in the article. Additionally, A.V. Rusov prepared the draft of the manuscript. F. Shahriaran performed an independent analytical calculation confirming the correctness of the results and carefully read and checked the manuscript. Prof. Dr. Th. Mannel provided the idea of this project, supervised the calculation and discussed the results, and optimized the manuscript to its final version.

Available online at www.sciencedirect.com

ScienceDirect

Nuclear Physics B 921 (2017) 211–224

NUCLEAR PHYSICS B

www.elsevier.com/locate/nuclphysb

Inclusive semitauonic B decays to order $\mathcal{O}(\Lambda_{\rm QCD}^3/m_b^3)$

Thomas Mannel [a,*], Aleksey V. Rusov [a,b,*], Farnoush Shahriaran [a,*]

[a] *Theoretische Physik 1, Naturwissenschaftlich-Technische Fakultät, Universität Siegen, D-57068 Siegen, Germany*
[b] *Department of Theoretical Physics, P.G. Demidov Yaroslavl State University, 150000, Yaroslavl, Russia*

Received 10 February 2017; received in revised form 22 May 2017; accepted 23 May 2017
Available online 29 May 2017
Editor: Tommy Ohlsson

Abstract

We calculate the decay width and the τ-lepton energy distribution as well as relevant moments for inclusive $\bar{B} \to X_c \tau \bar{\nu}_\tau$ process including power corrections up to order $\Lambda_{\rm QCD}^3/m_b^3$ and QCD corrections to the partonic level. We compare the result with the sum of the standard-model predictions of the branching fractions of the exclusive semileptonic $\bar{B} \to (D, D^*, D^{**})\tau\bar{\nu}_\tau$ decays as well as with the relevant experimental data. Our prediction is in agreement with the LEP measurement and is consistent with the standard-model calculation of the exclusive modes. We discuss the impact from physics beyond the Standard Model.

1. Introduction

Semitauonic B decays have attracted renewed attention after the measurements of the exclusive channels $\bar{B} \to D^{(*)}\tau\bar{\nu}$, which exhibit a tension with the Standard Model (SM) [1–4]. In fact, the theoretical predictions within the SM turn out to be quite precise, since one of the relevant form factors can be inferred from the decays into light leptons (electrons and muons), while the longitudinal form factor that appears only for the heavy τ lepton can be related to the known one by heavy quark symmetries (HQS). Although the use of HQS implies corrections of the order $\Lambda_{\rm QCD}/m_c$, a good precision is maintained due to the fact, that the contribution of the longitudinal form factor receives an additional suppression factor m_τ^2/m_B^2.

* Corresponding author.
E-mail addresses: mannel@physik.uni-siegen.de (T. Mannel), rusov@physik.uni-siegen.de (A.V. Rusov), shahriaran@physik.uni-siegen.de (F. Shahriaran).

http://dx.doi.org/10.1016/j.nuclphysb.2017.05.016

However, there is another problem with the current data on exclusive semitauonic B decays which is related to the degree of saturation of the inclusive $\bar{B} \to X_c \tau \bar{\nu}$ rate. There is on the one hand a measurement of this inclusive rate based on the b-hadron admixture as it was generated by LEP [5],

$$\mathrm{Br}(b\text{-admix} \to X \tau \bar{\nu}) = (2.41 \pm 0.23)\ \%$$

which to leading order in the heavy quark expansion (HQE) should be the branching ratio for each individual hadron. On the other hand, one may also compute the inclusive semitauonic ratio $R(X_c) = \Gamma(\bar{B} \to X_c \tau \bar{\nu}) / \Gamma(\bar{B} \to X_c \ell \bar{\nu})$, where ℓ is a light lepton. This ratio does not depend on V_{cb} and can been computed within the HQE very precisely. In combination with the accurately measured branching ratio $\mathrm{Br}(\bar{B} \to X_c \ell \bar{\nu})$ one finds in the $1S$ scheme including corrections up to $1/m_b^2$ [7]

$$\mathrm{Br}(B^- \to X_c \tau \bar{\nu}) = (2.42 \pm 0.05)\ \%$$

in full agreement with the LEP measurement. Taking the current data for $R(D)$ and $R(D^*)$ at face value, the two exclusive decay modes $\bar{B} \to D \tau \bar{\nu}$ and $\bar{B} \to D^* \tau \bar{\nu}$ would at least fully saturate (if not oversaturate) the inclusive rate.

This situation has motivated us to perform an independent calculation of $\bar{B} \to X_c \tau \bar{\nu}$ within the HQE. The calculation presented in [6] makes use of the $1S$ scheme and includes terms up to order $1/m_b^2$. In this paper we present a calculation in the kinetic scheme and include terms up to order $1/m_b^3$, improving the existing calculations by including the next order in the HQE. In the light of the quite precise prediction for the inclusive $\bar{B} \to X_c \tau \bar{\nu}$ rate we discuss the theoretical predictions for the exclusive channels $\bar{B} \to D^{(*,**)} \tau \bar{\nu}$ and compare to the current experimental situation.

2. The inclusive $\bar{B} \to X_c \tau \bar{\nu}$ decay

2.1. Outline of the calculation

The matrix element for the $\bar{B} \to X_c \ell \bar{\nu}$ ($\ell = e, \mu, \tau$) decay can be written in terms of the low energy effective Hamiltonian for the weak process $b \to c \ell \bar{\nu}$:

$$\mathcal{H}_W = \frac{G_F V_{cb}}{\sqrt{2}} J_L^\alpha J_{H\alpha} + \mathrm{h.c.}, \tag{2.1}$$

where $J_L^\alpha = \bar{\ell} \gamma^\alpha (1 - \gamma^5) \nu$ and $J_H^\alpha = \bar{c} \gamma^\alpha (1 - \gamma^5) b$ are the leptonic and hadronic currents, respectively, and V_{cb} is the CKM matrix element involved in the decay.

We express the triple-differential distribution for $\bar{B} \to X_c \ell \bar{\nu}$ in terms of the energies of the lepton and neutrino E_ℓ and E_ν and the dilepton invariant mass $q^2 = (p_\ell + p_\nu)^2$ as

$$\frac{d\Gamma}{dE_\ell dq^2 dE_\nu} = \frac{G_F^2 |V_{cb}|^2}{16\pi^3} L_{\alpha\beta} W^{\alpha\beta}, \tag{2.2}$$

where $L_{\alpha\beta}$ and $W_{\alpha\beta}$ are called the leptonic and hadronic tensors, respectively. In the Standard Model, the leptonic tensor takes the form

$$\begin{aligned} L^{\alpha\beta} &= \sum_{\text{lepton spin}} \langle 0 | J_L^{\dagger\alpha} | \ell \bar{\nu} \rangle \langle \ell \bar{\nu} | J_L^\beta | 0 \rangle \\ &= 8 (p_\ell^\alpha p_\nu^\beta + p_\ell^\beta p_\nu^\alpha - g^{\alpha\beta} (p_\ell \cdot p_\nu) - i \varepsilon^{\rho\alpha\sigma\beta} p_{\ell_\rho} p_{\nu_\sigma}) \end{aligned} \tag{2.3}$$

and the hadronic tensor is defined as

$$W^{\alpha\beta} = \frac{1}{4}\sum_{X_c}\frac{1}{2m_B}(2\pi)^3\langle\bar{B}|J_H^{\dagger\alpha}|X_c\rangle\langle X_c|J_H^{\beta}|\bar{B}\rangle\delta^{(4)}(p_B - q - p_{X_c}). \tag{2.4}$$

Its general decomposition into scalar functions $W_j = W_j((v\cdot q), q^2)$, $j = 1, \cdots, 5$ reads

$$W^{\alpha\beta} = -g^{\alpha\beta}W_1 + v^\alpha v^\beta W_2 - i\epsilon^{\alpha\beta\rho\sigma}v_\rho q_\sigma W_3 + q^\alpha q^\beta W_4 + (q^\alpha v^\beta + q^\beta v^\alpha)W_5\,. \tag{2.5}$$

After contraction of leptonic and hadronic tensors the triple differential decay rate takes the form:

$$\frac{d\Gamma}{dE_\ell\, dq^2 dE_\nu} = \frac{G_F^2|V_{cb}|^2}{2\pi^3}\left\{q^2\,W_1 + \left(2E_\ell E_\nu - \frac{q^2}{2}\right)W_2 + q^2(E_\ell - E_\nu)W_3\right. \tag{2.6}$$
$$\left. + \frac{1}{2}m_\ell^2\left[-2\,W_1 + W_2 - 2\,(E_\nu + E_\ell)\,W_3 + q^2\,W_4 + 4E_\nu W_5\right] - \frac{1}{2}m_\ell^4 W_4\right\}.$$

Due to the optical theorem, the hadronic tensor $W^{\alpha\beta}$ is related to the discontinuity of a time-ordered product of currents:

$$T^{\alpha\beta} = -\frac{i}{4}\int d^4x\, e^{-iqx}\,\frac{\langle\bar{B}|\mathrm{T}\left\{J_H^{\dagger\alpha}(x)J_H^{\beta}(0)\right\}|\bar{B}\rangle}{2m_B} \tag{2.7}$$

via the relations

$$-\frac{1}{\pi}\,\mathrm{Im}\,T_j = W_j \tag{2.8}$$

with the structure functions T_i defined in analogy to $W^{\alpha\beta}$:

$$T^{\alpha\beta} = -g^{\alpha\beta}T_1 + v^\alpha v^\beta T_2 - i\epsilon^{\alpha\beta\rho\sigma}v_\rho q_\sigma T_3 + q^\alpha q^\beta T_4 + (q^\alpha v^\beta + q^\beta v^\alpha)T_5\,. \tag{2.9}$$

Inserting $p_b = m_b v + k$ for the momentum of the b quark and expanding in the residual momentum $k \sim \mathcal{O}(\Lambda_{\mathrm{QCD}})$ yields the standard OPE as it is used for the light leptons. A simple way to derive this OPE at tree level based on an external-field method has been derived in [8].

In order to calculate τ-lepton energy spectrum and decay width we need to define the kinematic boundaries of the variable involved in the triple differential decay rate (2.6). We introduce the following dimensionless variables

$$\hat{q}^2 = \frac{q^2}{m_b^2}, \qquad x = \frac{2E_\nu}{m_b}, \qquad y = \frac{2E_\tau}{m_b} \tag{2.10}$$

and the mass parameters

$$\rho = \frac{m_c^2}{m_b^2}, \qquad \eta = \frac{m_\tau^2}{m_b^2}. \tag{2.11}$$

We first perform an integration over the energy of the final state neutrino E_ν and in terms of corresponding dimensionless variable x the limits of integration are determined as

$$\frac{\hat{q}^2 - \eta}{y_+} \le x \le \frac{\hat{q}^2 - \eta}{y_-}, \qquad y_\pm = \frac{1}{2}\left(y \pm \sqrt{y^2 - 4\eta}\right). \tag{2.12}$$

Subsequently we perform the integration over variable $\hat{q}^2$ with corresponding boundaries:

$$y_- \left(1 - \frac{\rho}{1-y_-}\right) \le \hat{q}^2 \le y_+ \left(1 - \frac{\rho}{1-y_+}\right), \tag{2.13}$$

and one gets the τ-lepton energy distribution. Integration over all possible values of the τ-lepton energy

$$2\sqrt{\eta} \le y \le 1 + \eta - \rho \tag{2.14}$$

allows us to calculate decay width.

In this way we obtain the analytic result for the decay width which can be presented in the following form:

$$\Gamma(\bar{B} \to X_c \tau \bar{\nu}) = \Gamma_0 (1 + A_{ew}) \left[C_0^{(0)} + \frac{\alpha_s}{\pi} C_0^{(1)} + C_{\mu_\pi^2} \frac{\mu_\pi^2}{m_b^2} + C_{\mu_G^2} \frac{\mu_G^2}{m_b^2} + C_{\rho_D^3} \frac{\rho_D^3}{m_b^3} + C_{\rho_{LS}^3} \frac{\rho_{LS}^3}{m_b^3} \right], \tag{2.15}$$

where nonperturbative parameters μ_π^2, μ_G^2, ρ_D^3, ρ_{LS}^3 are defined as:

$$2m_B\, \mu_\pi^2 = -\langle B(p)|\bar{b}_v (iD)^2 b_v|B(p)\rangle, \tag{2.16}$$

$$2m_B\, \mu_G^2 = \langle B(p)|\bar{b}_v (iD_\mu)(iD_\nu)(-i\sigma^{\mu\nu}) b_v|B(p)\rangle, \tag{2.17}$$

$$2m_B\, \rho_D^3 = \langle B(p)|\bar{b}_v (iD_\mu)(iv\cdot D)(iD^\mu) b_v|B(p)\rangle, \tag{2.18}$$

$$2m_B\, \rho_{LS}^3 = \langle B(p)|\bar{b}_v (iD_\mu)(iv\cdot D)(iD_\nu)(-i\sigma^{\mu\nu}) b_v|B(p)\rangle\,. \tag{2.19}$$

Note that this corresponds to a "covariant" definition of these parameters using the full covariant derivatives instead of only their spatial components, for a more detailed discussion see [8].

The coefficients $C_0^{(0)}$, $C_0^{(1)}$, $C_{\mu_\pi^2}$, $C_{\mu_G^2}$, $C_{\rho_D^3}$, $C_{\rho_{LS}^3}$ depend on ρ and η, and we define

$$\Gamma_0 = \frac{G_F^2 |V_{cb}|^2 m_b^5}{192\pi^3}. \tag{2.20}$$

The calculation of the decay width revealed that – as in the case of a massless lepton – the corresponding coefficients $C_{\rho_{LS}^3}$ for massive τ-lepton also vanishes, $C_{\rho_{LS}^3} = 0$. The explicit analytic expressions for coefficients $C_0^{(0)}$, $C_{\mu_\pi^2}$, $C_{\mu_G^2}$, $C_{\rho_D^3}$ as functions of ρ and η can be found in Appendix A. The derived expressions for $C_0^{(0)}$, $C_{\mu_\pi^2}$ and $C_{\mu_G^2}$ are in agreement with the corresponding results of [9,10], while analytic formula for $C_{\rho_D^3}$ represents a new result of this paper which in the particular case $m_\ell \to 0$ (or equivalently $\eta \to 0$) reproduces the corresponding expression in [8] originally derived in [11]. Moreover, we include perturbative radiative corrections to the partonic level of the decay width using results of [12]. This correction is presented as $C_0^{(1)}$ in eq. (2.15). Additionally, we include the electroweak correction $A_{\rm ew}$ to the decay width which is well-known and can be found in [13]:

$$1 + A_{\rm ew} \approx \left(1 + \frac{\alpha_{\rm em}}{\pi} \ln \frac{M_Z}{m_b}\right)^2 \approx 1.014. \tag{2.21}$$

Moreover, we calculate the τ-lepton energy distribution and their moments. We define the moments of the τ-lepton energy distribution as in [14]

$$M_\tau^n \equiv \langle E_\tau^n \rangle_{E_\tau > E_{\rm cut}} = \frac{\int_{E_{\rm cut}}^{E_{\rm max}} dE_\tau\, E_\tau^n \frac{d\Gamma}{dE_\tau}}{\int_{E_{\rm cut}}^{E_{\rm max}} dE_\tau \frac{d\Gamma}{dE_\tau}} \tag{2.22}$$

Table 1
The values of the parameters involved in the decay width given in kinetic scheme. The corresponding matrix of the correlations between the parameters can be found in [17].

Parameter	Value	Units	Source
$m_b^{\rm kin}$	4.561 ± 0.020	GeV	
$m_c^{\rm kin}$	1.092 ± 0.020	GeV	
μ_π^2	0.464 ± 0.067	GeV^2	
μ_G^2	0.333 ± 0.061	GeV^2	
ρ_D^3	0.175 ± 0.040	GeV^3	[17]
ρ_{LS}^3	-0.146 ± 0.096	GeV^3	
$V_{cb} \times 10^{-3}$	42.04 ± 0.67		
α_s	0.218 ± 0.018		
G_F	1.16637×10^{-5}	GeV^{-2}	
m_τ	1.777	GeV	[5]
τ_{B^+}	1.638	ps	
τ_{B^0}	1.520	ps	

and the central moments

$$\overline{M}_\tau^n \equiv \langle (E_\tau - \langle E_\tau \rangle)^n \rangle_{E_\tau > E_{\rm cut}}, \tag{2.23}$$

where $E_{\rm cut}$ denotes the energy cut of τ-lepton and $E_{\rm max}$ is its maximal value.

2.2. Numerical analysis and results

We evaluate the rate and the moments in the kinetic scheme. To this end, we re-write the pole mass in (2.15) in terms of the kinetic mass, using the one loop relation from [15]

$$m_Q^{\rm pole} = m_Q^{\rm kin}(\mu) \left(1 + r_Q(\mu) \frac{\alpha_s}{\pi}\right) \tag{2.24}$$

with $Q = b$ or c and auxiliary coefficient r_Q:

$$r_Q(\mu) = \frac{4}{3} C_F \frac{\mu}{m_Q^{\rm kin}(\mu)} \left(1 + \frac{3}{8} \frac{\mu}{m_Q^{\rm kin}(\mu)}\right). \tag{2.25}$$

Inserting (2.24) into (2.15) allows us to absorb parts of the one-loop QCD corrections into the mass definition. In a similar way as for the light leptons, the remaining corrections are small and thus allow us a precise prediction.

The numerical values of the parameters used in our analysis are given in Table 1. For a simple comparison to the massless case we show the dependence of the coefficients C_0, $C_{\mu_\pi^2}$, $C_{\mu_G^2}$, $C_{\rho_D^3}$ in the kinetic scheme on the mass of the τ lepton in Fig. 1.

Table 2 shows a breakdown of the various contributions for the total branching fraction, where we use the PDG values for the lifetimes. We can now compute the total rate, and with the input of the measured lifetime we get for the branching fraction of the inclusive $B^+ \to X_c \tau^+ \nu_\tau$ decay

$$\mathrm{Br}(B^+ \to X_c \tau^+ \nu_\tau) = (2.37 \pm 0.08)\ \%, \tag{2.26}$$

where the uncertainty appears due to a variation of the input parameters within their intervals including the correlations between them. The corresponding matrix of correlations between parameters shown in Table 1 is not presented here and can be found in [17]. The uncertainty in

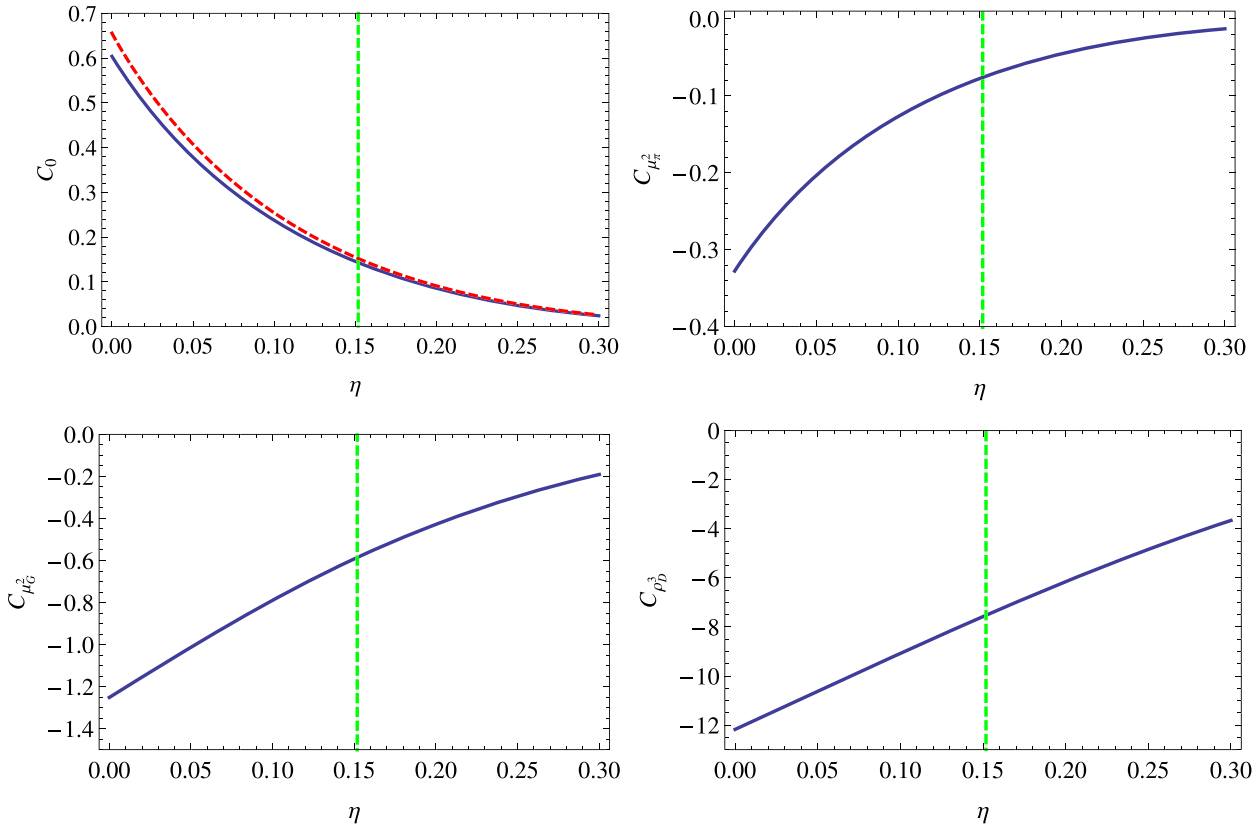

Fig. 1. Dependence of C_0, $C_{\mu_\pi^2}$, $C_{\mu_G^2}$, $C_{\rho_D^3}$ on the parameter η, with $C_0 = C_0^{(0)} + \alpha_s/\pi\, C_0^{(1)}$. In the left top plot the red dashed curve corresponds to $C_0^{(0)}$ and the blue solid one represents C_0 including the radiative correction. The vertical dashed lines correspond to the central value of the parameter η used in our analysis. All curves are plotted for central values of the input parameters. (For interpretation of the references to color in this figure legend, the reader is referred to the web version of this article.)

Table 2
Values of the branching fraction of the inclusive $B^+ \to X_c^0 \tau^+ \nu_\tau$ decay depending on the different kinds of perturbative and power corrections included there. The last row represents our final prediction for this process. Here the following value of charged B-meson life time $\tau_B^+ = 1.638$ ps is used [5]. In order to get results for neutral mode $B^0 \to X_c^- \tau^+ \nu_\tau$ it is sufficient to multiply values given in table by factor $\tau_B^0/\tau_B^+ \approx 0.928$ [5].

Accuracy	$\mathrm{Br}(B^+ \to X_c \tau^+ \nu_\tau)$ [%]
LO	3.06 ± 0.12
LO $+ 1/m_b^2$	2.84 ± 0.11
LO $+ 1/m_b^2 + 1/m_b^3$	2.56 ± 0.09
NLO	2.87 ± 0.12
NLO $+ 1/m_b^2$	2.65 ± 0.10
NLO $+ 1/m_b^2 + 1/m_b^3$	2.37 ± 0.08

(2.26) includes also an estimate of the higher power contribution of order $\mathcal{O}(\Lambda_{\mathrm{QCD}}^4/m_b^4)$ where the relevant coefficient is conservatively assumed to be of order one. Moreover, we include the estimate of the contributions of the higher order radiative corrections. We note that the correc-

tions of order $\mathcal{O}(\alpha_s^2)$ have been computed in the on-shell scheme in [16] and were found to be small. Thus we assume that the impact of the $\mathcal{O}(\alpha_s^2)$ corrections in the kinetic scheme is within the quoted in (2.26) uncertainties.

Alternatively, we can compute the ratio $R(X_c) = \text{Br}(B^+ \to X_c \tau^+ \nu_\tau)/\text{Br}(B^+ \to X_c \ell^+ \nu_\ell)$ for which we obtain

$$R(X_c) = 0.212 \pm 0.003. \tag{2.27}$$

Combining this with the recent world average, $\text{Br}(B \to X_c \ell \nu_\ell) = (10.65 \pm 0.16)$ %, quoted by HFAG [23], we can avoid the uncertainty in V_{cb}, and we thus find an even more precise prediction

$$\text{Br}(B^+ \to X_c \tau^+ \nu_\tau) = (2.26 \pm 0.05)\ \%\,, \tag{2.28}$$

with a slightly smaller central value compared to (2.26), which is, however, within the 1σ range. We note that the uncertainty of our result (2.28) is comparable with one in [7]. However, our analysis shows that the coefficient in front of ρ_D^3 is of the order of ten, similar to what is observed for the case of a massless lepton. The result of including the $1/m_b^3$ corrections is thus a significant shift of the central value compared to the analysis up to $1/m_b^2$ as the one presented in [7], see also Table 2.

Our predictions are also consistent with the measurement of the inclusive branching fraction of the LEP admixture of bottom baryons [5]

$$\text{Br}(b\text{-admix} \to X \tau^\pm \nu) = (2.41 \pm 0.23)\ \%\,. \tag{2.29}$$

Moreover, we also show the resulting τ-lepton energy distribution in Fig. 2. However, these curves cannot be interpreted on a point-by-point basis, since the OPE breaks down in the endpoint region. Note that this region is in fact larger than in the case of massless leptons due to the sizable mass of the τ lepton. However, moments of these spectra can be interpreted in the $1/m_b$ expansion.

In [6] the authors also derived standard model predictions for the τ energy distribution as well as dilepton invariant mass spectrum in the inclusive $B \to X_c \tau \bar{\nu}$ decay including $\Lambda_{\text{QCD}}^2/m_b^2$ and α_s corrections in the 1S mass scheme. In additions, they estimated the effects from shape functions in the endpoint region. In our paper we focus on the τ energy distribution, including the $\Lambda_{\text{QCD}}^3/m_b^3$ corrections. In our analysis we use the kinetic scheme which explains some visible differences between the shapes of the curves presented in Fig. 2 of our paper and in Fig. 2 of [6].

In the case of the light leptons the lepton energy distribution and the relevant moments are the measurable observables. However, for τ leptons, these observables will be more difficult to access, since the τ has to be reconstructed from its decay products. Nevertheless, it is instructive to show the τ-lepton energy moments defined by eqs. (2.22) and (2.23) as a function of the cutoff energy E_{cut} for the sake of comparison with the light lepton case. We present our results in Fig. 3 and give the numerical results for several values of E_{cut} in Table 3. Once abundant data on this decay becomes available, appropriate inclusive observables have to be defined, which should take into account the decay of the τ lepton. The construction of such observables will be subject of future work.

3. The exclusive $\bar{B} \to D^{(*,**)} \tau \bar{\nu}$ decays

Finally, we compare the inclusive result to the sum of identified exclusive states. The decays $\bar{B} \to D^{(*)} \tau \bar{\nu}$ into the two ground-state mesons D and D^* are described in terms of six form

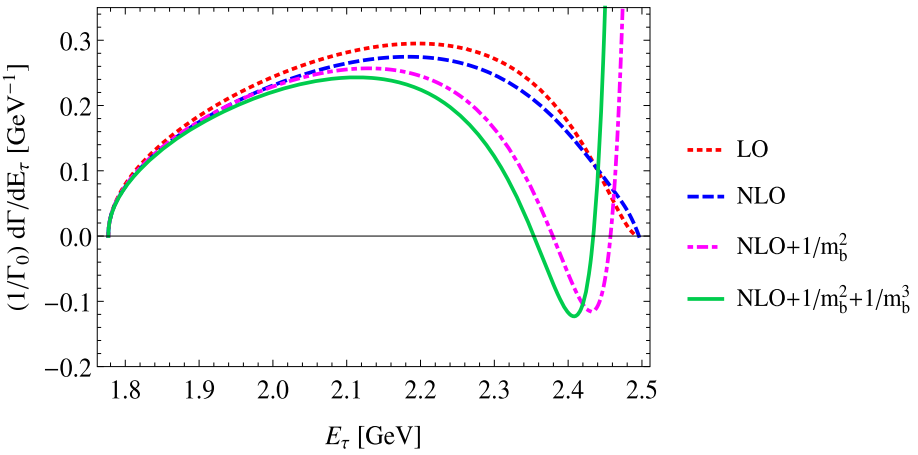

Fig. 2. τ-Lepton energy spectrum of the inclusive $\bar{B} \to X_c \tau \bar{\nu}_\tau$ decay.

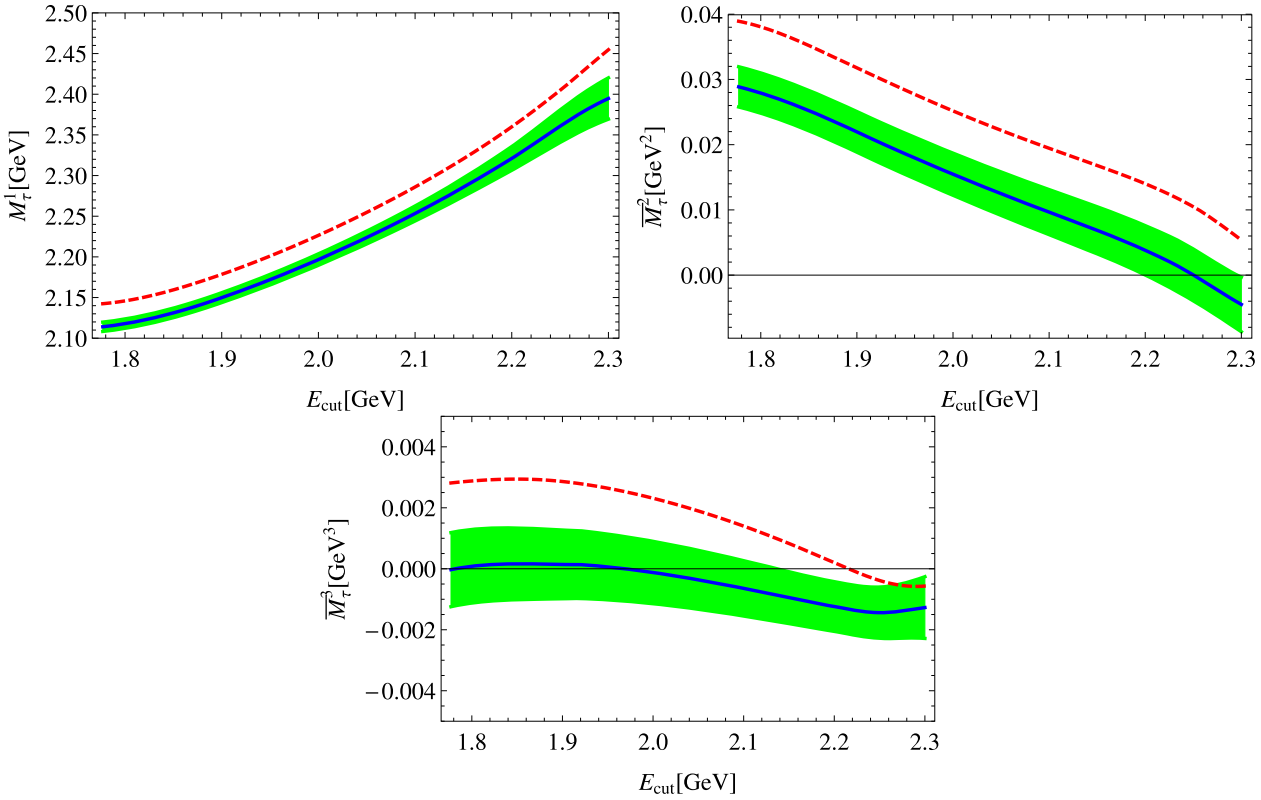

Fig. 3. Dependence of the moments of τ-lepton energy spectrum on the value of the cutoff energy $E_{\rm cut}$. The left plot corresponds to the first moment $M_\tau^1(E_{\rm cut})$, the middle plot contains the second central moment $\overline{M}_\tau^2(E_{\rm cut})$, the right plot contains the third central moment $\overline{M}_\tau^3(E_{\rm cut})$. The solid curves with green shaded areas indicating uncertainties are the result of the full calculation, the dashed ones are without $1/m_b^3$ corrections.

Table 3
The values of the moments of the τ-lepton energy distribution for three different values of the cutoff energy $E_{\rm cut}$.

Moment	$E_{\rm cut} = 1.8$ GeV	$E_{\rm cut} = 2.0$ GeV	$E_{\rm cut} = 2.2$ GeV
M_τ^1 [GeV]	2.118 ± 0.006	2.197 ± 0.007	2.321 ± 0.015
$\overline{M}_\tau^2$ [GeV^2]	0.028 ± 0.003	0.015 ± 0.003	0.004 ± 0.004
$10^3 \times \overline{M}_\tau^3$ [GeV^3]	0.08 ± 1.21	-0.12 ± 1.02	-1.24 ± 0.82

Table 4
SM predictions and experimental results concerning the branching fraction of $B^+ \to D^{(*,**)0}\tau^+\nu_\tau$ decays. In the second column the SM predictions of [18] and [20] are presented and in the third column the values extracted from combined data provided by HFAG [23] and PDG [5] are given.

Mode	Theory (SM)	Experiment (HFAG + PDG)
$\mathrm{Br}(B^+ \to D^0\tau^+\nu_\tau)$	(0.75 ± 0.13) %	(0.91 ± 0.11) %
$\mathrm{Br}(B^+ \to D^{*0}\tau^+\nu_\tau)$	(1.25 ± 0.09) %	(1.77 ± 0.11) %
$\mathrm{Br}(B^+ \to (D^0 + D^{*0})\tau^+\nu_\tau)$	(2.00 ± 0.16) %	(2.68 ± 0.16) %
$\sum_{D^{**}} \mathrm{Br}(B^+ \to D^{**0}\tau^+\nu_\tau)$	(0.14 ± 0.03) %	–

factors, some of which can be accessed in the corresponding decays into light leptons. However, due to the sizable mass of the τ lepton there are two form factors which cannot be accessed from light-lepton data. For these one may make use of heavy quark symmetries to get at least an estimate. Still a quite precise prediction can be made due to the fact that the contribution of these form factors come with a suppression factor m_τ^2/m_B^2. Also the decays into the first orbitally excited mesons have been studied in the heavy mass limit. Using QCD sum rules for the form factors appearing in these processes one may get an estimate for these decays, which we shall generically denote as $\bar{B} \to D^{**}\tau\bar{\nu}$.

In Tab. 4 we quote the recent SM predictions for these processes, referring to [18] for exclusive $\bar{B} \to D\tau\bar{\nu}$ and $\bar{B} \to D^*\tau\bar{\nu}$ decays and to [19] and [20] for $\bar{B} \to D^{(**)}\tau\bar{\nu}$. We note that the SM predictions for the exclusive channels $B^+ \to D^{(*,**)0}\tau^+\nu$ imply

$$\mathrm{Br}(B^+ \to D^0\tau^+\nu_\tau) + \mathrm{Br}(B^+ \to D^{*0}\tau^+\nu_\tau) + \sum_{D^{**}} \mathrm{Br}(B^+ \to D^{**0}\tau^+\nu_\tau) = (2.14 \pm 0.16)\ \%\,. \tag{3.1}$$

It is important to mention the recent paper [21] where the most precise prediction for $R(D) = 0.299 \pm 0.003$ was derived based on the combination of the experimental data and the result of the lattice calculation of the both $B \to D$ scalar and vector form factors [22]. However, in our paper we focus on the calculation of the branching fraction of the inclusive decay and on the comparison with the corresponding branching fractions of the exclusive modes, and at this level the value given in eq. (3.1) is sufficient for our purpose. From (3.1) one can see that the decays into the two ground state D mesons already saturate the predicted inclusive rate to about 85%, the lowest orbitally excited states add another 6%, leading to a saturation of the predicted inclusive rate at a level of 90%. This is in agreement with the expectation from the decays into light leptons, where the measured decay rates to the two ground state D mesons saturate the measured inclusive rate at a level of about 72%. Note that due to the sizable τ lepton mass we expect a lesser degree of saturation for the light leptons, so the overall picture is very consistent.

In Tab. 4 we also show the recent experimental data on $\bar{B} \to D\tau\bar{\nu}$ and $\bar{B} \to D^*\tau\bar{\nu}$. We use the HFAG values for $R(D)$ and $R(D^*)$ and combine them with the PDG values for the branching ratios with light leptons to get the branching ratios for the semitauonic decays. Summing the experimental values for branching ratios into the two ground state D mesons, we find an indication that these two decays alone already over-saturate the predicted inclusive rate, however, only at a level of 2σ. We take this as an indication of an inconsistency, which needs to be clarified.

4. Discussion and conclusions

The tension of the recent data for $R(D)$ and $R(D^*)$ with the theoretical predictions for these exclusive channels has been intensively discussed recently, including a possible explanation through effects from "New Physics" (NP). However, as it has been noticed before, there is also information on the inclusive rate, experimental as well as theoretical.

On the theoretical side, the heavy quark expansion allows us to perform a precise calculation of the inclusive semitauonic decay rates as well as of spectral moments. In the present paper we performed this calculation up to and including term at order $1/m_b^3$, thereby improving the existing calculations by one order in the $1/m_b$ expansion. On the experimental side we have a measurement of the inclusive rate from LEP which, however, is not precise enough to allow for a stringent test.

There have been various attempts to explain the tension in $R(D)$ and $R(D^*)$ in terms of different NP scenarios. We do not go into a detailed discussion of all possible scenarios, we rather parametrize the effects of NP by a simple extension of the effective Hamiltonian

$$\mathcal{H}_{\rm NP} = \frac{G_F V_{cb}}{\sqrt{2}} \left(\alpha\, O_{V+A} + \beta\, O_{S-P}\right) \tag{4.1}$$

with the new operators

$$\begin{aligned} O_{V+A} &= \left(\bar{c}\gamma_\mu(1+\gamma_5)b\right)\left(\bar{\tau}\gamma^\mu(1-\gamma_5)\nu\right), \\ O_{S-P} &= \left(\bar{c}(1-\gamma_5)b\right)\left(\bar{\tau}(1-\gamma_5)\nu\right) \end{aligned} \tag{4.2}$$

and the dimensionless couplings α and β. Our main motivation is to study the effect of (4.1) on the inclusive rate on the basis of this example.

We may discuss this effective low-energy interaction in the context of a standard-model effective theory (SMEFT) with linear realization of the Higgs field. It is interesting to note that the above operator structures cannot be obtained at the leading order of the SMEFT expansion, since we insist on having lepton-universality violation. At dimension 6 we can write

$$P_{V+A} = \left(\bar{c}_R\gamma_\mu b_R\right)\left(\phi^\dagger(i\,D^\mu)\phi\right) \tag{4.3}$$

where ϕ is the SM Higgs doublet field. After spontaneous symmetry breaking, this operator generates an anomalous coupling of the W to the right handed $b \to c$ current. Since the SM coupling to the W is lepton universal, the insertion of this operator into the SM Lagrangian would lead to a lepton-universal effect. Thus we would need to combine this with another new-physics operator which will have dimension six and which generates a lepton-universality violating coupling of the W to the left handed $\tau \to \nu$ current. Upon integrating out the W boson, the combination of the two dimension-six operators generates the same effects as the dimension eight operators we shall discuss now. In fact, writing the left-handed $SU(2)_L$ doublets as L for the leptons and Q for the quarks, we can construct the relevant $SU(2)_L \times U(1)_Y$ invariant operators of dimension eight

$$O'_{V+A} = \left(\bar{c}_R\gamma_\mu b_R\right)\left((\bar{L}\cdot\phi^\dagger)\gamma^\mu(\tilde{\phi}\cdot L)\right), \tag{4.4}$$

$$O'_{S-P} = \left(\bar{c}_R(\phi^\dagger\cdot Q)\right)\left(\bar{\tau}_R(\tilde{\phi}^\dagger\cdot L)\right), \tag{4.5}$$

where $\tilde{\phi}$ is the charge conjugate Higgs field. Once the Higgs field acquires its VEV

$$\langle\phi\rangle = \frac{1}{\sqrt{2}}\begin{pmatrix}0\\ v\end{pmatrix}, \quad \langle\tilde{\phi}\rangle = \frac{1}{\sqrt{2}}\begin{pmatrix}v\\ 0\end{pmatrix},$$

we obtain $8\,O'_{V+A} = v^2 O_{V+A}$ and $8\,O'_{S-P} = v^2 O_{S-P}$. To this end, we infer that within the SMEFT power counting we have

$$\alpha, \beta = \mathcal{O}\left(\frac{v^4}{\Lambda_{NP}^4}\frac{1}{V_{cb}}\right). \tag{4.6}$$

However, the purpose of our simple ansatz (4.1) is not a sophisticated analysis of NP effects, rather we want to study the effect of NP on the inclusive rate. It is a straightforward exercise to add (4.1) to the effective Hamiltonian of the SM and to re-compute the exclusive decay rates for $\mathrm{Br}_{\mathrm{NP}}(B \to D^{(*)}\ell\nu_\ell)$ including the NP effects, using the heavy-quark limit for the form factors (see e.g. [18]). Assuming that there is no effect in the decays into light leptons, the resulting expressions for $R(D)$ and $R(D^*)$ are quadratic forms in the parameters α and β. We define the corresponding NP ratios $R_{\mathrm{NP}}(D^{(*)})$ by

$$R_{\mathrm{NP}}(D^{(*)}) = \frac{\mathrm{Br}_{\mathrm{NP}}(\bar{B} \to D^{(*)}\tau\nu_\tau)}{\mathrm{Br}(\bar{B} \to D^{(*)}\ell\nu_\ell)}. \tag{4.7}$$

The values of parameters α and β are extracted by requiring consistency with the corresponding experimental data on $R(D)$ and $R(D^*)$. Our ansatz is designed to describe both $R(D)$ and $R(D^*)$ simultaneously, and a fit yields

$$\alpha = -0.15 \pm 0.04, \quad \beta = 0.35 \pm 0.08 \tag{4.8}$$

for the parameters α and β. Note that there is a second solution, which exhibits destructive interference with the SM contribution. This solution yields a smaller (in comparison with the first scenario) value for the inclusive rate, which is in tension with the measurement of the sum of the branching fractions of the exclusive $B^+ \to D^0\tau^+\nu_\tau$ and $B^+ \to D^{0*}\tau^+\nu_\tau$ decays. It is interesting to note that the values (4.8) obtained in our fit are not in conflict with the above SMEFT discussion since putting $v = 250$ GeV, $\Lambda_{\mathrm{NP}} \sim 1$ TeV, $V_{cb} \simeq 0.041$ in (4.6) yields $\alpha, \beta \sim 0.1$.

It is worthwhile to point out a subtlety in the extraction of the parameters α and β from the exclusive decays. The experimental analysis of $R(D)$ and $R(D^*)$ assumes the SM shapes for the kinematic distributions, which are used to extract e.g. efficiencies. However, including the NP operators (4.2) will change the shapes of the spectra, and hence the extracted values could shift. As in most other NP analyses we assume that this is only a small effect; a full analysis of this is clearly beyond the scope of this paper.

We are now ready to study the impact of this NP model on the inclusive rate by including the NP operators (4.2) into the calculation. Inclusion of NP modifies the parametrization (2.15), which becomes

$$\Gamma_{\mathrm{NP}} = \Gamma_{\mathrm{SM}} + \Gamma_0\left[A_1\,\alpha + A_2\,\alpha^2 + C_{12}\,\alpha\beta + B_1\,\beta + B_2\,\beta^2\right], \tag{4.9}$$

with coefficients $C_0, A_1, A_2, B_1, B_2, C_{12}$ depending on parameters $\rho = m_c^2/m_b^2$ and $\eta = m_\tau^2/m_b^2$, and Γ_{SM} is the expression given in (2.15).

In Fig. 4 we show the dependence of the inclusive rate on the parameters α and β. The green dot together with the ellipse indicate the best fit value and one-sigma range, respectively, of the parameters α and β (4.8) extracted from $R(D)$ and $R(D^*)$. The shaded bands indicate the one-sigma intervals for $\mathrm{Br}(B^+ \to X_c\tau^+\nu_\tau)$: the red band is our SM prediction (2.26), the green

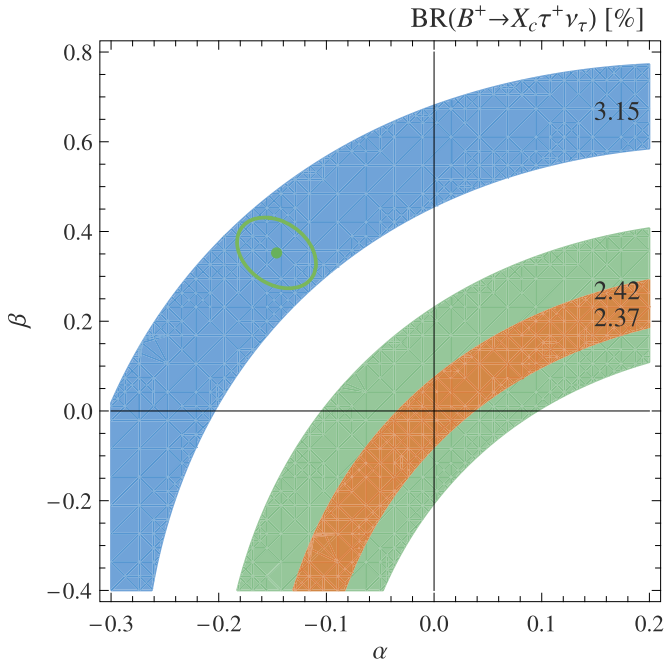

Fig. 4. Contour plot for the branching fraction of $B^+ \to X_c \tau^+ \nu_\tau$ (4.9) as function of α and β. The green dot together with the ellipse indicate the best fit value and one-sigma range of the parameters α and β extracted from $R(D)$ and $R(D^*)$, see (4.8). The shaded bands indicate the one-sigma intervals of $\mathrm{Br}(B^+ \to X_c \tau^+ \nu_\tau)$: the red band is our SM prediction (2.26), the green area represents the LEP measurement (2.29), and the blue band is our prediction for inclusive $B^+ \to X_c \tau^+ \nu_\tau$ decay including contribution from NP (specified in Table 5). (For interpretation of the references to color in this figure legend, the reader is referred to the web version of this article.)

area represents the LEP measurement (2.29), and the blue band is our prediction for inclusive $B^+ \to X_c \tau^+ \nu_\tau$ decay including the contribution (4.1) from NP (specified in Table 5). The error estimate of the latter value contains also the uncertainties from α and β, including the correlation between them. The NP prediction brings the inclusive rate into agreement with the data on exclusive decays, but is now in visible tension with the LEP data.

Recently, the constraints on NP in the $b \to c\tau\bar{\nu}$ transition from the tauonic B_c decay have been discussed, however, with a different ansatz for the NP operators [24–26]. In fact, adding the new physics contribution (4.1) yields a modification of the decay rate $B_c \to \tau\bar{\nu}$, which reads

$$\Gamma(B_c \to \tau\bar{\nu}_\tau) = \frac{M m_\tau^2 f_{B_c}^2 G_F^2 |V_{cb}|^2}{8\pi} \left(1 - \frac{m_\tau^2}{M^2}\right)^2 \left| 1 - \alpha - \frac{M^2}{m_\tau (m_b + m_c)} \beta \right|^2 , \tag{4.10}$$

where M is the mass of the B_c meson and f_{B_c} is its decay constant, defined in the usual way. It has been pointed out in [24] that even relatively small values of β may have a significant effect in the decay rate, since the pre-factor $M^2/(m_\tau(m_b + m_c)) \sim 4$ enhances the contribution of O_{S-P}.

Using the parametrization (4.1) together with our fit values implies a reduction of the tauonic branching fraction for the B_c compared to the SM, since the extracted value of $\beta = 0.35$ is positive and yields in combination with the corresponding pre-factor the relative contribution of order ~ 1 but with a opposite sign compared to $(1 - \alpha)$ contribution, as one can see from (4.10). We conclude that the width of leptonic $B_c \to \tau\bar{\nu}_\tau$ decay including our parametrization of NP is not in tension with the measured B_c lifetime.

Thus we arrive at a different conclusion compared to [24]. However, the reason is that we dropped the assumption that only the leading order in the SMEFT expansion is taken into account. Thus, attributing a possible NP effect leading to the $R(D^{(*)})$ puzzle to dimension-eight

Table 5
Summary of predictions for different mode of semitauonic B-meson decays in the framework of SM and including NP effects in comparison with relevant experimental data. NP predictions presented here correspond to the first scenario for parameters α, β (4.8). We do not quote an uncertainty for the exclusive NP calculations; for fixed $\{\alpha, \beta\}$ the uncertainties are of the same size as the SM ones.

	SM	NP	Experiment
$\mathrm{Br}(B^+ \to D^0 \tau^+ \nu_\tau)$	(0.75 ± 0.13) %	0.93 %	(0.91 ± 0.11) %
$\mathrm{Br}(B^+ \to D^{*0} \tau^+ \nu_\tau)$	(1.25 ± 0.09) %	1.65 %	(1.77 ± 0.11) %
$\mathrm{Br}(B^+ \to X_c \tau^+ \nu_\tau)$	(2.37 ± 0.08) %	(3.15 ± 0.19) %	(2.41 ± 0.23) %

operators can lift the constraint obtained in [24]. We have pursued a different purpose with this simple model, but this observation might deserve a more detailed analysis.

Acknowledgements

TM thanks Martin Jung for useful discussions. This work was supported by the Research Unit FOR 1873, funded by the German research foundation DFG. AR and FS acknowledge the support by a Nikolai-Uraltsev Fellowship of Siegen University.

Appendix A

Here the explicit analytic expressions of the coefficients introduced in the $B \to X_c \tau \nu_\tau$ decay width (2.15) as functions of dimensionless variables ρ and η are given:

$$C_0 = \sqrt{R}\left[1 - 7\rho - 7\rho^2 + \rho^3 - (7 - 12\rho + 7\rho^2)\eta - 7(1+\rho)\eta^2 + \eta^3\right] \tag{A.1}$$
$$- 12\left[\rho^2 \ln\frac{(1+\rho-\eta-\sqrt{R})^2}{4\rho} - \eta^2 \ln\frac{(1+\eta-\rho+\sqrt{R})^2}{4\eta}\right.$$
$$\left. - \rho^2\eta^2 \ln\frac{(1-\rho-\eta-\sqrt{R})^2}{4\rho\eta}\right],$$

$$C_{\mu_\pi^2} = -\frac{\sqrt{R}}{2}\left[1 - 7\rho - 7\rho^2 + \rho^3 - (7 - 12\rho + 7\rho^2)\eta - 7(1+\rho)\eta^2 + \eta^3\right] \tag{A.2}$$
$$+ 6\left[\rho^2 \ln\frac{(1+\rho-\eta-\sqrt{R})^2}{4\rho} - \eta^2 \ln\frac{(1+\eta-\rho+\sqrt{R})^2}{4\eta}\right.$$
$$\left. - \rho^2\eta^2 \ln\frac{(1-\rho-\eta-\sqrt{R})^2}{4\rho\eta}\right],$$

$$C_{\mu_G^2} = \frac{\sqrt{R}}{2}\left[-3 + 5\rho - 19\rho^2 + 5\rho^3 + (5 + 28\rho - 35\rho^2)\eta - (19 + 35\rho)\eta^2 + 5\eta^3\right] \tag{A.3}$$
$$- 6\left[\rho^2 \ln\frac{(1+\rho-\eta-\sqrt{R})^2}{4\rho} - \eta^2 \ln\frac{(1+\eta-\rho+\sqrt{R})^2}{4\eta}\right.$$
$$\left. - 5\rho^2\eta^2 \ln\frac{(1-\rho-\eta-\sqrt{R})^2}{4\rho\eta}\right],$$

$$
\begin{aligned}
C_{\rho_D^3} = \frac{2}{3\rho^2\sqrt{R}}\Big\{&\eta^7 - \eta^6(5\rho+7) + \eta^5\left(6\rho^2+22\rho+21\right) \\
&+ \eta^4\left(\rho^3-9\rho^2-35\rho-35\right) \\
&+ \eta^3(-5\rho^4-2\rho^3-8\rho^2+20\rho+35) + \eta^2\left(3\rho^5-\rho^4-4\rho^3+18\rho^2+5\rho-21\right) \\
&+ \eta(1-\rho)^3\left(2\rho^3+6\rho^2+11\rho+7\right) + (\rho-1)^5(\rho+1)^2 \\
&- R\Big[\eta^5 - \eta^4(3\rho+5) + \eta^3\left(-3\rho^2+8\rho+10\right) + \eta^2\left(37\rho^3+27\rho^2-6\rho-10\right) \\
&+ \eta\left(32\rho^4-18\rho^3-9\rho^2+5\right) - 4\rho^5+10\rho^4-3\rho^3-15\rho^2+\rho-1\Big]\Big\} \\
&+ 8\left\{\eta^2(5\rho^2+\eta-1)\,\ln\left[\frac{(1-\rho-\eta-\sqrt{R})^2}{4\eta\rho}\right]\right. \\
&\left. - (\eta-1)\,\ln\left[\frac{(1+\rho-\eta-\sqrt{R})^2}{4\rho}\right]\right\},
\end{aligned}
\tag{A.4}
$$

where $R = \eta^2 - 2\,\eta\,(\rho+1) + (\rho-1)^2$.

References

[1] J.P. Lees, et al., BABAR Collaboration, Phys. Rev. D 88 (2013) 072012.
[2] J.P. Lees, et al., BABAR Collaboration, Phys. Rev. Lett. 109 (2012) 101802.
[3] R. Aaij, et al., LHCb Collaboration, Phys. Rev. Lett. 115 (2015) 111803.
[4] Y. Sato, et al., Belle Collaboration, Phys. Rev. D 94 (2016) 072007.
[5] C. Patrignani, et al., Particle Data Group, Chin. Phys. C 40 (2016) 100001.
[6] Z. Ligeti, F. Tackmann, Phys. Rev. D 90 (2014) 034021.
[7] M. Freytsis, Z. Ligeti, J.T. Ruderman, Phys. Rev. D 92 (2015) 054018.
[8] B.M. Dassinger, Th. Mannel, S. Turczyk, J. High Energy Phys. 03 (2007) 087.
[9] A. Falk, Z. Ligeti, M. Neubert, Y. Nir, Phys. Lett. B 326 (1994) 145–153.
[10] S. Balk, J.G. Körner, D. Pirjol, K. Schilcher, Z. Phys. C 64 (1994) 37–44.
[11] M. Gremm, A. Kapustin, Phys. Rev. D 55 (1997) 6924.
[12] M. Jezabek, L. Motyka, Nucl. Phys. B 501 (1997) 207.
[13] A. Sirlin, Nucl. Phys. B 71 (1974) 29; Rev. Mod. Phys. 50 (1978) 573.
[14] P. Gambino, C. Schwanda, Phys. Rev. D 89 (2014) 014022.
[15] D. Benson, I.I. Bigi, T. Mannel, N. Uraltsev, Nucl. Phys. B 665 (2003) 367.
[16] S. Biswas, K. Melnikov, J. High Energy Phys. 1002 (2010) 089.
[17] A. Alberti, P. Gambino, K.J. Healey, S. Nandi, Phys. Rev. Lett. 114 (2015) 061802.
[18] P. Biancofiore, P. Colangelo, F. De Fazio, Phys. Rev. D 87 (2013) 074010.
[19] R. Klein, T. Mannel, F. Shahriaran, D. van Dyk, Phys. Rev. D 91 (2015) 094034.
[20] F.U. Bernlochner, Z. Ligeti, Phys. Rev. D 95 (2017) 014022.
[21] D. Bigi, P. Gambino, Phys. Rev. D 94 (2016) 094008.
[22] H. Na, et al., HPQCD Collaboration, Phys. Rev. D 92 (2015) 054510; Erratum: Phys. Rev. D 93 (2016) 119906.
[23] Heavy Flavor Averaging Group, http://www.slac.stanford.edu/xorg/hfag.
[24] R. Alonso, B. Grinstein, J. Martin Camalich, Phys. Rev. Lett. 118 (2017) 081802.
[25] A. Celis, M. Jung, X.Q. Li, A. Pich, arXiv:1612.07757 [hep-ph].
[26] X.Q. Li, Y.D. Yang, X. Zhang, J. High Energy Phys. 1608 (2016) 054.

Chapter 6

Summary and discussion

In this thesis, several semileptonic exclusive and inclusive B-meson decays were studied. The hadronic input for these decays was calculated in the framework of QCD-based methods and the new predictions for the observables were obtained.

At first, the FCNC exclusive $B \to \pi\ell^+\ell^-$ decays were studied. The main focus was put on an analysis of the most difficult underlying input – the nonlocal hadronic amplitudes. The latter ones are generated by a nonlocal overlap of the weak transition with the electromagnetic lepton-pair emission. At timelike region of momentum transfer squared the nonlocality involves long distances, including the formation of hadronic resonances – the vector mesons. To avoid complications related to the long-distance part of the nonlocal effects, the nonlocal contributions have been calculated one by one, combining QCDF and LCSR methods at spacelike region of the momentum transfer squared q^2, where the quark-level diagrams are well defined. The accuracy of the calculation was improved by taking into account, in addition to the factorizable quark-loop effects and the factorizable NLO corrections, also the important nonfactorizable contributions: the soft gluon emission, spectator scattering and weak annihilation. The quark-level calculations were then combined with the hadronic dispersion relation and the parameters of the latter were fitted to access the $q^2 > 0$ region. As a result, the q^2-dependent correction to the Wilson coefficient of the semileptonic operator O_9 was obtained.

This result was used for predictions of the various observables including the differential branching fraction, direct CP-asymmetry and the isospin asymmetry. This analysis has been performed for the exclusive $B \to \pi\ell^+\ell^-$ decays which were recently measured by the LHCb collaboration. These measurements were compared with our predictions in the recent LHCb paper. Furthermore, we have extended the analysis for another yet unobserved $B_s \to K\ell^+\ell^-$ decay channel.

Moreover, the higher twist effects in the LCSR for the heavy-to-light transition vector form factor were estimated within factorization approximation. To this end, the light-cone expansion of the massive quark propagator including for the first time the higher derivatives of the gluon field strength was derived. This new expression was found consistent with the known massless quark limit. This result has a more general relevance since it can be used in any other application of LCSR where one needs the light-cone expansion of the massive quark propagator. Additionally, the analytical expressions for the factorizable twist-5 and twist-6 contributions to the LCSR for the $B \to \pi$ vector form factor have been derived. The relevant numerical analysis revealed that these effects are extremely suppressed, that justifies the conventional truncation of the operator product

expansion in the light-cone sum rules up to twist-4 terms adopted in the previous LCSR analyses.

The results described above have then been taken into account for updating the $B \to P$ form factors from LCSR. The revised $B_s \to K$ vector form factor in the large recoil region was used to predict the ratio of the integrated $B_s \to K\ell\nu_\ell$ decay width and $|V_{ub}|^2$. This result can be used to determine this CKM matrix element from the future data on $B_s \to K\ell\nu_\ell$ in the kinematically dominant large recoil region.

Additionally, the $B \to \pi$, $B \to K$ and $B_s \to K$ form factors updated from LCSR were used to obtain new predictions for the binned branching fraction and binned direct CP-asymmetry in the FCNC processes $B \to \pi\ell^+\ell^-$, $B \to K\ell^+\ell^-$ and $B_s \to K\ell^+\ell^-$. In these decays the contributions of the nonlocal hadronic amplitudes were also taken into account in a systematic way described above.

Furthermore, we suggested a new way of determination of CKM parameters from observables in FCNC $B \to K\ell^+\ell^-$, $B \to \pi\ell^+\ell^-$ and $B_s \to K\ell^+\ell^-$ decays. Recently, $|V_{td}|$, $|V_{ts}|$ and their ratio were determined by the LHCb collaboration from the measured $B \to \pi\ell^+\ell^-$ and $B \to K\ell^+\ell^-$ partial decay widths. We suggested to make the extraction of CKM parameters from these decays more accurate and systematic. To this end, it was found more convenient to switch to the Wolfenstein parametrization of the CKM matrix. In this form, three observables: the width of $B \to K\ell^+\ell^-$, the ratio of $B \to \pi\ell^+\ell^-$ and $B \to K\ell^+\ell^-$ widths and the direct CP-asymmetry in $B \to \pi\ell^+\ell^-$, are sufficient to extract the three Wolfenstein parameters A, η and ρ from experimental data, provided the parameter λ is known quite precisely from the global CKM fit. Two additional observables for the same determination are given by the yet unmeasured $B_s \to K\ell^+\ell^-$ decay. Future more accurate data on the $B \to K\ell^+\ell^-$ and $B \to \pi\ell^+\ell^-$ decays will allow to use this method to extract the CKM parameters with an accuracy comparable to the other determinations.

Finally, a calculation of the inclusive $B \to X_c\tau\nu_\tau$ decay including the terms up to order $\Lambda^3_{\rm QCD}/m_b^3$ was performed improving the existing accuracy by one order more within HQE. A new explicit analytic expression for the coefficient of the Darwin term in the total decay width of the inclusive $B \to X_c\tau\nu_\tau$ has been derived. Updated predictions for the branching fraction and the moments of the τ-lepton energy distribution in $B \to X_c\tau\nu_\tau$ are of interest for experimental collaborations aiming at more precise measurement of these observables. Furthermore, in the light of the current anomalies in $R(D)$ and $R(D^*)$, we considered a certain NP scenario as an example to demonstrate a correlation between the NP predictions for exclusive and inclusive semileptonic B-meson decay modes induced by flavour changing $b \to c$ transition current.

In conclusion, we emphasize that all the results are of great interest for experimental collaborations aiming at more precise measurements of the discovered decay modes and for exploring yet unobserved channels. Some other results derived in the thesis can be used as an input in the further phenomenological analysis of the other various B- and D-meson decays.

Acknowledgements

First of all, I am very grateful to my supervisor Prof. Dr. Alexander Khodjamirian who provided me a possibility to write this dissertation, who always supported and appreciated my work. I am also very thankful to him for fruitful discussions of the projects, for encouraging me to participate in plenty of various conferences, seminars, schools and workshops and for the help to settle a lot of formalities.

I also thank Prof. Dr. Thomas Mannel, the head of the theoretical particle physics group, for providing excellent working conditions. Additionally, I am grateful to him for a fruitful collaboration on the project resulting in publication of one of our papers. I appreciate very much his friendliness and generous hospitality and also his regular Christmas and barbecue parties organised at his home.

Furthermore, I would like to specially thank some of my colleagues. First, my special thanks to Bastian Müller for a plenty of nice and fruitful discussions during our work in the group. I also thank him for some useful comments on the thesis and for the help with the German translation of the abstract. Philipp Böer is thanked for many interesting discussions on physics and I appreciated our various joined academic trips especially to CERN and Dubna. I thank Dr. Markus Suta for helpful advices on settling some formalities related with the cumulative thesis.

I also would like to thank my other co-authors Dr. Christian Hambrock and Farnoush Shahriaran for a productive collaboration on the projects.

I thank the whole theoretical particle physics group for the nice working atmosphere as well as for the hospitality and support.

My special thanks belong to my parents. Despite they live far away from Siegen I appreciate very much their moral support during my PhD-study and life abroad.